TUM School of Engineering and Design
Technische Universität München

Coordinating Decentralized Energy Systems with Local Energy and Flexibility Markets — From Consumer and Prosumer to Flexumer

Michel Zade, M.Sc.

Vollständiger Abdruck der von der TUM School of Engineering and Design der Technischen Universität München zur Erlangung eines

Doktors der Ingenieurwissenschaften (Dr.-Ing.)

genehmigten Dissertation.

Vorsitz:

Prof. Dr.-Ing. Harald Klein

Prüfer*innen der Dissertation:

Prof. Dr.-Ing. Ulrich Wagner
Prof. Dr.-Ing. Stefan Niessen

Die Dissertation wurde am 15. März 2022 bei der Technischen Universität München eingereicht und durch die TUM School of Engineering and Design am 14. Juni 2022 angenommen.

Abstract

The electrification of final energy demand and expansion of renewable generation units and storage systems lead to an increasing number of controllable and decentralized assets in energy systems. Consumers become prosumers by installing their own generation units, can transform into active participants with their controllable assets, and prefer electricity products with specific quality attributes. Consequently, energy systems become climate-neutral, decentralized, and volatile, while costs to maintain grid stability and security of supply rise. To cost-effectively ensure security of supply while expanding renewable energies and electrifying the mobility and heating sectors, it will be essential to integrate and coordinate consumers, prosumers, and their controllable assets. This results in the need for energy models that reflect both the coordination of active participants and their interests.

In the first part of this dissertation, I present a library of coordination mechanisms and a bidding format that allow to model an increasing number of active consumers and prosumers in local energy markets. The coordination models are examined and evaluated using a Monte Carlo simulation. Based on the simulation results, an innovative auction-based coordination mechanism is identified that verifiably satisfies consumer preferences, considers their willingness to pay a premium for heterogeneous energy qualities, and increases local electricity coverage.

Furthermore, I introduce a blockchain implementation of a local energy market that allows to evaluate the added value of the technology compared to a centralized setup. Characteristics of the blockchain implementation are evaluated in a comparative performance analysis and a qualitative assessment of application-specific requirements for local energy markets. Results of the analyses show that the blockchain technology does not fulfill essential requirements for local energy markets such as data privacy and scalability, and therefore cannot empower decentralized participants to host their own energy trading applications at its current stage of development.

The final part of this dissertation presents a new model that quantifies and prices market-based flexibility potentials of consumers' and prosumers' controllable assets, thereby transforming them into flexumers. The functional capabilities of the model are demonstrated in a case study for electric vehicles with field trial mobility data from California and Germany, various electricity tariffs, and charging strategies. The case study results reveal that electric vehicles can provide both positive and negative flexibility. Power and energy quantities depend on the time of day, electricity tariff, charging strategy, and maximum charging power. Owners of controllable appliances can be incentivized to pay grid operators to call their flexibility potential.

Researchers, energy experts, and regulators can use the coordination mechanisms and flexibility model to investigate the market-based integration and coordination of increasingly distributed participants in a more electrified world and a carbon-neutral energy system.

Zusammenfassung

Die Elektrifizierung des Endenergiebedarfs und der Ausbau von erneuerbaren Erzeugungsanlagen und Speichersystemen führt zu einer steigenden Anzahl von steuerbaren und dezentralen Anlagen in Energiesystemen. Konsumenten werden durch die Installation eigener Erzeugungsanlagen zu Prosumenten, können mit ihren steuerbaren Anlagen zu aktiven Teilnehmern werden und besitzen Präferenzen für Energieprodukte mit bestimmten Qualitätsattributen. Dies trägt zur Klimaneutralität des Energiesystems bei, erhöht gleichzeitig Dezentralität und Volatilität. Die Kosten für die Aufrechterhaltung der Netzstabilität und Versorgungssicherheit steigen. Um die Versorgungssicherheit kosteneffizient zu gewährleisten und gleichzeitig die erneuerbaren Energien auszubauen sowie den Mobilitäts- und Wärmesektor zu elektrifizieren, müssen die Konsumenten, Prosumenten und ihre steuerbaren Anlagen integriert und koordiniert werden. Daraus ergibt sich die Notwendigkeit von Modellen, die die Koordinationsmechanismen zwischen und die Interessen der aktiven Teilnehmer in Energiesystemen widerspiegeln.

Im ersten Teil dieser Dissertation stelle ich Koordinierungsmechanismen und ein Gebotsformat vor, die es ermöglichen, eine wachsende Anzahl von aktiven Konsumenten und Prosumenten in lokalen Energiemärkten zu modellieren. Die Koordinationsmodelle werden mit Hilfe einer Monte-Carlo-Simulation untersucht und bewertet. Basierend auf den Simulationsergebnissen wird ein innovativer auktionsbasierter Koordinationsmechanismus identifiziert, der die Konsumentenpräferenzen und zusätzlichen Zahlungsbereitschaften für heterogene Energiequalitäten berücksichtigt und nachweislich erfüllt sowie den lokalen Deckungsgrad erhöht.

Darüber hinaus stelle ich eine Blockchain-Implementierung eines lokalen Energiemarktes vor, die es erlaubt, den Mehrwert der Technologie im Vergleich zu einem zentralen Aufbau zu bewerten. Die Eigenschaften der Blockchain-Implementierung werden in einer vergleichenden Leistungsanalyse und einer qualitativen Bewertung der anwendungsspezifischen Anforderungen an lokale Energiemärkte bewertet. Die Ergebnisse der Analysen zeigen, dass die Blockchain-Technologie wesentliche Anforderungen für lokale Energiemärkte wie Datenschutz und Skalierbarkeit nicht erfüllt und es daher in ihrem derzeitigen Entwicklungsstadium dezentralen Marktteilnehmern nicht ermöglicht, eigene Anwendungen zum lokalen Handel von Energie zu betreiben.

Der letzte Teil dieser Dissertation stellt ein neues Modell vor, das die marktbasierten Flexibilitätspotenziale der steuerbaren Anlagen von Konsumenten und Prosumenten quantifiziert und bepreist, wodurch Konsumenten und Prosumenten zu Flexumenten werden. Die Funktionsfähigkeit des Modells wird in einer Fallstudie für Elektrofahrzeuge mit Mobilitätsdaten aus Feldversuchen in Kalifornien und Deutschland, verschiedenen Stromtarifen und Ladestrategien demonstriert. Die Ergebnisse der Fallstudie zeigen, dass Elektrofahrzeuge sowohl positive als auch negative Flexibilität anbieten können. Leistung und Energie hängen von der Tageszeit, dem Stromtarif, der Ladestrategie und der maximalen Ladeleistung ab. Darüber hinaus können Besitzer von steuerbaren Geräten dazu veranlasst werden, Netzbetreiber für die Inanspruchnahme ihres Flexibilitätspotenzials zu bezahlen.

Forscher, Energieexperten und Regulierungsbehörden können die präsentierten Koordinierungsmechanismen und das Flexibilitätsmodell nutzen, um die marktbasierte Integration und Koordination von zunehmend dezentralen Teilnehmern in einer stärker elektrifizierten Welt und einem klimaneutralen Energiesystem zu modellieren.

Acknowledgements

Throughout my doctoral candidacy I have received support from various people to whom I would like to express my gratitude.

I am grateful for the colleagues with whom I was able to collaborate, share knowledge, and have fruitful and insightful discussions over the past five years. Special thanks go to Clara Orthofer, Daniel Zinsmeister, and Sebastian Dirk Lumpp who became close friends and whose feedback I learned to appreciate very much and helped me to enhance my personal and scientific toolsets. I thank Johannes Honold for supervising me as master student and taking me in as his office mate in the first years of my PhD. I am thankful to Wessam El-Baz, Yasin Incedag, Babu Kumaran Nalini, and Zhengjie You for working with me on the C/sells project and sharing their views with me. Additionally, I thank the students I worked with for their support. Another thank you goes to the RegHEE project partners Sylke Schlenker-Wambach, Ulrich Sperling, and Josef Lipp for sharing their experiences and continuously supporting our research.

I thank my supervisor Professor Dr.-Ing. Ulrich Wagner and mentor Dr.-Ing. Peter Tzscheutschler who have given me the opportunity to do my PhD on decentralized energy systems, the freedom to explore new research fields, guidance on how to become a tutor and scientist, and support throughout my time at the institute of Energy Economy and Application Technology. Furthermore, I would like to thank Prof. Dr.-Ing. Stefan Niessen for his support as co-examiner and the exchanges about our research projects.

Finally, I thank my wife Sandra for always being there for me and proofreading first drafts, thank my friends for their final reviews and my family for their support and constant belief in my ability to succeed.

Michel Zade March 2022

Contents

Chapter 1

Introduction

1.1 Motivation and research questions

In 2022, scientists of the Intergovernmental Panel on Climate Change observed that human-induced global warming already had caused more frequent and extreme weather events and led to irreversible impacts, which human and natural systems cannot adapt to [1]. To limit future impact of climate change on human and planetary health, the energy system must become carbon-neutral [1].

1.1.1 Transformation of the energy system

Generating Variable Renewable Electricity (VRE) is becoming increasingly cheaper compared to conventional fossil-fueled generation [2]. As a result, since 2015 more than 50 % of annually installed generation capacity has been renewable energies [2], globally reaching a total capacity of 2.8 TW in 2020 [3]. However, this transformation can only be a starting point to limit global warming to 1.5° Celsius compared to pre-industrial temperature levels [4]. Current projections outline that approximately 30 TW of renewable generation capacity is required by 2050 to maintain the 1.5° Celsius limit [2, 5].

In this context, consumers are transforming into prosumers by installing generation units and storage systems for renewable energies on their premises, temporarily supplying their energy demands, and feeding into and consuming energy from the public grid. In Germany, the total number of generation units increased from 1.2 million in 2011 to over 2 million in 2020, leading to an increase in the renewable share of gross electricity consumption from 20 % to 45 % (see figure 1.1 and [6, 7]).

These increasing numbers of generation units and storage systems and the intermittency of the electricity feed-in make the transportation, trading, and balancing of renewable energies significantly more complex compared to conventional fossil fueled power plants, which offer reliable and steady operation schedules. This complexity combined with insufficiently expanded power grids causes costly grid congestion management and ultimately increases consumers' energy bills (see figure 1.1).

Energy system scenarios for 2050 estimate that the global final energy demand will be supplied by more than 50 % with electricity [2, 5]. Electricity will be used to charge 1.8 billion Electric Vehicles (EVs) and power 400 million Heat Pumps (HPs) by mid-century

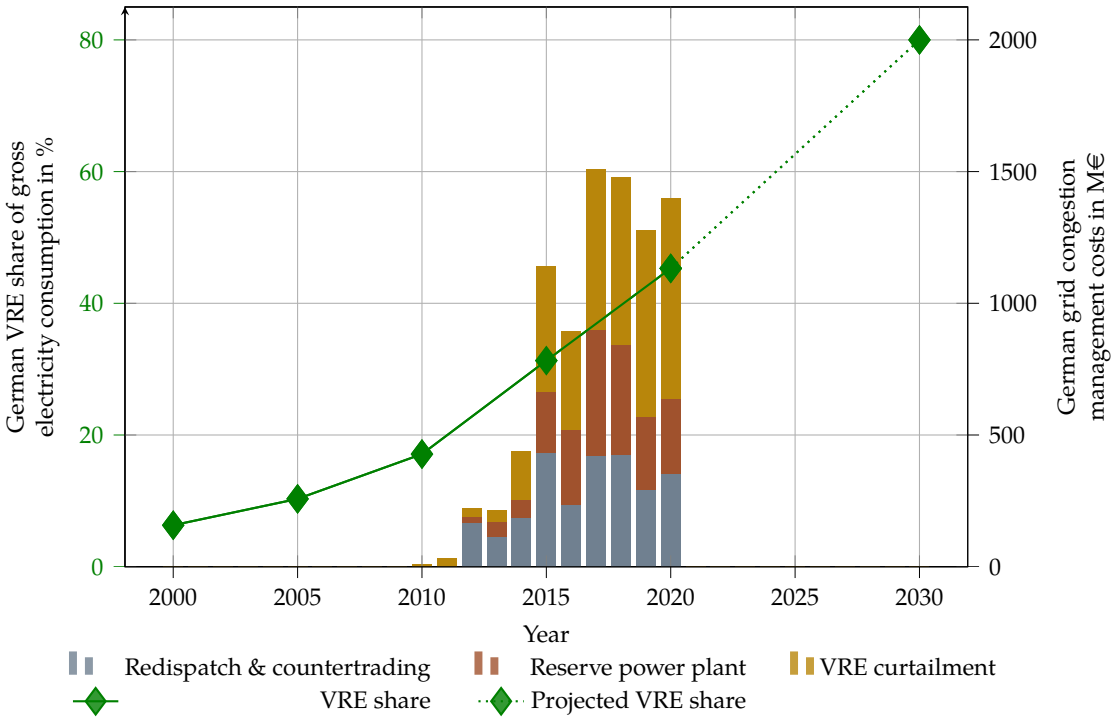

Figure 1.1: German grid congestion management costs according to [8, 9, 10, 11]. *Renewable energy share of gross electricity consumption from 2000 to 2020* [12]. *Projection of VRE share based on coalition agreement of German government* [13].

[2, 14]. EVs and HPs can be used as controllable assets to shift consumption behavior, participate in Local Energy Markets (LEMs), and offer valuable and cost-efficient grid services that support a continuous expansion of volatile renewable energies while maintaining security of supply.

The increasing electrification of the final energy demand changes the role of currently passive consumers. They will be incentivized to offer their flexibility in carbon-neutral energy systems, thereby becoming more active participants [15]. In this dissertation, flexibility refers to deviations from controllable assets' operation schedules that will be traded in a market-based setting (see definition in 1.3.3).

Failing to adequately coordinate these small-scale and controllable assets while phasing-out fossil-fueled power plants and neglecting to sufficiently expand power grids could cause additional infrastructure costs, power losses, and reduce energy systems' security of supply [16, 17]. With this in mind, I formulate the following Research Questions (RQs).

RQ#1 What do coordination mechanisms look like that allow consumers and prosumers to be integrated as active participants into the energy system, to trade energy locally, and to take into account their preferences for energy qualities such as *green* or *local*?

RQ#2 How can consumers and prosumers become flexumers that provide market-based flexibility to grid operators and how much flexibility at what time and price can be expected from them?

1.1.2 Technological advancements

In recent years, multiple technological advancements were introduced that can help to integrate and coordinate the aforementioned billions of controllable assets as active and flexible components in energy systems. Future households will most probably be equipped with Home Energy Management Systems (HEMSs) and Smart Meters (SMs) [18] since they have promising features and form the basis for the transformation of market participants from consumers to prosumers and flexumers.

HEMSs are discussed in the literature as demand response tools that communicate with home appliances, optimize their schedules based on user preferences, forecasts, and costs, and control their operation [19]. Today, companies such as Sonnen, KiwiGrid, and GridX are developing and offering commercial products for private households worldwide that visualize energy consumptions and feed-ins from household appliances. Once HEMSs are able to control household appliances, a wide range of grid services and applications will be possible by intelligently controlling each appliances' operation schedule, reducing household energy bills, and ideally optimizing the overall system efficiency [20].

Another important technology that enables the provision and billing of grid-stabilizing services is the smart metering infrastructure. A smart metering infrastructure measures the energy consumed or fed into the grid and allows metering operators to receive metering values in Real-Time (RT) [21]. As soon as SMs are installed in households and grid operators set up appropriate coordination mechanisms, it will be possible to set tailored incentives for consumers, prosumers, and their controllable assets that can be automatically processed and used to cost-efficiently avoid grid congestions [22].

In parallel, a decentralized and potentially disruptive technology, known as blockchain, and its potential to empower consumers and prosumers to host their own energy trading applications was discussed among researchers and energy experts [23, 24, 25, 26, 27]. A blockchain is a distributed database, does not rely on a central entity hosting the infrastructure, and allows to execute code decentralized with smart contracts. For a more detailed description please refer to section 1.3.2. Since 2016, a variety of studies were published theoretically assessing blockchains in the energy sector. Studies were released describing promising characteristics such as process automation, transparency, decentralization, and tamper-resistance [27, 28] and evaluated a variety of energy-related blockchain use cases [29]. Interviews among energy experts were conducted investigating the potential impact of the blockchain technology on the energy economy [30, 31]. However, how the blockchain technology can empower consumers, prosumers, and flexumers and what role it will take in the coordination of them is still an open question. Therefore, I formulate the following RQ.

RQ#3 What value can blockchain technology add in coordinating consumers and prosumers, particularly in LEMs compared to centralized implementations?

To answer the aforementioned RQs, energy models are needed that represent both the coordination of individual participants and their interests. Furthermore, the models should be implementable on varying systems such as a blockchain.

1.2 Structure

This dissertation presents two energy models that allow to investigate coordination mechanisms for and flexibility potentials of consumers, prosumers, and flexumers, and the evaluation of the potential added value that recent technological advances can provide. The overall structure of this dissertation is visualized in figure 1.2.

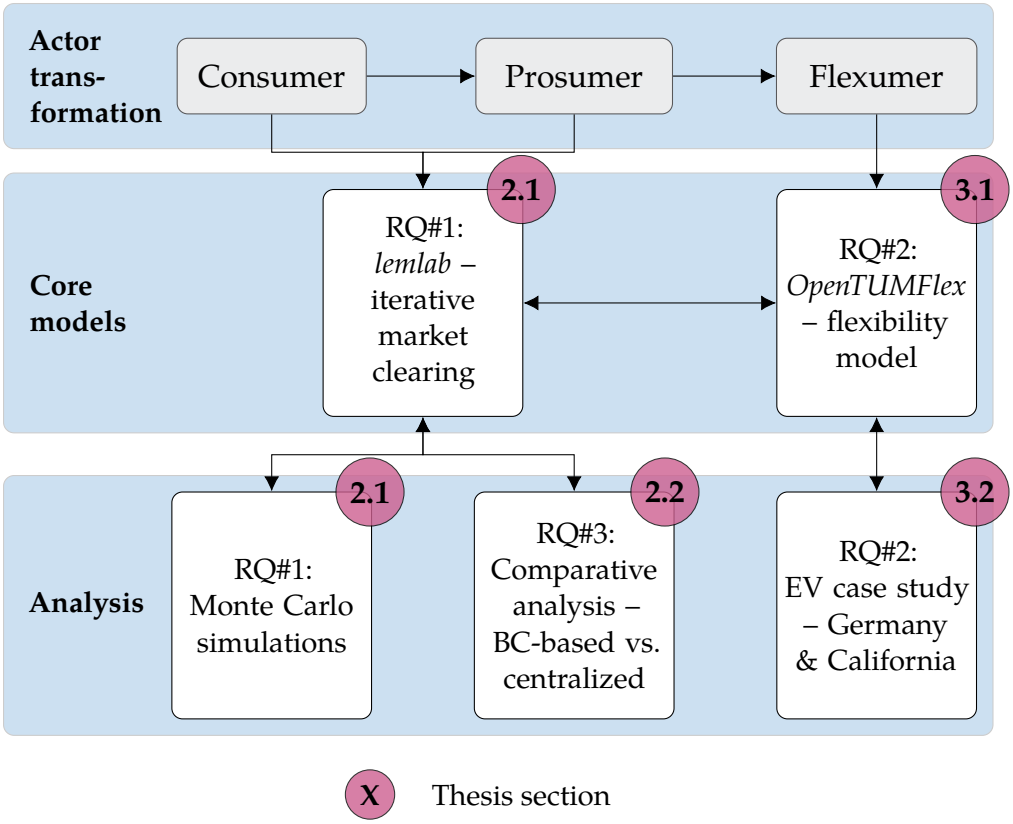

Figure 1.2: Schematic of the dissertation and the chapters therein. Red circles are links to the corresponding sections in this dissertation. lemlab and OpenTUMFlex are models developed as part of this dissertation and in collaboration with colleagues [32, 33].

The transformation from consumers to flexumers is the overarching theme of this thesis. Formerly passive consumers are transforming into active participants of the energy system with controllable loads and preferences for electricity from specific generation types and locations. Simultaneously, consumers who install generation units and storage systems on their premises are becoming prosumers, which temporarily supply their own demand and feed-in and consume electricity from the public grid. Consumers and prosumers who are able to calculate their flexibility potential and offer it to grid operators transform into flexumers.

In section 2.1, I present an article introducing a new coordination model for active consumers and prosumers. This coordination model is based on a new bidding format and a newly developed library of auction-based Iterative Market Clearing Algorithms (IMCAs) that considers and verifiably satisfies consumers' preferences for specific energy qualities and their Willingness To Pay a Premium (WTPP). WTPP refers to an additional amount of money a user is willing to pay for an electricity product with specific attributes such as a regional provider or a certain share of VRE [34, 35]. To demonstrate the capabilities and characteristics of the newly developed coordination model, the results of Monte Carlo simulations are presented. The model library is publicly available as part of the open-source project *lemlab* [32].

Section 2.2 analyzes how the introduction of blockchain could empower consumers and prosumers to self-responsibly host their own LEM applications. A comparative performance analysis of a blockchain-based and centralized implementation indicates what added value the blockchain technology can provide in the context of LEMs. The blockchain-based LEM implementation and the performance analysis are publicly available as part of the open-source project *lemlab* [32]. Additionally, I briefly introduce a preparatory study I conducted and published on the power demand of the Bitcoin and Ethereum blockchain network.

In section 3.1, I present an article introducing a flexibility quantification and pricing model for flexumers' market-based flexibility potential. The capability of the model is demonstrated in a case study with mobility data from field trials in California and Germany, varying electricity tariffs, and charging strategies that allow to investigate future flexibility offers of EVs (see section 3.2). The model is publicly available as part of the open-source project *OpenTUMFlex* [33].

Finally, section 4 concludes this dissertation, puts key findings into the broader scientific context, and makes recommendations for future research.

1.3 Definitions

Before presenting the articles of this dissertation, I will specify the most important terms for this dissertation since there is no distinct definition of these terms in the literature.

1.3.1 Consumer, prosumer, and flexumer

Consumer

Consumers are households that obtain energy from the grid. Furthermore, consumers can be subdivided into active and passive participants. Passive consumers are participants that do not actively control their consumption behavior whereas active consumers express their preferences for certain energy qualities, participate in LEMs, and optimize the operation of their controllable loads.

Prosumer

Prosumers are consumers that install a decentralized energy generation unit on their premise, temporarily supply their own energy demands, feed excess energy into and con-

sume energy from the public grid. Prosumers can participate in LEMs based on forecasts and optimize their energy costs but do not consider external limitations such as grid congestions.

Flexumer

Flexumers are consumers or prosumers that own controllable household appliances, can calculate flexibility offers, communicate them to a market platform, and control them accordingly if being called to prevent grid congestions (see flexibility in 1.3.3).

1.3.2 Local energy markets

LEMs allow non-professional participants to trade excess and deficit energy in a defined regional area [36].

The **value proposition** of a LEM is to exchange energy locally; thereby economically strengthening local communities, increasing their acceptance for VREs, reducing grid fees and grid expansion costs [36].

The **roles** in a LEM involve multiple parties dependent on the national regulatory framework the design is implemented in. Non-professional and professional participants such as prosumers and aggregators act as Distributed Energy Resource (DER) operators on the LEM. Retailers are simultaneously connected to a whole-sale market and a LEM to ensure market liquidity (see market thickness in [37]). Market operators provide the information and communication infrastructure for the exchange of data. Grid operators and regulators are not directly involved but observe the market and use outcomes to calculate power flows and monitor market operations.

Coordination types of distributed energy resources

The differentiation of coordination types is mainly based on a review article published in [38] and is in line with previous review articles [39, 40].

In **centrally optimized** LEMs coodinators collect information from all connected DERs, optimize their operations, and control them. This approach has the advantage to find a cost-optimal solution and is capable to incorporate grid constraints. However, this coordination strategy quickly becomes computationally expensive with a high number of DERs and requires the disclosure of personal information to coordinating entities. Aggregating or controlling DERs as a virtual power plant are subsets of this coordination type.

Peer-to-peer markets are fully decentralized coordination mechanisms that allow participants to directly communicate with each other; thereby reducing the disclosed information and transparency. Over-the-counter contracts and power purchase agreements can be understood as large-scale examples of Peer-to-Peer (P2P) mechanisms.

In **community-based markets**, participants send pre-defined data to an independent entity that processes the data based on agreed coordination rules. Afterwards, participants self-responsibly react and control their devices with respect to the market outcome. An example would be the spot market of the EPEX SPOT or auction-based LEMs.

Functions

I distinguish four fundamental LEM functions.

User and meter management allows to create, initialize, edit, delete user accounts, and map connected HEMSs and SMs to users.

Market clearing is the core function of a LEM. This function calculates the exchangeable market volume and price based on inputs from market participants. Once, the volume and price have been calculated, user accounts are credited or debited with the appropriate quantities.

Settlement is executed after energy has been matched, physically exchanged among market participants, and logged with SMs. The function calculates balancing energies, grid fees, and taxes. These calculated quantities are then credited or debited from the users' accounts.

Labelling energy quantities refers to the assignment of energy quality labels to energy quantities that are fed into the grid, matched in the market clearing, and metered by SMs. Energy quality labels can for example be generation-unit-specific, region-specific, or CO_2-specific.

Requirements

To objectively compare different setups of LEMs objective requirements are necessary. In the case of a LEM, these requirements can be categorized in market clearing and infrastructure.

Market clearing requirements are specified to evaluate whether a matching algorithm satisfies user preferences for heterogeneous energy qualities, incorporates users' WTPP, increases local coverage of demand and supply, and ensures individual rationality and computational tractability.

Infrastructure requirements are defined to assess whether an infrastructure such as a blockchain ensures data security, reliability, scalability, tamper resistance, and low operating costs.

Heterogeneous energy qualities and preferences

Heterogeneous energy qualities are labels that a community can assign to electricity quantities fed into the grid, cleared on a market, or consumed and metered through a SM. Labels can be based on generation types, CO_2-emissions, geographic distance or arbitrarily chosen. DER owners are able to label their placed market bids with an energy quality and consumers can in return indicate their preference for a particular energy quality on a LEM. Within this thesis, I use the quality labels *NA, local, green-local* to indicate whether a certain electricity quantity originated from a non-local, local, or a CO_2-neutral and local generation unit.

Willingness to pay a premium

WTPP refers to an amount of money a consumer is willing to additionally pay for a specific product with distinct attributes. Studies use choice experiments to estimate consumers'

WTPP for certain product attributes [41, 42, 35, 43].

Bidding format

The bidding format defines what information participants need to provide to place valid market bids on a LEM. Whereas conventional double auctions only require a price and a quantity, I extended the bidding format to include the WTPP and heterogeneous energy quality label (see section 2.1).

Iterative market clearing algorithms

IMCAs refer to a newly developed set of market clearing algorithms that iteratively use a Periodic Double Auction (PDA) to verifiably satisfy heterogeneous energy quality preferences. A PDA refers to a market mechanism where market bids are collected in a closed book and cleared at predefined intervals [44, 45]. The publication in section 2.1 presents two general architectures and multiple combinations of IMCAs.

Blockchain

This definition is mainly based on [46] if not indicated otherwise. Blockchains are virtual state machines. Changes to the blockchain's state are stored in blocks on distributed network nodes. The total amount of data that can be inserted into a block is limited to ensure synchronicity among all network nodes. Each appended block consists of transactions that represent validated state transition requests and the hash value of the previous block, thereby building a chain of blocks.

Hashing functions are one-way mathematical functions that compute a unique hash value of a predefined length for any kind of input [47]. One-way refers to a function that makes it very difficult or impossible to reproduce the input data based on the output. Due to their characteristics, hashing functions are used in the mining process and for connecting consecutive blocks in blockchains.

A blockchain node requests a state transition by sending out a **transaction**. In the most basic form a transaction consists of a sender, a receiver, and a value. However, transactions are also used to deploy programmable scripts also known as smart contracts.

Smart contracts are programmable scripts that can be deployed to a blockchain. Once deployed to a blockchain they allow to modify a blockchain's state variably. **Off- & on-chain** refer to the executing infrastructure of a function. On-chain means that a function is executed inside a deployed smart contract on a blockchain and off-chain that it is executed on a conventional non-blockchain system but uses the blockchain infrastructure eventually.

lemlab

lemlab is a modular and agent-based simulation toolbox for LEMs that allows to connect to RT and emulated test beds, centralized and decentralized data base infrastructures such as blockchains, simulate various market mechanisms, prosumer strategies and characteristics, and integrate a variety of time series [32]. *lemlab* was developed at the Chair

of Energy Economy and Application Technology as part of the research project RegHEE [32]. The bidding format, IMCAs, and analyses presented in chapter 2 are published as add-ons in *lemlab*.

1.3.3 Market-based flexibility

Flexibility

Flexibility refers to a designated deviation from a planned operating schedule [48]. This definition includes large-scale measures such as redispatch, feed-in management, sheddable loads, and small-scale market-based flexumer offers presented in chapter 3. However, within this dissertation I focus on market-based flexibility where provider and grid operators negotiate a compensation for flexibility [49]. Furthermore, flexibility can be subdivided into a positive and negative type: negative is the reduction of electricity feed-in or the consumption of non-scheduled energy and positive the delay of energy consumption or non-scheduled feed-in [50].

Flexibility platform or market

A flexibility platform is used to match flexibility demands and offers. Demands come from grid operators who need to stabilize grid operations, and offers come from DER operators who can quantify, price, and control the operation of their assets accordingly.

Flexibility offers consist of positive and negative power, available energy, price, and a time step in which the offer is valid. The price has to at least ensure that the flexibility provider does not experience an economical disadvantage. The location of the DER can be explicitly added or is implicitly included through the identifier of the offering operator.

Vehicle availability

To quantify the flexibility potential of EVs we need to know when a vehicle is parked and available for charging at a certain location. This information is referred to as vehicle availability and is described by the following parameters: an identifier for the location, the arrival and departure time of the vehicle, and the distance the vehicle has travelled since its last departure. Based on these parameters *OpenTUMFlex* calculates flexibility offers.

OpenTUMFlex

OpenTUMFlex is an open-source market-based flexibility model, which quantifies and prices flexibility potentials of controllable household appliances [33]. The model was developed at the Chair of Energy Economy and Application Technology as part of the research project SINTEG C/sells [22]. Chapter 3 presents the theoretical basis and the functional capabilities of *OpenTUMFlex*.

Chapter 2

Local energy markets for active consumers and prosumers

At the turn of the millennium, energy systems in the European Union (EU) and North America were liberalized with the aim of establishing a competitively efficient energy market and strengthening consumer rights [51, 52]. Formerly integrated energy supply companies were subdivided into separate entities, operating power grids, generating, and distributing electricity (see EU directive 96/92/EC [53]). Nowadays, producers and retailers trade electricity in competitive markets, consumers can freely choose and change their retailers, and prosumers in Germany for example get a fixed price for their VRE feed-ins [52].

In 2003, the EU went one step further and formulated the idea to label electricity according to its environmental impact and transparently communicate these labels (see EU directive 2003/54/EC [54]). This concept was further specified in the EU directive 2009/28/EC with the aim to label the origin of electricity for consumers, anticipating increased demands for VREs, thereby supporting the expansion of renewable generation units [55].

These market mechanisms and subsidy systems were designed for formerly centralized energy systems with fossil-fueled power plants and renewable generation units, which were not yet competitively marketable [56, 39]. Nowadays, these systems cause high grid congestion management costs, have not created the expected incentives, and slow down the integration of additional VREs [57, 58, 56]. Therefore, new market designs are necessary that consider the location dependency, intermittency, and uncertainty of VREs [56].

LEMs are discussed in the literature as coordination mechanisms that can fulfill the aforementioned needs such as the integration of consumers and prosumers as active participants into energy systems and the reduction of transmission losses and grid expansion costs [40, 36, 39]. Furthermore, LEMs are divided into three coordination types: centrally optimized, P2Ps, or community-based markets (see definitions in section 1.3.2). Within this dissertation, I will refer to a LEM as a community-based market platform that enables non-professional participants such as consumers and prosumers to engage in market-based, local and self-responsible electricity trading.

2.1 Considering energy qualities and preferences

Scientific context

Concurrently to the aforementioned introduction of energy quality labels, studies showed how consumers are developing preferences and are actively asking for specific electricity products with distinct attributes (see table 2.1), thereby transforming from formerly passive to active consumers. These product attributes can mark whether the electricity originates completely or partially from carbon-neutral energy sources, from regional retailers or producers, or whether a certain security of supply level can be ensured. Within this dissertation, I refer to these product attributes as heterogeneous energy qualities and consumer preferences (see definition in 1.3.2).

Table 2.1: Electricity product attributes analyzed in consumer surveys with choice experiments in [34, 59, 43, 60, 35, 41, 61, 62, 63, 64, 42, 65, 66, 67, 68, 69].

Attribute	Description
Generation type mix	Shares of generation types e.g. wind or nuclear
Generation location mix	Shares of locally, regionally, or nationally generated electricity
Retailer ties	Whether retailer have local, regional, or national ties
Security of supply	Outage frequency and duration per time period
Visual landscape	Impact on the visual appearance of the landscape

These heterogeneous consumer preferences are studied by marketing and social scientists who conduct choice experiments with electricity products to analyze consumer preferences and their WTPP [70]. Whereas most studies conclude that the price is the key attribute of electricity products [35, 41, 66, 34], the studies also show that consumers are interested in locally generated renewable electricity and have a WTPP for the listed attributes [59, 43, 35, 41, 42, 65, 66, 68].

However, current market designs only insufficiently allow consumers to express these preferences or verifiably satisfy them [71, 72]. Nowadays, consumers in liberalized European energy systems sign contracts with retailers that ensure their electricity supply. If consumers ask for VRE, retailers purchase sufficient Renewable Energy Certificates (RECs) within a year to meet the energy demand of VRE-demanding consumers on a balance sheet basis [58]. This is possible because RECs are valid for a year and can be traded separately from the physical electricity feed-in (see EU directive 2009/28/EC [55]). Consequently, consumers cannot know whether they are consuming renewable energy and modify their behavior to satisfy their preference for VRE.

This discrepancy between verified heterogeneous consumer preferences and energy market models, which do not consider them, is criticized in the literature because the energy transition is a social process and a holistic analysis requires the inclusion of social and individual preferences [73, 74, 71, 72]. Narrowing down the literature to auction- and community-based LEMs only one relevant publication can be found, which addresses heterogeneous consumer preferences. Richter et al. introduced a market mechanism that contains separate markets for each energy quality; thereby allowing consumers to purchase electricity with their heterogeneous energy quality preference [71]. This publica-

tion is an important first step but lacks an analysis of the algorithm's efficiency, and a consideration of consumers' WTPP for heterogeneous energy qualities.

Contribution

This section presents an article introducing a library of IMCAs and a new bidding format that allow to integrate and coordinate an increasing number of active consumers and prosumers and consider their heterogeneous energy qualities and preferences. The newly developed set of IMCAs iteratively use a PDA to ensure a verifiable satisfaction of consumer preferences. Consumer preferences are dynamically communicated through an energy quality preference field and the corresponding WTPP in each market bid. Furthermore, the IMCA library consists of two subcategories of market clearing algorithms: the Check and Curtail (CC) and Preference Prioritization (PP). While the PP algorithms are enhancements and variations of the algorithm presented in [71], the CC variant represents an innovative approach to clear heterogeneous consumer preferences without the creation of separate market clearings for each energy quality. Finally, the library also includes combinations of the two subcategories and standard PDAs, which allow to integrate consumers' WTPP.

Since no realistic consumer and prosumer behavior data is available for such a new bidding format and market mechanism, the performance of the IMCA library was evaluated with Monte Carlo simulations and a scalability analysis. Monte Carlo simulations were chosen in this context because they allow to estimate unbiased expected market outcomes such as market prices and volumes within a finite amount of time while data for realistic user behavior is not available for the newly presented market designs.

Based on the Monte Carlo simulation results, we identified a market clearing algorithm that verifiably matches prosumers who supply electricity with a specific energy quality label with consumers who ask for an electricity product with the same attributes, considers consumers' WTPP for heterogeneous electricity qualities, and increases coverage of local demand and local supply compared to conventional LEM models. Furthermore, results from the scalability analysis show that all presented algorithms are capable of matching up to 10,000 market bids on average within less than two minutes.

In conclusion, the paper introduces for the first time a library of auction-based coordination mechanisms that allow consumers and prosumers to become active participants in energy systems and express their heterogeneous energy preferences, to increase local electricity coverage while not significantly affecting social welfare. The presented analyses verify the described benefits and indicate potential for future improvements. Future research should investigate how the library can be used in whole-sale markets with conditional market bids and cross-border trades.

Publication #1: Satisfying user preferences in community-based local energy markets – Auction-based clearing approaches

Authors Michel Zade, Sebastian Dirk Lumpp, Peter Tzscheutschler, Ulrich Wagner

Publication medium Applied Energy, Volume 306, Part A

Digital object identifier https://doi.org/10.1016/j.apenergy.2021.118004

Open-source repository all models and analysis modules are publicly available in the open-source repository *lemlab* [32].

Author contributions

Michel Zade:	65 %	Conceptualization, Methodology, Software, Investigation, Visualization, Writing – original draft, Writing – review & editing.
Sebastian Dirk Lumpp:	15 %	Conceptualization, Software, Resources, Writing – review & editing.
Peter Tzscheutschler:	15 %	Conceptualization, Methodology, Investigation, Writing – review & editing, Project administration, Funding acquisition.
Ulrich Wagner:	5 %	Investigation, Writing – review & editing, Supervision, Funding acquisition.

Applied Energy 306 (2022) 118004

Contents lists available at ScienceDirect

Applied Energy

journal homepage: www.elsevier.com/locate/apenergy

Satisfying user preferences in community-based local energy markets — Auction-based clearing approaches

Michel Zade *, Sebastian Dirk Lumpp, Peter Tzscheutschler, Ulrich Wagner

Technical University of Munich, Arcisstrasse 21, Munich, 80333, Bavaria, Germany

ARTICLE INFO

Keywords:
Local energy market
Heterogeneous energy qualities
Willingness-to-pay a premium
Auction-based clearing
Open-source

ABSTRACT

The advancing energy transition is leading to a constantly increasing number of prosumers and active participants in the energy system. Local energy markets are considered a promising approach to coordinate those active participants efficiently, increase acceptance among the population, and decrease grid expansion costs. However, energy models and markets do not consider heterogeneous user preferences which are considered crucial for the progressing energy transition. Therefore, this paper proposes new auction-based local energy market models that consider user preferences and users' willingness to pay a premium for heterogeneous energy qualities. In order to account for the unknown and stochastic user behavior in such a new market setting, we simulate and compare existing and newly developed auction-based clearing algorithms with an unbiased Monte Carlo method and evaluate whether they fulfill pre-defined key characteristics. Based on the results, we conclude and identify a clearing algorithm that verifiably satisfies user preferences, considers willingness to pay a premium, increases local coverage of electricity, maintains individual rationality, and computational tractability. The presented clearing algorithms enable new market designs that can help to increase acceptance and accelerate the expansion of renewable energies. All market models and simulations are publicly available in the open-source repository *lemlab*. Future research will validate the presented results in a field trial in Germany with 20 households.

1. Introduction

In 2007, authors of the Intergovermental Panel on Climate Change (IPCC) report concluded that a migration to Renewable Energy Sources (RESs) would provide "proven benefits linked with energy access, distributed energy, health, equity and sustainable development" [1]. They further conclude that a Decentralized Energy System (DES) offers advantages such as reduced need of transmission infrastructures, reduced power losses, and a higher share of zero-carbon electricity [1]. In the following years, the installed capacity of RES more than doubled from 1.3 TW to 2.8 TW from 2011 to 2020 [2]. At the same time, the total number of generation units in Germany increased from 1.2 to over 2 million [3,4]. The formerly centralized energy system is continuously being transformed into a decentralized, renewable, volatile, and complex one. This transformation impacts in various ways the energy trilemma of energy security, energy equity, and environmental sustainability [5,6].

In this context, regulators in the European Parliament and the Council of the European Union recognize the potential of an increasing number of prosumers and designed a directive to enable the active participation of individual and grouped prosumers as part of citizen energy communities in electricity and flexibility markets [7,8]. Furthermore, the Australian Energy Security Board pursues reforms that overcome current challenges that hinder an efficient market integration of Distributed Energy Resources (DERs) [9]. Challenges include access barriers to markets, high costs, and static pricing structures. Even though specific regulations are not widespread yet, the aforementioned initiatives and directives indicate a future empowerment of prosumers.

Local Energy Markets (LEMs) are discussed as one possible implementation of a citizen energy community to coordinate the increasing number of DES [10–12]. LEMs are a branch of transactive energy, ideally consider prosumers' perspectives, ensure safe and efficient system operation, reduce grid expansion and transmission costs, and strengthen local communities by enabling prosumers to actively negotiate and trade their energy and flexibility [11–13]. Participants of LEMs can be generators, prosumers, retailers, grid operators, and potentially mediators who serve as intermediaries between them.

In order to describe LEMs in a standardized way, Zhang et al. derived a three dimensional, four-layered architecture that categorizes the relevant spatial, functional, and temporal dimension [14]. The first dimension splits the functionality into a power grid, information and

* Corresponding author.
E-mail address: michel.zade@tum.de (M. Zade).

https://doi.org/10.1016/j.apenergy.2021.118004
Received 2 June 2021; Received in revised form 29 September 2021; Accepted 1 October 2021
Available online 20 October 2021

communication, control, and business layer. The second dimension describes the spatial resolution from a small premise to an entire region, and the third dimension describes the temporal sequence of a LEM. In this paper, we will focus on auction-based market clearing algorithms that take place in a local community and before the energy has been exchanged (ex-ante). Therefore, we will be talking about the pre-exchange time period, the business layer, and premises' market agents in terms of the four-layered architecture.

Despite of the aforementioned description methods, LEMs are nowadays mostly distinguished by their interaction and coordination processes. Coordination processes in LEMs define what kind of information market participants need to exchange and whether mediators or coordinators are involved or not. Generally, we distinguish three coordination types: a centralized/coordinated system in which a coordinator decides and optimizes each participant's device control, a fully decentralized Peer-to-Peer (P2P) system in which all participants communicate directly with each other, and a community-based market where participants communicate pre-defined and limited private information to a market coordinator that returns a price signal [13,15,16]. Centralized implementations have the advantage of considering network constraints but require the disclosure of private information to central entities, and quickly become computationally expensive [12,13]. On the other hand, fully decentralized P2P approaches bear the risk of being inefficient and make it difficult for grid operators to ensure security of supply [13,15,16]. In a community-based market, market participants or their market agents disclose bidding information to a central community platform where the clearing is executed. Thereby, this community platform becomes a potential single point of failure and must be designed and secured accordingly. Even though a community-based market does not offer the same level of data privacy as a full P2P approach, the disclosed information is reduced to a minimum compared to centrally optimizing approaches while allowing grid operators access to the platform in order to ensure system stability. In this paper, we focus on a community-based LEM and explicitly exclude full P2P and centrally optimized approaches. For simplicity, we will abbreviate community LEMs to LEM.

Many papers in the literature use auction-based approaches to trade electricity between multiple buyers and sellers in a LEM [12]. Generally, we distinguish two forms of two-sided auctions: the Continuous Double Auction (CDA) and the Periodic Double Auction (PDA), often called a clearinghouse or call market [17,18]. In both auction types, agents place their bids with a price and a quantity in an order book [18]. In a CDA, the mechanism tries immediately to match the bid with other bids from the order book. This continuous design, however, encourages high frequency trading, and diminishes welfare of "slow" traders [19,20]. Therefore, we consider PDAs, where bids are collected and cleared at predefined intervals, to be better suited for LEMs with non-professional participants and will focus on them for the remainder of the paper.

PDAs are used in stock exchanges, electricity markets, and are considered allocationally efficient mechanisms [18,21]. In this context, a mechanism is "allocationally efficient if those who value the goods most are able to buy them from those who can produce them at the lowest cost" [21]. However, market participants express their valuation in a conventional double auction only through a price that cannot capture participants' differentiated valuation for heterogeneous energy qualities. Therefore, we argue that the definition of allocative efficiency needs to be adapted to auction-based LEMs that incorporate user preferences for heterogeneous energy qualities. Nevertheless, LEMs must adhere to basic market design principals: Individual Rationality (IR), thickness, and tractability [18,22,23]. A LEM is individually rational if market participants receive a non-negative gain from participating, thick if enough supply and demand are brought together, and tractable if executable in a reasonable amount of time. For a more detailed description of those properties, please refer to [18,22,23].

In parallel to the increasing expansion of RES and research interest in LEMs, many studies have investigated consumer preferences based on choice experiments. In choice experiments, participant's are asked to choose between electricity tariffs that contain a variation of different characteristics. Recurring characteristics are location of suppliers (international, national, regional, local), energy generation types (nuclear, renewable, fossil), costs, and reliability of electricity supply. Based on the participant's choices, a WTPP for specific types of electricity is calculated. Even though quantitative results are heavily dependent on the presented choices, the region and demographic background of the participants, qualitative valuations of the participants for certain characteristics can be extracted. Many studies identify the cost of electricity as the decisive characteristic [24,25]. One study concludes that the electricity source is the most important attribute [26], other studies find it in second place [24,25,27]. Regional generation units and headquarters of suppliers are in third position [24,25,28,29]. A WTPP for reliability of electricity supply was not investigated in comparison to other characteristics [30].

While previously mentioned studies identify a WTPP and heterogeneous user preferences for renewable and regional energy generation, only few publications can be found that incorporate those user preferences into their auction-based market designs that are considered crucial for the continuous energy transition [31]. A review conducted in 2018 on LEMs, their interaction types, market clearing approaches, and requirements, found that most auction-based publications have the objective to either maximize social welfare which refers to the sum of consumer and producer surplus or to minimize operational costs [12]. The satisfaction of heterogeneous user preferences or WTPP were not listed as an objective. In 2018, the concept of a Federated Power Plant (FPP) was formulated that may satisfies heterogeneous energy preferences of consumers [10]. More recent publications on auction-based LEMs analyzed whether a PDA can be performed by smart contracts in a blockchain network. Wang et al. Troncia et al. and Zahid et al. implemented and demonstrated the feasibility of a trading and digital certification platform for electricity in smart contracts [32–34]. Oprea et al. implement two different settlement functions in smart contracts and compare their performance in multiple scenarios with each other [35]. Khorasany et al. investigated a two-stage auction design to allow last minute adjustments to schedules and to reduce energy costs [36]. However, only one publication was found that considers heterogeneous user preferences in an auction-based LEM [37]. Richter et al. propose a market mechanism that considers heterogeneous user preferences by creating separate markets for separate preferences [37]. Even though this publication is an important first step, it lacks an analysis of the algorithm's efficiency, and the consideration of participants' WTPP for heterogeneous energy qualities.

Therefore, we present six alternative auction-based LEM algorithms that satisfy user preferences and consider WTPP for heterogeneous energy qualities. In order to analyze and objectively compare the core characteristics of the different LEM algorithms and due to the lack of realistic user data, we present the results of a Monte Carlo simulation. The evaluated characteristics are: how efficient the algorithms are compared to conventional ones, whether they are individual rational, verifiably satisfy user preferences, consider WTPP, maximize local electricity coverage, and tractability.

The rest of the paper is organized as follows. Section 2 describes a standard PDA and presents six alternative auction-based LEM algorithms. Section 3 explains the setup of the Monte Carlo simulation and the computed results. A thorough discussion and comparison of the developed algorithms is provided in Section 3.2. Section 4 concludes the paper.

2. Auction-based clearing algorithms for local energy markets

This section describes auction-based clearing algorithms for LEMs that we found in the literature and developed ourselves in order to

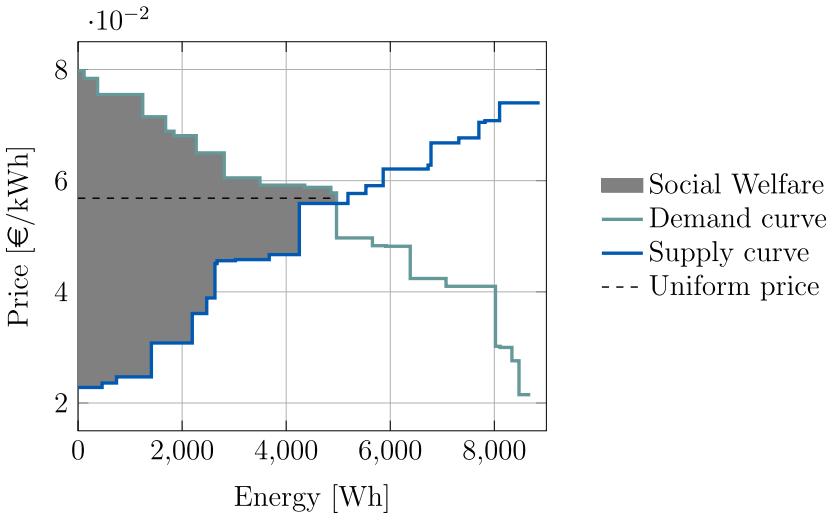

Fig. 1. Graphical visualization of a double auction. With the utilities of the interested buyers and marginal costs of the suppliers of electricity. The shaded area represents the social welfare and the dashed line the uniform market clearing price.

Table 1
Bidding format of a LEM that incorporates heterogeneous user preferences and WTPP. This format is publicly available in the open-source project *lemlab* [38].

Parameter	Description
id_{user}	User identification number or string
qty_{energy}	Quantity of energy a user would like to ask or buy for
$price_{\text{energy}}$	Price a user is willing to sell or buy for
$quality_{\text{energy}}$	Quality (preference) label a user is offering/asking for
$wtpp_{\text{quality}}$	Willingness to pay a premium for energy if a certain quality is supplied
$type_{\text{bid}}$	Bid type (e.g. ask or buy)
ts_{delivery}	Timestamp of delivered energy quantity
n_{position}	Bid number for a user who wants to place multiple bids for one timestamp

satisfy heterogeneous user preferences, users' WTPP, and to increase coverage of local demand and local supply. Section 2.1 starts by outlining the bidding format. Section 2.2 provides an overview of a standard PDA with additional features for non-professional traders such as prosumers. Section 2.3 describes basic Iterative Market Clearing Algorithms (IMCAs). Finally, Section 2.4 describes combinations of IMCA and how a WTPP is considered in them. The presented clearing algorithms are publicly available as part of an open-source project [38].

2.1. Bidding format

A key component of a LEM is the market mechanism and the corresponding bidding format [11]. The bidding format describes what kind information participants need to exchange with a trading platform in order to express a willingness to trade. In a conventional electricity market, this exchanged information is called a bid with a buy or an ask price and an energy quantity. A buy price refers to an electricity demand by the participant and an ask price to the supply of electricity. On the trading platform, all placed bids are stored in an order book.

In our special case of LEMs, conventional bidding formats are expanded to incorporate heterogeneous user preferences and their WTPP. Therefore, Table 1 summarizes not only parameters for a conventional PDA but also for alternative market models presented later in this paper that incorporate heterogeneous user preferences and WTPP.

Whereas parameters such as id_{user}, qty_{energy}, and $price_{\text{energy}}$ are self-explanatory, the remaining parameters require further elaboration. $quality_{\text{energy}}$ refers to a quality label a prosumer can give his bid, if it fulfills certain pre-defined characteristics. Characteristics can be that the electricity is produced within a certain region, from a certain generation type, or without the use of fossil fuels. The same parameter can however also be used by buyers to express their preference for a specific electricity quality. $wtpp$ is a parameter that represents the user's willingness to pay a price premium if the market mechanism can ensure the satisfaction of the bidder's transmitted quality preference. A WTPP can be expressed in absolute values or in percent of the price a user is willing to pay for electricity ($price_{\text{energy}}$). $type_{\text{position}}$ is a flag that indicates whether it is an ask or a buy bid. In some implementations this indication can be omitted because a plus or minus in front of the communicated $price_{\text{energy}}$ indicates buy and ask bids. ts_{delivery} defines the starting point of the delivery period of electricity. If the market mechanism operates at quarter-hourly intervals and accepts bids 24 h in advance, prosumers can place bids for any of the 96 delivery periods. Finally, n_{position} represents the bid number of a user for a certain delivery period on the platform. The idea is that a user can place multiple, independent bids on the platform with potentially varying energy quantities and prices in order to account for uncertainties or probabilistic forecasts.

After defining the bidding format, the subsequent sections will describe the already existing and newly developed market mechanisms for satisfying user preferences in LEMs.

2.2. Periodic double auction

Double auctions have been used in the last 100 years throughout the world to trade stocks, electricity and other homogeneous products. Even though double auctions achieve very efficient allocations and prices, a theoretical explanation is missing [17,18]. Nevertheless, a commonly used measure of efficient allocation is social welfare. Mathematically, social welfare is formulated by the sum of the bidders' utility minus the sum of producers' costs [12]. The goal of a PDA is to maximize social welfare (see Eq. (A.1)). A utility function maps an agent's level of interest for a certain state to real numbers [18]. In PDAs, bidders express their utilities and costs for electricity via a price (see $price_{\text{energy}}$ in Table 1). Geometrically, social welfare is the area surrounded by the demand and supply curve and the price axis (see shaded area in Fig. 1) [39]. A mathematical formulation of the PDA clearing algorithm is provided in (A.1).

In PDAs, bids are collected in an order book. At clearing time, all buy bids are sorted by price from biggest to lowest and ask bids from lowest to highest. All bids where the buy price exceeds or equals the ask price are matched. If all buy prices are above the offer prices, all bids are matched that fulfill the market clearance condition (supply energy quantity equals demand energy quantity). In a final step, the

clearing prices are calculated. Here, multiple calculation methods can be used such as uniform, discriminatory, or discriminatory midpoint pricing [39]. For simplicity we will only use uniform prices throughout this paper. A graphical visualization of demand and supply curve, social welfare, and uniform prices is shown in Fig. 1.

For LEMs and non-professional participants, we inserted a shuffling of bids before the sorting in order to further discourage high frequency trading and ensure that bidders are not penalized for a slower internet connection.

This market mechanism ensures a competitive equilibrium in which agents prefer their allocation over any other allocation, supplied and demanded electricity are equal, and participants receive non-negative gains (IR). What this mechanism does not reflect, are the users' heterogeneous user preferences for certain electricity qualities. Therefore, we will introduce alternative auction-based clearing algorithms in the following subsections that verifiably satisfy heterogeneous user preferences and incorporate WTPP.

2.3. Iterative market clearing algorithms

Since PDAs do not consider any form of heterogeneous preferences, we introduce one existing and three newly developed IMCAs that verifiably satisfy heterogeneous user preferences. Preferences refer to the parameter $quality_{\text{energy}}$ in a LEM bid (see bidding format in Table 1).

2.3.1. Check and curtail

In order to verifiably satisfy heterogeneous user preferences, we present one variant that clears a PDA, checks whether all buyer preferences are satisfied by matched ask bids, and potentially curtails unsatisfied buy bids before re-initiating the entire process. Hence, we call this variant the Check and Curtail clearing algorithm (CC). This algorithm starts by computing a PDA independent of any energy qualities and preferences. Then, the algorithm checks whether the preferences of all buy bids are satisfied by all cleared ask bids. If that is the case, the algorithm is done within one iteration. However, if not all buy bids can be satisfied with the cleared ask bids, the algorithm curtails the lowest priced buy bids that could not be satisfied. After curtailing unsatisfied bids, the algorithm re-initiates a PDA without curtailed buy bids. Curtailed bids are then excluded from this CC clearing but market agents can place the same or altered bids in consecutive clearings for the same time of delivery. This process continues until all cleared buy bids are verifiably satisfied by cleared ask bids. A mathematical formulation of the CC clearing algorithm is provided in Appendix A.2. Fig. 2 visualizes the algorithm as a flowchart.

Optionally, the algorithm can consider a quality order that can "assign" higher energy qualities to lower energy preferences. This is possible if the quality order is designed so that higher energy qualities include their lower ones (e.g. na, local, local-green). Otherwise, the algorithm could not label buy preferences for local energy as satisfied even if there exists excess local-green electricity on the market because local-green would represent a separate energy quality.

The CC algorithm is implemented in a while-loop since it cannot be foreseen how many iterations it will take to satisfy all cleared buy bids. Potentially, the algorithm does not find a solution because bid curtailment ultimately leads to a steeper demand curve, which leads to a smaller possible market volume and fewer ask bids that can satisfy bidders' preferences. A maximum number of iterations or execution time can be defined to limit computational costs (see $n_{\text{max,iterations}}$ in Fig. 2). This number should be chosen heuristically based on expected traded energy quantities and market granularity.

In conclusion, this IMCA variant ensures that bidders' preferences are satisfied by cleared ask bids. However, the algorithm's computational costs can vary significantly and potentially does not find a solution at all. Therefore, the next subsection introduces three alternative clearing algorithms that can satisfy heterogeneous user preferences with reduced and foreseeable computational costs.

2.3.2. Preference prioritization

Preference Prioritization clearing algorithms (PP) describe a subset of IMCAs that compute a PDA for each energy quality and preference. Hence, PP clearings compute as many PDAs as there are energy qualities ($n_{\text{qualities}}$). In this paper, we propose and analyze three PP variants. The variants differ in the sequence of market clearing of the heterogeneous energy classes (prioritization) and whether they consider uncleared bids in subsequent clearings. Fig. 3 visualizes the general structure of a PP clearing as a flowchart.

First, buy and ask bids are extracted by quality. Which of the qualities are extracted first and last differs by variant. Then, a PDA computes the matched bids and calculates a market clearing price. Optionally, uncleared buy bids can be reinserted into subsequent clearing rounds (see paragraph). A PP clearing is done when one PDA was computed for every electricity quality. This algorithm calculates for every energy

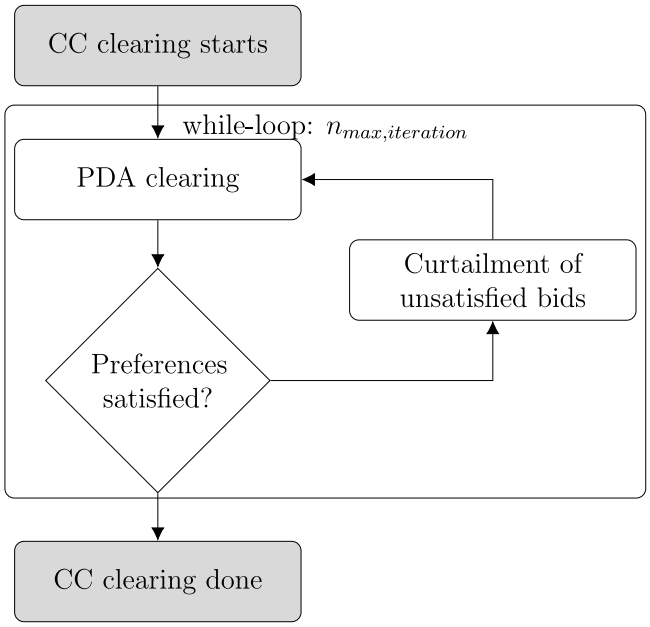

Fig. 2. Flowchart of the CC clearing algorithm. PDA clearing refers to a periodic double auction (see Section 2.2).

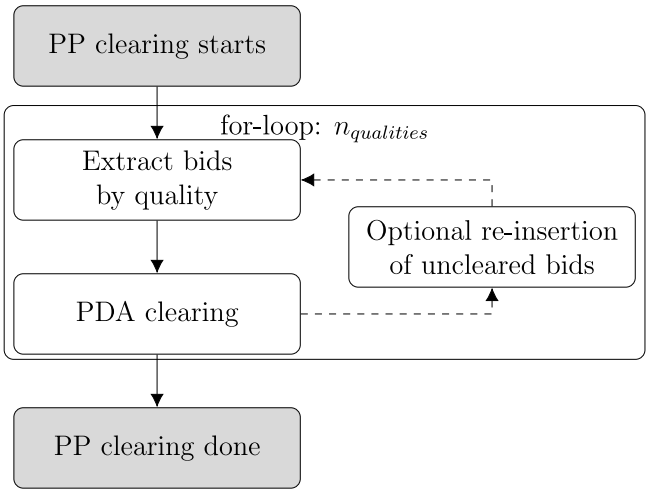

Fig. 3. Flowchart of the preference prioritization clearing algorithm.

quality preference a specific clearing price and thereby uses discriminatory prices. A mathematical formulation of the PP clearing algorithm is provided in Appendix A.3. The following paragraphs describe the specific characteristics of the three variants.

Preference separation. Richter and others introduced an auction-based market clearing that treats separate energy qualities and preferences as different goods [37]. This variant matches offers of a certain energy quality with bids that explicitly ask for this energy quality. The order of PDA executions does not change the outcome of the clearing algorithm because all energy qualities are treated independent of each other. Uncleared bids are not reinserted in subsequent clearing iterations. We call this variant the Preference Separation clearing algorithm (SEP).

This approach ensures that consumers are only matched with producers that fulfill their exact preference. However, this approach does not allow consumers who ask for local energy to be matched with producers who offer local & green energy because this quality potentially is offered only in a separate clearing iteration. Therefore, we potentially not match a significant amount of buy bids that could have been matched while still satisfying the consumers' preferences. Hence, we introduce two alternative variants that are able to incorporate ask bids of higher qualities into clearings for lower preferences.

Highest-to-lowest preference. Since SEPs potentially compute inefficient allocations of heterogeneous bids, we present the Highest-to-Lowest clearing algorithm (H2L) that performs $n_{\text{qualities}}$ PDAs and allows the reinsertion of uncleared ask bids of higher qualities into clearings for lower user preferences. This variant clears the highest energy preferences first and the lowest ones last.

In a first step, the algorithm computes a PDA for ask and buy bids with the highest energy quality. In the second iteration, unmatched ask bids of the highest energy quality and ask bids of the second-highest energy quality are matched with buy bids that request the second highest energy preference. This is possible if the quality order is designed so that higher energy qualities include their lower ones (e.g. none, local, local-green). Unmatched buy bids with the highest energy preference cannot be reinserted because their preference satisfaction cannot be ensured since ask bids of lower quality are included. This procedure continues until a clearing for the lowest energy quality is computed. Due to the reinsertion of unmatched ask bids of higher quality in subsequent clearing iterations, this variant matches ask bids of higher energy quality more often than ask bids with lower qualities and therefore prioritizes higher energy qualities.

This approach ensures that consumers are supplied with energy that fulfills or exceeds buyers communicated preferences and therefore leads to more efficient allocations of buy and ask bids. However, this variant potentially matches a buyer that places a buy bid for a specific quality of energy with a lower price than a buyer that placed a buy bid for any kind of energy with a high price because higher energy qualities are cleared before lower ones are. In order to prevent this aforementioned case, the following paragraph describes a third variant that flips the order of clearing executions.

Lowest-to-highest preference. Since the H2L variant potentially clears buyers that request higher energy qualities with a lower price than buyers who ask for lower energy qualities, we introduce the third PP variant Lowest-to-Highest clearing algorithm (L2H). This third variant computes consecutive PDAs starting with the lowest buyers' preference and concluding with the highest and inserts ask bids of higher qualities into clearings for lower preferences.

In the first iteration, the algorithm matches buy bids that request the lowest energy quality with all available ask bids. This is possible if the quality order is designed so that higher energy qualities include their lower ones (e.g. none, local, local-green). Therefore, consumers do not experience any disadvantage if they are matched with ask bids of higher quality. The second round will then consider buy bids of the second-lowest preference and match them with all remaining ask bids that fulfill or exceed the second-lowest energy quality. This procedure continues for all energy qualities and preferences until the highest energy quality is cleared.

This variant ensures that consumers are supplied with energy that fulfills or exceeds buyers' communicated preferences and a buyer that asks for any kind of energy will be matched more likely than a buyer that asks for a specific higher type. This variant prioritizes buy bids that ask for lower energy qualities because they are cleared with the maximum number of ask bids and ask bids of higher qualities because they are reinserted in multiple clearings for lower preferences.

2.4. Combining iterative market clearing algorithms

All of the presented IMCA in Section 2.3 satisfy verifiably heterogeneous user preferences. However, one variant potentially does not find a solution (CC) and none of the presented algorithms consider a WTPP. Therefore, we investigated multiple combinations of the previously mentioned clearing algorithms that compensate the drawbacks of the single IMCA and incorporate users' WTPP for heterogeneous energy qualities. Here, we present two of the most promising combinations. Interested readers may refer to [38] for all investigated combinations.

2.4.1. Matching curtailed bids

One major drawback of the CC clearing algorithm is that potentially no matching is possible because no PDA satisfies the cleared buyer bids or the computational costs are too high to find a feasible solution. In those cases, curtailed and uncleared bids can be re-inserted in a consecutive PP clearing variant.

Hence, we propose a combination of a CC and a H2L clearing. We call this variant Check and Curtail combined with Highest-to-Lowest clearing algorithm (CC-H2L). First, a CC clearing is performed, once this algorithm ends, all uncleared and curtailed bids are reinserted in a consecutive H2L clearing. This only makes sense if uncleared ask bids request a lower price than uncleared and curtailed buy bids.

This combination allows suppliers and buyers to be matched even though the CC did not match them or did not find a feasible solution in a given number of iterations or period of time. All other characteristics that were described above for the CC and H2L remain true for the combination of the two.

2.4.2. Integrating willingness-to-pay a premium

A WTPP for certain types of energy qualities are expressed in the literature mostly as some percentage of some reference cost (see Section 1). So far, the presented IMCA did not consider any kind of WTPP for a certain type of electricity. They would either satisfy the bids and their corresponding preferences by the available ask bids or leave buy bids uncleared.

Consumers can communicate their WTPP for certain energy qualities via the parameter $wtpp_{\text{quality}}$ (see Table 1). By doing so, they express their willingness to pay a price premium if they can be ensured, that they are matched with ask bids that fulfill their energy preference. If they cannot be ensured to be matched with their preferred energy quality, then only their regular $price_{\text{energy}}$ is valid.

On the market platform, buy bids are first inserted with their specified preferences and their WTPP into an IMCA which ensures consumers' preference satisfaction. In a second phase of the clearing, buy and ask bids that are not cleared in the IMCA are then inserted into a PDA. In this second phase, no WTPP are considered since it cannot be ensured that bidders will be supplied with their preferred type of electricity. With this combination, bidders' preferences can verifiably be satisfied and their WTPP for a specific energy quality can be considered.

As discussed in the beginning of this subsection, we will present the results of the most promising combination (Check and Curtail combined with Highest-to-Lowest and Periodic Double Auction clearing algorithm (CC-H2L-PDA)).

The key characteristics of the proposed market clearing algorithms are further analyzed and discussed in the following sections.

3. Analyzing of clearing algorithms for local energy markets

In this section, we evaluate the performance of the presented clearing algorithms. Therefore, we formulate key properties a LEM for non-professional participants should possess. A LEM should:

1. verifiably satisfy heterogeneous user preferences for different electricity qualities,
2. incorporate users' WTPP for specific energy qualities,
3. increase coverage of local demand and local supply,
4. motivate investments in high energy qualities,
5. be individually rational, and
6. be tractable.

A LEM verifiably satisfies heterogeneous user preferences when the market matches supplier and buyer bids so that buyers' preferences are fulfilled in quantity and quality. In order to incorporate a WTPP, a LEM needs to ensure that the WTPP is only applied if the market can supply the buyer with the requested electricity quality. Furthermore, it is desirable that the LEM increases the quantities exchanged within the community and decreases its energy exchange with non-local participants. In order to motivate participants to invest in generation units that produce electricity of higher quality (e.g., wind turbines), a LEM should not price local electricity qualities lower than non-local ones. Finally, basic design principals such as IR and tractability should be met.

After defining those key characteristic, a proper analysis method must allow an unbiased analysis of them. Many publications use case studies as a method to demonstrate certain characteristics of new market designs (see [37,39,40]). Even though the results and conclusions drawn are heavily dependent on the design of the case studies, this makes sense in settings where input data can be easily modeled or was collected in previous field trials. In our case, we introduce a new market design and a new bidding format that require user input that is difficult to model and has not been collected in field trials in the past. Furthermore, modeled input data would influence the outcomes of the clearing algorithms so that an unbiased analysis is not possible.

Another approach to estimate outcomes of models whose input parameters are unknown and all possible input variations cannot be executed in a feasible amount of time is the Monte Carlo method [41]. There, we approximate deterministic quantities such as cleared market volumes or market clearing prices by an average of random values that are computed in simulations with independent and identically distributed (i.i.d.) random input data. This is possible because the Strong Law of Large Numbers (SLLN) is at the core of the Monte Carlo method and states that the average of the randomly computed outcomes becomes equal to the expected value if the number of simulations (N) goes to infinity (inf). In order to reach "good approximations" of the expected value in a finite amount of time, the number of simulations can be calculated (see Appendix B.3) [41,42].

In the past, Monte Carlo methods have been used in energy related research to model stochastic processes. Hardi modeled the energy demand of last mile deliveries and used Monte Carlo simulations to model stochastic drop-off locations [43]. Other publications use Monte Carlo simulations to incorporate the uncertainty of electricity demand, solar, and wind energy availability [44,45]. Nikmehr et al. use Monte Carlo simulations to model uncertain behavior of DES [46].

With this in mind, we find Monte Carlo simulations an appropriate method to model stochastic input data to LEM, objectively evaluate the newly presented clearing algorithms, and their key characteristics. The setup of the Monte Carlo simulations with a description of the input data, extracted key parameters, necessary number of simulations, and computing environment can be found in Appendix B. The results are summarized in the following subsections.

3.1. Results

This section visualizes and describes the results of the Monte Carlo method. The 10,000 simulations of the seven clearing algorithms were computed in approximately 7 h. Based on the calculation of the necessary simulations in the previous section, we consider our results robust and stable.

3.1.1. Cleared energy quantities, prices, and welfare

Fig. 4 shows the average cleared energy quantity, price, and welfare for each clearing algorithm. Dashed lines indicate the reference lines of the PDA clearing algorithm. In the following paragraphs, each plot is described separately.

Cleared energy quantities. The cleared energy quantities vary from −8.8 % to 36.4 % compared to the standard PDA. The standard PDA clears on average approximately 23.7 kWh. Whereas SEP and L2H clear slightly less energy with 23.3 kWh and 23.5 kWh, the H2L algorithm clears slightly more energy with 24.2 kWh. CC clears the least energy with only 21.6 kWh. This can be explained by the curtailment of unsatisfied buy bids if they cannot be fulfilled. Additionally, the algorithm does not clear any bids if the maximum number of iterations is reached. CC-H2L clears 25 kWh which is an increase of 5.4 % compared to the PDA. If we add price premiums with the CC-H2L-PDA, the algorithm clears 32.3 kWh which is an increase of 36.4 % compared to the standard PDA. The latter two clearing algorithms, CC-H2L and CC-H2L-PDA, benefit from the combination of complementary clearing methods that increases the total amount of cleared energy on the LEM.

Clearing prices. The clearing prices vary from −9 % to 12 % compared to the standard PDA. The standard PDA and the SEP algorithm clears the energy on average for 0.05 $\frac{e}{\text{kWh}}$. This clearing price corresponds to the mean of the lower and upper bounds of the energy prices set in Table B.3. H2L and CC-H2L calculate a clearing price that is slightly below the PDA prices with 0.049 $\frac{e}{\text{kWh}}$. CC and L2H clear the market at 0.048 $\frac{e}{\text{kWh}}$ and 0.046 e/kWh respectively. The CC algorithm curtails the lowest cleared buy bids if they cannot be satisfied, thereby increases the slope of the demand curve, and ultimately leads to lower clearing prices. The L2H computes the lowest clearing prices because it considers all ask bids in the first clearing iteration and thereby computes the least increasing supply curve. CC-H2L-PDA clears the energy on average for the highest cost with 0.056 $\frac{e}{\text{kWh}}$ which corresponds to a 12 % increase compared to the PDA. This price increase is a direct consequence of the incorporation of WTPP for heterogeneous electricity qualities in the CC-H2L-PDA.

Welfare. Welfare is the sum of consumer and producer surplus. In a PDA this value can be visualized as the area surrounded by the price axis, the demand, and supply curve (see Fig. 1). In the case of IMCA, the welfare is calculated as the sum of the single welfares computed in each clearing execution. Among the seven clearing algorithms, the welfare varies from −17 % to 74 %. Clearing algorithms PDA, SEP, H2L, and CC-H2L all calculate a similar welfare in the range from 0.68 € to 0.7 €. L2H and CC calculate a welfare of 0.58 € and 0.61 €, which corresponds to −17 % compared to the PDA results. This decrease of welfare can be explained by the curtailment of unsatisfied buy bids in the case of CC and by not efficient allocations in the case of L2H. Due to the consideration of WTPP, the CC-H2L-PDA reaches the highest welfare of 1.22 € which corresponds to an increase of 74 %.

After having summarized the overall results of the clearing algorithms, the following subsections illustrate how many shares of specific heterogeneous electricity qualities and user preferences are cleared and what clearing prices were computed for each electricity quality.

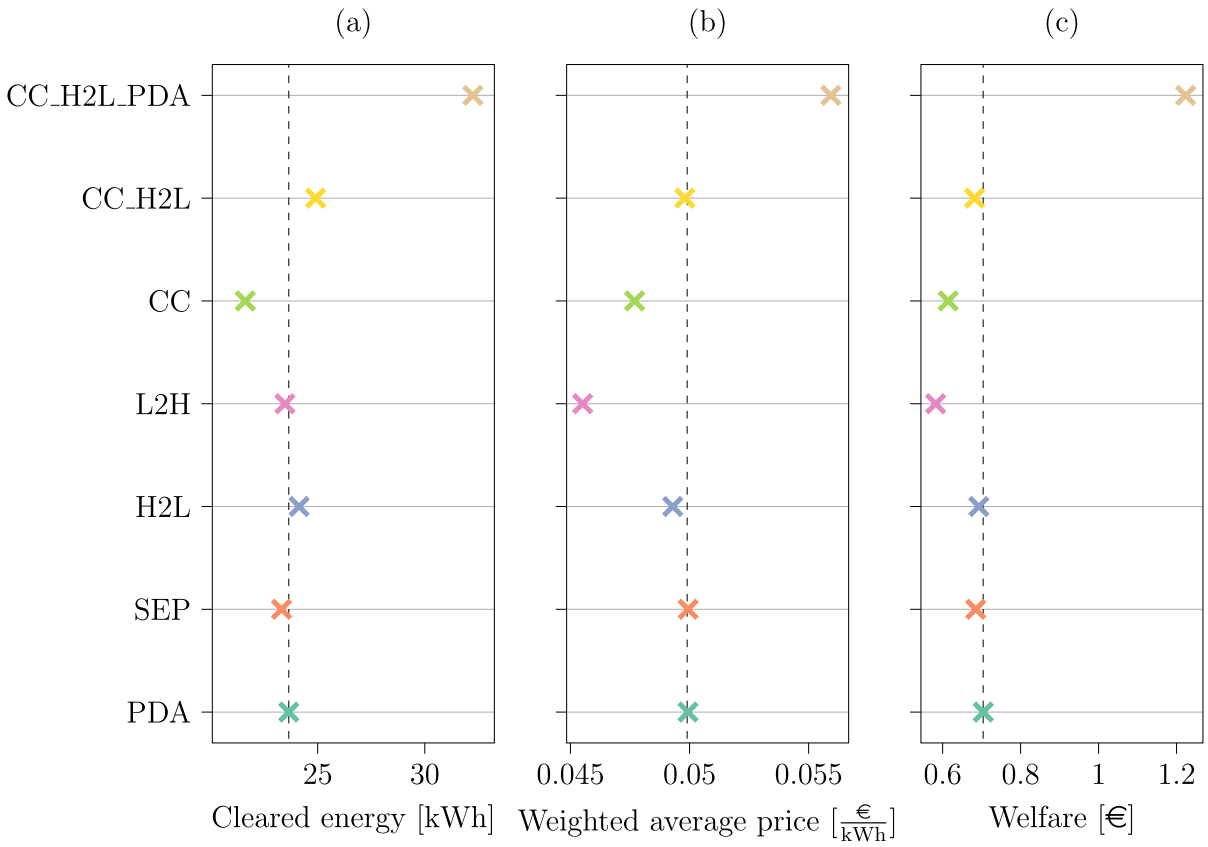

Fig. 4. Monte Carlo simulation results for cleared energy quantities, clearing prices and welfare for each one of the seven clearing algorithms. Markers indicate the mean within a 99 % CI.

3.1.2. Cleared energy qualities

Fig. 5 shows the shares of cleared ask bids with a specific quality label for each clearing algorithm.

The algorithms PDA, SEP, and CC clear each quality with an equal probability of 33.3 %. Algorithms H2L, L2H, CC-H2L and CC-H2L-PDA clear ask bids of higher qualities more often than the ones of lower qualities. The range varies from the lowest to the highest qualities from 16.7 % to 49.8 %.

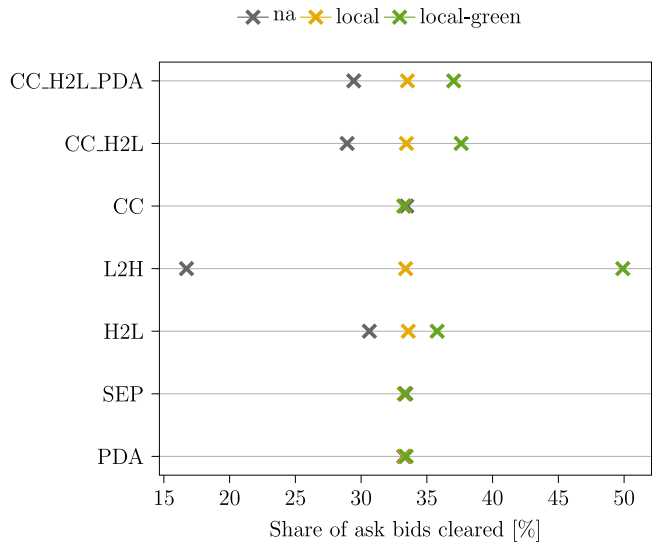

Fig. 5. Shares of ask bids cleared with a specific quality label. Marker represent the mean with a CI of 99 %. Each row represents one clearing algorithm.

Whereas the results of the H2L, CC-H2L and CC-H2L-PDA only vary from 28.9 % to 37.6 %, the greatest difference is recognizable in the results of the L2H algorithm. The L2H approach starts by clearing buy bids with the lowest energy preference with all available ask bids. This is possible because ask bids with higher energy qualities satisfy lower energy preferences. In the second round, buy bids with the second-lowest preferences are cleared with all remaining ask bids that fulfill the preference requirement or exceed them. This procedure continues until all types of bid preferences are cleared. Therefore, ask bids with high energy qualities are cleared more often than ask bids of lower qualities.

The H2L algorithm clears first buy bids with the highest energy preference and ask bids that fulfill this requirement. Then, bids with the second-highest energy preference are cleared with ask bids that fulfill this requirement and the ones that were not cleared in the first iteration (see Section 2). Therefore, ask bids of higher energy qualities also have multiple chances of being cleared in subsequent clearings. The CC-H2L, and CC-H2L-PDA algorithms are a combination of the aforementioned algorithms and therefore inherit their characteristics.

In summary, the clearing algorithms H2L, L2H, CC-H2L, and CC-H2L-PDA clear ask bids of higher energy qualities more often than ask bids of lower quality. In the next section, we analyze the cleared buy bids.

3.1.3. Cleared user preferences

Fig. 6 shows the shares of buy bids cleared with a specific preference from each clearing algorithm. PDA and SEP clear all preferences with equal probabilities since those algorithms treat all energy preferences equally. All other algorithms clear bids with lower ranked energy preferences more often than bids with higher ranked preferences. However, the value ranges vary significantly between the clearing algorithms.

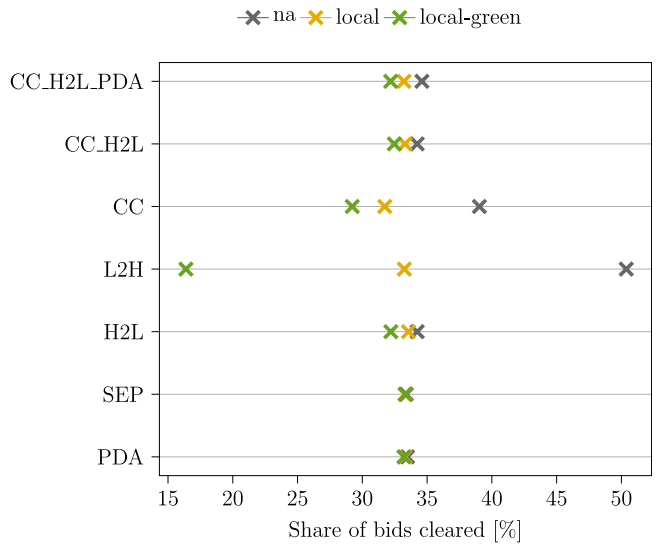

Fig. 6. Shares of buy bids cleared with a certain energy preference. Markers indicate the mean within a 99 % CI. Each row represents one clearing algorithm.

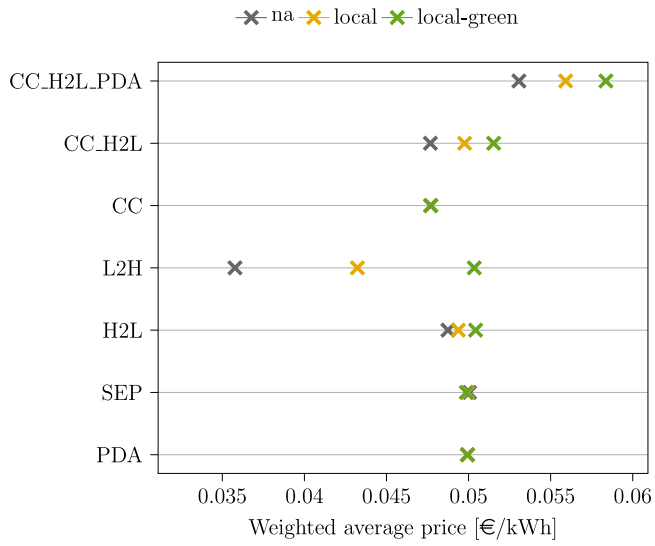

Fig. 7. Weighted average clearing prices per clearing algorithm and quality. Markers represent the means with a CI of 99 %. Each row represents one clearing algorithm.

The markers for the PDA and SEP algorithm are stacked on top of each other and show that all buy bids are cleared with an equal probability of 33.3 % independent of their preferences. Clearing algorithm H2L, CC-H2L, and CC-H2L-PDA indicate that buy bids with higher energy preferences are cleared slightly less often compared to buy bids with lower preferences. The ranges vary from 32.2 % to 34.2 %. Clearing algorithms, L2H and CC, amplify this behavior significantly. Buy bids that ask for local-green energy have a probability of only 16.4 % whereas buyer who do not care about their energy quality would be matched 2 times more often. This happens because the clearing algorithm starts to match the bids with the lowest preferences first with all available ask bids. Buy bids with higher preferences are only cleared in subsequent steps with the remaining uncleared ask bids. The CC algorithm shows a similar behavior. However, the range varies only from 29.2 % to 39.1 %. This behavior is the consequence of the curtailment of unsatisfied buy bids in the CC algorithm.

3.1.4. Prices of cleared energy qualities

Fig. 7 visualizes the weighted average clearing prices for each clearing algorithm and energy quality. The clearing prices for different energy qualities are the same at 0.05 $\frac{€}{\text{kWh}}$ for the PDA and SEP algorithms. Clearing algorithm CC computes a slightly lower clearing price of 0.048 $\frac{€}{\text{kWh}}$ because unsatisfied bids are curtailed and the downwards slope of the demand curve increases which leads to slightly lower clearing prices. H2L, L2H, CC-H2L, and CC-H2L-PDA algorithms show a price increase with the rank of energy quality. However, the value ranges in which the prices rise vary significantly.

In the H2L and CC-H2L clearing algorithms, clearing prices for the lowest to the highest energy quality vary from 0.048 €/kWh to 0.052 €/kWh. This range corresponds to a price difference of ±4 % compared to the PDA clearing prices. Clearing prices of the CC-H2L-PDA algorithm show an increase due to the incorporation of price premiums. The range is slightly larger and goes from 0.053 €/kWh to 0.058 €/kWh. These results can be explained by the H2L algorithm that clears ask bids of higher quality with a higher price because of limited ask bids that can satisfy preferences of the higher quality. Ask bids with the lowest quality are cleared with the lowest prices of approximately 0.036 €/kWh in the L2H algorithm. This happens because ask bids with the lowest energy quality are cleared only in one clearing iteration in which all ask bids are also included, and thereby the supply curve has the least increasing slope. Clearing prices from the L2H clearing vary from 0.036 €/kWh to 0.05 €/kWh.

The next section will discuss the implications of those results, their limitations, and whether the initially formulated key characteristics can be met.

3.2. Discussion

At the beginning of this section we formulated key requirements a LEM should satisfy. In this subsection, we discuss whether the presented clearing algorithms can fulfill those key requirements, what the results of the Monte Carlo method imply, and what the results' limits are.

Two of the reasons for introducing LEMs are the satisfaction of user preferences and the consideration of WTPP (see Section 1). All of the presented IMCA verifiably satisfy user preferences due to their market design. WTPP for heterogeneous energy qualities are considered only in the CC-H2L-PDA algorithm. However, the same method of applying WTPP in a first stage and then clearing a PDA without them in a second stage 2.4.2, can be applied to any of the presented LEM clearing algorithms that verifiably satisfy user preferences. From all investigated combinations presented in this paper and in *lemlab*, the CC-H2L-PDA algorithm showed the best performance.

Another goal is to increase coverage of local demand and local supply of electricity. The results of the Monte Carlo method showed that H2L, L2H, CC-H2L, and CC-H2L-PDA algorithms clear offers of higher energy qualities more often than those of lower qualities. Higher qualities refer, in our simulations, to local and local-green electricity generation (see Appendix B). Hence, the aforementioned algorithms increase the coverage of local demand and supply compared to conventional PDAs, whereas PDA, SEP and CC algorithms clear all qualities equally. Therefore, market designers should choose a LEM algorithm that contains the H2L or L2H method, in order to increase coverage of local supply and demand of electricity.

Price results showed that H2L, L2H, CC-H2L, and CC-H2L-PDA algorithms calculate a higher clearing price for higher energy qualities than for lower ones. On the one hand, this characteristic motivates suppliers to invest in new generation units that generate electricity of higher qualities. On the other hand, some user behavior studies have shown that electricity prices are the most decisive selection criterion for consumers [24,25]. Therefore, price spreads between electricity qualities and realistic user behavior need to be investigated further.

One of the basic design rules is that a market needs to provide non-negative gains to its participants and thereby be individually rational [22,23]. All of our clearing algorithms fulfill this requirement

because the double auction mechanism is at the core of all presented algorithms.

A LEM is a real world application that must be tractable for small communities in a finite amount of time. From the presented market clearing algorithms, the PDA is the computationally cheapest option. A single clearing for a PDA with 200 random market bids takes approximately $t_{PDA} = 0.1$ s on an Intel(R) Core(TM) i7-8550U. The execution time for PP and CC algorithms can be calculated by Eq. (1) and (2).

$$t_{\mathrm{PP}} = n_{\mathrm{qualities}} \times t_{\mathrm{PDA}} \tag{1}$$

$$t_{\mathrm{CC}} = [t_{\mathrm{PDA}}, n_{\mathrm{max,iterations}} \times t_{\mathrm{PDA}}] \tag{2}$$

$n_{\mathrm{qualities}}$ is the number of distinct electricity qualities and $n_{\mathrm{max,iterations}}$ the maximal number of while-loop iterations in the CC clearing algorithm. Whereas the execution times of the PDA and PP clearing algorithms are rather insignificant compared to the current time granularity of 15 min in electricity markets, the execution time of CC algorithms potentially is more critical. Due to the iterative while-loop design, the algorithm's execution time cannot be precisely calculated. Only a time range with a lower and upper bound can be provided. Hence, the choice of $n_{\mathrm{max,iterations}}$ becomes a critical design decision due to its direct impact on the upper bound of execution time. Additionally, the pure CC algorithm does not clear any bids if the maximum number of iterations are reached. Therefore, we declare the pure CC algorithm as potentially intractable for LEMs.

In order to evaluate the scalability of our newly developed clearing algorithms, we computed a time complexity analysis and summarized the results in Appendix C. For 10,000 bids the computationally most expensive clearing algorithm consumes on average only 2 min. Hence, we assume our clearing algorithms to be scalable for the use case of LEMs that trade quarter-hourly. More importantly, the time complexity results of all presented clearing algorithms are subject to a linear growth rate. Furthermore, we want to point out that our clearing algorithms do not contain non-deterministic functions and are therefore reproducible.

Another important property of clearing algorithms is which buy bids they clear more often. The iterative clearing algorithms clear buy bids with lower energy preferences more often than those with higher preferences. This happens because buy bids that request higher energy qualities have a more restricted pool of possible ask bids to be matched with. Therefore, a clearing algorithm that considers different electricity qualities ultimately clears buy bids with preferences for higher electricity qualities less often. However, the results in 6 indicate that the impact is not as significant in the H2L as in the L2H. In order not to motivate buyer to continuously ask for lower energy qualities, market designers should pay attention to this characteristic.

An essential part of the PP clearing algorithms is the order of energy qualities. In this paper we used the order na, local, local-green, which is convenient for a LEM. Nevertheless, the market models and their designs can be used for other commodities (e.g. heat) with similar characteristics (interchangeable but heterogeneous) as well. However, the definition of adequate quality/preference orders that are accepted by all market participants potentially remains a challenge. A democratic method to define this order was proposed using a Borda Count Scores [37].

In summary, the CC-H2L-PDA algorithm fulfills all of the formulated key characteristics. The algorithm verifiably satisfies heterogeneous user preferences, incorporates users' WTPP, increases local coverage of electricity, is individually rational, and tractable. The other presented algorithms were important intermediary market designs but lack the overall performance of the CC-H2L-PDA.

Table 2 summarizes the most important properties of the simulated clearing algorithms.

The results presented in this section are computed with i.i.d. random input data with the Monte Carlo method and allow an objective and unbiased comparison of the clearing algorithms' key features. This approach was used in order to incorporate the so far unknown and stochastic user behavior in such a new LEM design. Hence, we assume the Monte Carlo method to be currently the best approach to analyze the algorithms' key features. Once user behavior data for such a LEM design becomes available or can be appropriately modeled, case studies can be conducted to evaluate the performance of the clearing algorithms. Nevertheless, the newly designed bidding format and auction-based market clearing algorithms are ready to be used for real world implementations of local energy markets and allow to verifiably satisfy heterogeneous user preferences and users' WTPP. Currently, we are implementing the presented clearing algorithms in a field trial with 20 German households and try to validate the presented results.

Table 2
Key features of the presented auction-based clearing algorithms for a LEM.

Characteristic	PDA	SEP	H2L	L2H	CC	CC-H2L	CC-H2L-PDA
Satisfying user preferences	No	Yes	Yes	Yes	Yes	Yes	Yes
Considering price premiums	No	No	No	No	No	No	Yes
Increasing local coverage	No	No	Yes	Yes	Yes	Yes	Yes
Motivate high quality	No	No	Yes	Yes	Yes	Yes	Yes
Individual rational	Yes	Yes	Yes	Yes	Yes	Yes	Yes
Tractable	Yes	Yes	Yes	Yes	No	Yes	Yes

The next section concludes this paper and gives an outlook into future research goals.

4. Conclusion

Within this paper we introduced a new bidding format, investigated a variety of auction-based clearing algorithms for local energy markets and identified the CC-H2L-PDA that verifiably satisfies user preferences and incorporates users' willingness to pay a premium for heterogeneous electricity qualities. Furthermore, this clearing algorithm can increase coverage of local demand and local supply compared to conventional periodic double auctions, is individually rational, and tractable. This clearing algorithm is thereby the first auction-based approach for local energy markets that coordinates a constantly increasing number of distributed energy suppliers, consumers, retailers, and incorporates important user preferences in order to increase the acceptance of renewable energies and can fuel the advancing energy transition in the long term.

All presented and evaluated clearing algorithms and the conducted Monte Carlo simulation are implemented open-source in *lemlab* and offer interested parties the opportunity to reuse the implemented methods for their models, implement their own market models or verify our results [38]. Topics for future research could include but are not limited to modeling of realistic user behavior in local energy markets with heterogeneous energy qualities, a quantitative and qualitative comparison similar to [16,47] of our newly developed community-based clearing algorithms with fully decentralized peer-to-peer and centrally optimized approaches, and whether the markets can be gamed. Currently, we are setting up a field trial with 20 households in a German village where we want to validate our presented algorithms. This is part of the research project *RegHEE - Local Trade of Electricity from Renewables over a Blockchain Platform* and enables us to collect realistic load, generation profiles, and user behavior data [48].

5. Supplementary materials

All presented market mechanisms were implemented in the open-source *lemlab* software project [38]. The source code for all experiments presented in this publication are available under an open-source licence in the Github repository.

lemlab is an open-source tool for multi-agent-based development and testing of LEM applications. Interested parties are invited to clone our repository and use the toolbox to investigate their research questions. We explicitly invite collaboration and feedback regarding the toolbox.

CRediT authorship contribution statement

Michel Zade: Conceptualization, Methodology, Software, Investigation, Visualization, Writing – original draft, Writing – review & editing. **Sebastian Dirk Lumpp:** Conceptualization, Software, Resources, Writing – review & editing. **Peter Tzscheutschler:** Conceptualization, Methodology, Investigation, Writing – review & editing, Project administration, Funding acquisition. **Ulrich Wagner:** Investigation, Writing – review & editing, Supervision, Funding acquisition.

Acknowledgments

This work was supported by the Bavarian Ministry of Economic Affairs, Regional Development and Energy, Germany and Zentrum Digitalisierung.Bayern, Germany [grant number IUK589/001].

Appendix A. Mathematical formulations

This section provides mathematical formulations of the clearing algorithms. In the first part of this section we introduce relevant sets. Subsequent subsections show mathematical formulations of the presented clearing algorithms.

$S = \{1, 2, \dots, N_S\}$ refers to the set of all sellers and $B = \{1, 2, \dots, N_B\}$ to the set of all buyers. d represents an energy demand and s an energy supply. $Q = \{1, 2, \dots, Q_{max}\}$ is the set of all energy qualities, $M_B = \{1, 2, \dots, n_{mB}\}$ the subset of all matched buyers, $M_S = \{1, 2, \dots, n_{mS}\}$ of all matched suppliers, $U_B = \{1, 2, \dots, n_{uB}\}$ the subset of all unmatched buyers, and $U_S = \{1, 2, \dots, n_{uS}\}$ the subset of all unmatched suppliers. Consequently, $M_S, U_S \subseteq S$ and $M_B, U_B \subseteq B$.

A.1. Periodic double auction

Mathematically, social welfare SW is formulated by the sum of the bidders' utility U minus the sum of producers' costs C [12]. The goal of a PDA is to maximize social welfare (see Eq. (A.1)).

$$\max SW_{PDA} = \sum_{i=1}^{n_{mB}} U_i(d_i) - \sum_{j=1}^{n_{mS}} C_j(s_j) \tag{A.1}$$

s.t.

$$\sum_{i=1}^{n_{mB}} d_i = \sum_{j=1}^{n_{mS}} s_j \tag{A.2}$$

$\forall i \in M_B \quad \text{and} \quad j \in M_S$

A.2. Check and curtail

Mathematically, the CC clearing algorithm can be formulated as a social welfare maximization problem. We maximize social welfare in equation while satisfying buy bids with ask bids of equal or higher energy quality (see Eq. (A.3)). We ensure with the binary variable α that an ask bid is only matched once with a buy bid (see Eq. (A.5). Eq. (A.4) ensures that matched buy bids with a preference p are satisfied with supplies that offer a quality q that is equal or higher than the preference.

$$\max SW_{CC} = \sum_{q=1}^{Q_{max}} \left(\sum_{i=1}^{n_{mB}} U_{i,q}(d_{i,q}) - \sum_{j=1}^{n_{mS}} C_{j,q}(s_{j,q}) \right) \tag{A.3}$$

s.t.

$$\sum_{i=1}^{n_{mB}} d_{i,p} \leq \sum_{q=p}^{Q_{max}} \sum_{j=1}^{n_{mS}} s_{j,q} \alpha_{j,p} \tag{A.4}$$

$$\sum_{p=1}^{Q_{max}} \alpha_{j,p} \leq 1 \tag{A.5}$$

$\forall i \in M_B \quad \text{and} \quad j \in M_S \quad \text{and} \quad p, q \in Q \quad \text{and} \quad \alpha \in \{0, 1\}$

A.3. Preference prioritization

Mathematically, we formulate the PP clearing algorithm as a series of social welfare maximization for every energy quality preference (see Eq. (A.6) to (A.8)).

$$\max SW_{p_v} = \sum_{i=1}^{n_{mB}} U_{i,p_v}(d_{i,p_v}) - \sum_{q=p_v}^{Q_{max}} \sum_{j=1}^{n_{mS}} C_{j,q}(s_{j,q}) \tag{A.6}$$

$$\max SW_{p_w} = \sum_{i=1}^{n_{mB}} U_{i,p_w}(d_{i,p_w}) - \sum_{q=p_w}^{Q_{max}} \sum_{u=1}^{n_{uS}} C_{q,u}(s_{q,u}) \tag{A.7}$$

...

$$\max SW_{p_x} = \sum_{i=1}^{n_{mB}} U_{i,p_x}(d_{i,p_x}) - \sum_{q=p_x}^{Q_{max}} \sum_{u=1}^{n_{uS}} C_{q,u}(s_{q,u}) \tag{A.8}$$

$\forall i \in M_B \quad \text{and} \quad j \in M_S \quad \text{and} \quad u \in U_S \quad \text{and} \quad p, q \in Q$

In a first step, the algorithm maximizes social welfare for all buy bids that ask for preference p_v and ask bids that have the energy quality $q = p_v$ or higher. Then, all matched and unmatched bids are extracted. In a second iteration, the algorithm clears buy bids of preference p_w with ask bids that provide the energy quality $q = p_w$ or higher and are unmatched which is indicated by the index u.

Appendix B. Monte Carlo simulation — setup

In this section we describe the randomly generated input data, the extracted key outcomes of the clearing algorithms, the computing environment, and calculate how many Monte Carlo simulations are necessary to approximate the outcomes within a given CI.

B.1. Input data

The general idea of the Monte Carlo method is to approximate an outcome of a model or a function by inserting i.i.d. random input data and averaging the outcomes over all simulations. In order to compare the outcomes of all clearing algorithms, the same randomly generated input data is used for each of the clearing algorithms. Table B.3 summarizes all randomly varied input data, their value ranges and corresponding units.

In this simulation, we use the set of qualities $Q = \{1 : \text{na}, 2 : \text{na}, 3 : \text{local-green}\}$. Other qualities such as "green" could be considered as well. However, some algorithms benefit from the fact that we can assign ask bids of higher quality to buy bids of the same or lower energy quality preferences. In order to do so high energy qualities must include their lower ones. Since green energy could be produced locally or non-locally, this label cannot be considered in such a hierarchy. Therefore, we have only limited ourselves to this subset of qualities. A more elaborate description of what the different parameters represent can be found in Section 2.1. A total of 200 market bids was inserted into each market clearing to simulate a reasonably sized LEM.

Table B.3
Variables and corresponding value ranges for the Monte Carlo simulations. $U()$ refers to a uniform distribution in the provided value range. The $quality_{energy}$ set represents the order of qualities with *na* being the lowest quality and *local-green* being the highest electricity quality.

Parameter	Value range	Unit
$type_{\text{bid}}$	{buy, ask}	–
qty_{energy}	$U(1, 1000)$	Wh
$price_{\text{energy}}$	$U(0.02, 0.08)$	€/kWh
$quality_{\text{energy}}$	$\{na, local, local-green\}$	–
$wtpp_{\text{quality}}$	$U(0, 50)$	%

Table B.4
Extracted key parameters from market results.

Key parameter	Description
qty_{traded}	Quantity traded
$price_{\text{wavg}}$	Weighted average clearing price
$welfare$	Welfare (producer plus consumer surplus)
$share_{\text{ask,cld}}$	Share of ask bids cleared with a specific quality
$share_{\text{buy,cld}}$	Share of buy bids cleared with a specific preference
$price_{\text{quality}}$	Weighted average clearing prices per quality

B.2. Extraction of key parameters

In order to evaluate whether the clearing algorithms fulfill the formulated key characteristics, we extract a variety of key parameters from the market results and average them according to the Monte Carlo method. Table B.4 provides a list of all extracted key parameters.

qty_{traded} is the total amount of cleared energy quantity and $price_{\text{wavg}}$ the weighted average clearing price over all cleared market bids. $welfare$ is the sum of consumer and producer surplus. $share_{\text{ask,cld}}$ refer to the shares of buy and ask bids cleared with a specific preference or quality label. $price_{\text{quality}}$ are the prices paid for certain electricity qualities.

B.3. Number of simulations

After defining all input variables and key outcomes, we calculate the necessary number of simulations to get a "good" estimate of the outcomes with Eq. (B.1).

$$N \geq \left(\frac{\sigma * z}{\epsilon}\right)^2 \tag{B.1}$$

N represents the number of simulations one needs to perform in order to achieve a certain accuracy (ϵ) for an expected value with a standard deviation (σ). z represents the z-score of the CI of a normal distribution.

Before we calculate the number of simulations, we need to compute the standard deviations (σ) of the expected outcomes, define a desired accuracy, and a CI. σ is calculated by the outcomes of a small Monte Carlo simulation (e.g., with 100 simulations). The accuracy ϵ must be set to a value of the same unit as the standard deviation. In this simulation, we set the accuracy level to one percent of the calculated averages from the small Monte Carlo simulation. Furthermore, we choose a z-score of 2.58 which corresponds to a CI of 99 %.

Inserting σ, ϵ, and the z-score into Eq. (B.1) for each computed outcome from each of the seven clearing algorithm leads to a variety of necessary simulations. The numbers of simulations vary from 172 to 8922. In order to fulfill the desired accuracy and confidence level for all outcomes, we compute a total of 10,000 simulations for each clearing algorithm.

B.4. Computing environment

The clearing algorithms and the described Monte Carlo simulation setup are implemented in Python as part of the *lemlab* toolbox [38]. For the generation of i.i.d. random input variables, we use the Python built-in, pseudo-random number generator *random*. Furthermore, we simulate the clearing simulations in parallel with the help of the *multiprocessing* library on a computer with an Intel(R) Core(TM) i7-3930K with 6 cores and 48 GB of random-access memory (RAM).

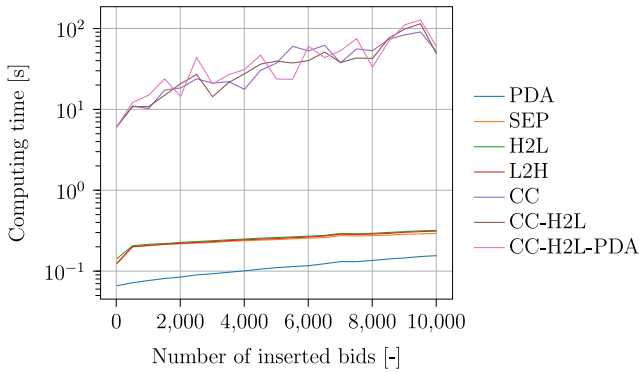

Fig. C.8. Results of the time complexity analysis for the seven clearing algorithms. The number of bids were increased from 10 to 10,010 bids with a step size of 500. The visualized results show the average from 100 samples for each number of bids.

Appendix C. Time complexity analysis

In this section we describe the results of a time complexity analysis in order to analyze the computing time of our newly developed auction-based clearing algorithms with an increasing number of inputs. The analysis was implemented in *lemlab* where all market clearing algorithms are available as an open-source project.

We inserted a linearly increasing number of bids from 10 to 10,010 with a step size of 500. Furthermore, we generated 100 samples for every number of bids and plotted their average in C.8. A high sample size is necessary because the CC clearing algorithm is not only dependent on the number of bids but also on the inserted user preferences and available energy qualities, which have a significant impact on the computing time.

For up to 10,000 bids the PDA needs only 0.15 s and the PP clearing algorithms up to 0.32 s of computing time. The fluctuating results of the CC, CC-H2L, and CC-H2L-PDA clearing algorithms indicate that the number of samples might not have been sufficiently high in order to even out the computing time's dependency on the user preferences and energy qualities of the bids. More importantly, the computing times of all clearing algorithms show a linear growth rate and can be described with the big O notation O(n) where n is the number of inserted bids.

Appendix D. Acronyms

LEM	Local Energy Market
WTPP	Willingness To Pay a Premium
IPCC	Intergovermental Panel on Climate Change
RES	Renewable Energy Source
DES	Decentralized Energy System
DER	Distributed Energy Resource
P2P	Peer-to-Peer
MEM	Microgrid Energy Market
FPP	Federated Power Plant
CDA	Continuous Double Auction
PDA	Periodic Double Auction
IR	Individual Rationality

IMCA	Iterative Market Clearing Algorithm
PP	Preference Prioritization clearing algorithms
SEP	Preference Separation clearing algorithm
L2H	Lowest-to-Highest clearing algorithm
H2L	Highest-to-Lowest clearing algorithm
CC	Check and Curtail clearing algorithm
CC-H2L	Check and Curtail combined with Highest-to-Lowest clearing algorithm
CC-H2L-PDA	Check and Curtail combined with Highest-to-Lowest and Periodic Double Auction clearing algorithm
CI	Confidence Interval
SLLN	Strong Law of Large Numbers
i.i.d.	independent and identically distributed

References

[1] Sims REH, Schock RN, Adegbululgbe A, Fenhann J, Konstantinaviciute I, Moomaw W, et al. Energy supply: Contribution of working group III to the fourth assessment report of the intergovernmental panel on climate change. 2007, URL https://www.ipcc.ch/site/assets/uploads/2018/02/ar4-wg3-chapter4-1.pdf,

[2] IRENA- International Renewable Energy Agency, editor. Renewable capacity statistics 2021. 2021, URL https://www.irena.org/publications/2021/March/Renewable-Capacity-Statistics-2021.

[3] Bundesnetzagentur, Bundeskartellamt, editors. Monitoringbericht 2016: Monitoringbericht gemäß § 63 Abs. 3 i. V. m. § 35 EnWG und § 48 Abs. 3 i. V. m. § 53 Abs. 3 GWB. 2016, URL https://www.bundesnetzagentur.de/SharedDocs/Mediathek/Monitoringberichte/Monitoringbericht2016.pdf?_blob=publicationFile&v=2.

[4] Bundesnetzagentur, Bundeskartellamt, editors. Monitoringbericht 2020: Monitoringbericht gemäß § 63 Abs. 3 i. V. m. § 35 EnWG und § 48 Abs. 3 i. V. m. § 53 Abs. 3 GWB. 2021, URL https://www.bundesnetzagentur.de/SharedDocs/Mediathek/Berichte/2020/Monitoringbericht_Energie2020.pdf?_blob=publicationFile&v=6.

[5] Pittel K. Das energiepolitische zieldreieck und die energiewende. 2012, URL https://www.ifo.de/DocDL/ifosd_2012_12_7.pdf,

[6] Bailey R, Sutherland J, Koh S, Hang Chen Q, Kocincova L, Suárez Rubio V, et al. World energy trilemma index 2020. 2020, URL https://www.worldenergy.org/assets/downloads/World_Energy_Trilemma_Index_2020_-_REPORT.pdf,

[7] European Parliament, Council of the European Union. Directive (EU) 2019/944 of the european parliament and of the council of 5 june 2019 on common rules for the internal market for electricity and amending directive 2012/27/EU (recast): directive (EU) 2019/944. 2019, URL https://eur-lex.europa.eu/legal-content/EN/TXT/?uri=uriserv:OJ.L_.2019.158.01.0125.01.ENG&toc=OJ:L:2019:158:TOC.

[8] Caramizaru A, Uihlein A. Energy communities: an overview of energy and social innovation, EUR 30083 EN. 2020, http://dx.doi.org/10.2760/180576,

[9] Energy Security Board, editor. Post-2025 market design: Directions paper. 2021, URL https://esb-post2025-market-design.aemc.gov.au/32572/1609802925-p2025-january-directions-paper.pdf.

[10] Morstyn T, Farrell N, Darby SJ, McCulloch MD. Using peer-to-peer energy-trading platforms to incentivize prosumers to form federated power plants. Nat. Energy 2018;3(2):94–101. http://dx.doi.org/10.1038/s41560-017-0075-y.

[11] Mengelkamp E, Gärttner J, Rock K, Kessler S, Orsini L, Weinhardt C. Designing microgrid energy markets. Appl Energy 2018;210:870–80. http://dx.doi.org/10.1016/j.apenergy.2017.06.054.

[12] Khorasany M, Mishra Y, Ledwich G. Market framework for local energy trading: A review of potential designs and market clearing approaches. IET Gener Transm Distrib 2018;12(22):5899–908. http://dx.doi.org/10.1049/iet-gtd.2018.5309.

[13] Tushar W, Yuen C, Saha TK, Morstyn T, Chapman AC, Alam MJE, et al. Peer-to-peer energy systems for connected communities: A review of recent advances and emerging challenges. Appl Energy 2021;282:116131. http://dx.doi.org/10.1016/j.apenergy.2020.116131.

[14] Zhang C, Wu J, Zhou Y, Cheng M, Long C. Peer-to-peer energy trading in a microgrid. Appl Energy 2018;220:1–12. http://dx.doi.org/10.1016/j.apenergy.2018.03.010.

[15] Parag Y, Sovacool BK. Electricity market design for the prosumer era. Nat. Energy 2016;1(4). http://dx.doi.org/10.1038/nenergy.2016.32.

[16] Sousa T, Soares T, Pinson P, Moret F, Baroche T, Sorin E. Peer-to-peer and community-based markets: A comprehensive review. Renew Sustain Energy Rev 2019;104:367–78. http://dx.doi.org/10.1016/j.rser.2019.01.036.

[17] Friedman D, Rust J, editors. The double auction market: Institutions, theories, and evidence ; proceedings of the workshop on double auction markets held june, 1991 in santa fe, new Mexico. In: Santa Fe institute studies in the sciences of complexity, vol. 14, Cambridge, Mass.: Perseus Publ; 1993.

[18] Shoham Y, Leyton-Brown K. Multiagent systems: algorithmic, game-theoretic, and logical foundations. Cambridge: Cambridge University Press; 2009, http://dx.doi.org/10.1017/CBO9780511811654.

[19] Wah E, Hurd D, Wellman M. Strategic market choice: Frequent call markets vs. Continuous double auctions for fast and slow traders. EAI Endorsed Trans. Serious Games 2015;3(10). http://dx.doi.org/10.4108/eai.8-8-2015.2260356.

[20] Budish E, Cramton P, Shim J. The high-frequency trading arms race: Frequent batch auctions as a market design response *. Q J Econ 2015;130(4):1547–621. http://dx.doi.org/10.1093/qje/qjv027.

[21] Gode DK, Sunder S. What makes markets allocationally efficient? Q J Econ 1997;112(2):603–30. http://dx.doi.org/10.1162/003355397555307.

[22] Myerson RB, Satterthwaite MA. Efficient mechanisms for bilateral trading. J Econom Theory 1983;29(2):265–81. http://dx.doi.org/10.1016/0022-0531(83)90048-0.

[23] Roth AE. The art of designing markets. Harv. Bus. Sch. Publ. Corp. 2007. URL https://scholar.harvard.edu/files/roth/files/hbr.artofdesigningmarkets.pdf.

[24] Kaenzig J, Heinzle SL, Wüstenhagen R. Whatever the customer wants, the customer gets? Exploring the gap between consumer preferences and default electricity products in Germany. Energy Policy 2013;53:311–22. http://dx.doi.org/10.1016/j.enpol.2012.10.061.

[25] Kalkbrenner BJ, Yonezawa K, Roosen J. Consumer preferences for electricity tariffs: Does proximity matter? Energy Policy 2017;107:413–24. http://dx.doi.org/10.1016/j.enpol.2017.04.009.

[26] Plum C, Olschewski R, Jobin M, van Vliet O. Public preferences for the swiss electricity system after the nuclear phase-out: A choice experiment. Energy Policy 2019;130:181–96. http://dx.doi.org/10.1016/j.enpol.2019.03.054.

[27] Günther N, Fait L, Groh E, Wetzel H. Gibt es eine zahlungsbereitschaft für regionalen Grünstrom? Energ.wirtsch. Tagesfr. 2019;69(11):35–8.

[28] Tabi A, Hille SL, Wüstenhagen R. What makes people seal the green power deal? — Customer segmentation based on choice experiment in Germany. Ecol Econom 2014;107:206–15. http://dx.doi.org/10.1016/j.ecolecon.2014.09.004.

[29] Sagebiel J, Müller JR, Rommel J. Are consumers willing to pay more for electricity from cooperatives? results from an online choice experiment in Germany. Energy Res. Soc. Sci. 2014;2:90–101. http://dx.doi.org/10.1016/j.erss.2014.04.003.

[30] Hensher DA, Shore N, Train K. Willingness to pay for residential electricity supply quality and reliability. Appl Energy 2014;115:280–92. http://dx.doi.org/10.1016/j.apenergy.2013.11.007.

[31] Senkpiel C, Dobbins A, Kockel C, Steinbach J, Fahl U, Wille F, et al. Integrating methods and empirical findings from social and behavioural sciences into energy system models—Motivation and possible approaches. Energies 2020;13(18):4951. http://dx.doi.org/10.3390/en13184951.

[32] Wang J, Wang Q, Zhou N, Chi Y. A novel electricity transaction mode of microgrids based on blockchain and continuous double auction. Energies 2017;10(12):1971. http://dx.doi.org/10.3390/en10121971.

[33] Zahid M, Ali I, Khan RJ, Noshad Z, Javaid A, Javaid N. Blockchain based balancing of electricity demand and supply. In: Barolli L, Hellinckx P, Enokido T, editors. Advances on broad-band wireless computing, communication and applications, Vol. 97. 2020, p. 185–98. http://dx.doi.org/10.1007/978-3-030-33506-9_17.

[34] Troncia M, Galici M, Mureddu M, Ghiani E, Pilo F. Distributed ledger technologies for peer-to-peer local markets in distribution networks. Energies 2019;12(17). http://dx.doi.org/10.3390/en12173249.

[35] Oprea SV, Bara A, Andreescu AI. Two novel blockchain-based market settlement mechanisms embedded into smart contracts for securely trading renewable energy. IEEE Access 2020;8:212548–56. http://dx.doi.org/10.1109/ACCESS.2020.3040764.

[36] Khorasany M, Razzaghi R, Gazafroudi AS. Two-stage mechanism design for energy trading of strategic agents in energy communities. Appl Energy 2021;295. http://dx.doi.org/10.1016/j.apenergy.2021.117036.

[37] Richter B, Mengelkamp E, Weinhardt C. Vote for your energy: A market mechanism for local energy markets based on the consumers' preferences. In: 16th international conference on the european energy market. [Piscataway, New Jersey]: IEEE; 2019?, p. 1–6. http://dx.doi.org/10.1109/EEM.2019.8916544.

[38] Lumpp SD, Zade M, Doepfert M. Lemlab. 2021, https://github.com/tum-ewk/lemlab.

[39] Zou X. Double-sided auction mechanism design in electricity based on maximizing social welfare. Energy Policy 2009;37(11):4231–9. http://dx.doi.org/10.1016/j.enpol.2009.05.019.

[40] Morstyn T, McCulloch MD. Multiclass energy management for peer-to-peer energy trading driven by prosumer preferences. IEEE Trans Power Syst 2019;34(5):4005–14. http://dx.doi.org/10.1109/TPWRS.2018.2834472.

[41] Graham C, Talay D. Stochastic simulation and monte carlo methods, Vol. 68. Berlin, Heidelberg: Springer; 2013, http://dx.doi.org/10.1007/978-3-642-39363-1.

[42] Lerche I, Mudford BS. How many Monte Carlo simulations does one need to do? Energy Exploration Exploitation 2005;23(6):405–27, URL http://www.jstor.org/stable/43754692.

[43] Hardi L. Modellgestützte energie- und CO2-bilanz der letzten meile des lieferverkehrs mit quelloffenen geodaten. München: Universitätsbibliothek der TU München; 2019.

[44] Das I, Bhattacharya K, Canizares C. Optimal incentive design for targeted penetration of renewable energy sources. IEEE Trans Sustain Energy 2014;5(4):1213–25. http://dx.doi.org/10.1109/TSTE.2014.2339172.

[45] Zalzar S, Bompard E, Purvins A, Masera M. The impacts of an integrated European adjustment market for electricity under high share of renewables. Energy Policy 2020;136:111055. http://dx.doi.org/10.1016/j.enpol.2019.111055.

[46] Nikmehr N, Najafi Ravadanegh S. Reliability evaluation of multi-microgrids considering optimal operation of small scale energy zones under load-generation uncertainties. Int J Electr Power Energy Syst 2016;78:80–7. http://dx.doi.org/10.1016/j.ijepes.2015.11.094.

[47] Moret F, Baroche T, Sorin E, Pinson P. Negotiation algorithms for peer-to-peer electricity markets: Computational properties. In: 2018 Power Systems Computation Conference. 2018, p. 1–7. http://dx.doi.org/10.23919/PSCC.2018.8442914.

[48] Zade M, Lumpp SD, Tzscheutschler P. RegHEE — Local trade and labelling of electricity from renewable sources on a blockchain platform. 2021, https://www.ei.tum.de/en/ewk/forschung/projekte/reghee/.

2.2 Evaluating the added value of blockchains

Scientific context

After the introduction of the blockchain technology and the rising interest among energy researchers and experts, the energy industry and academia began to discuss whether the blockchain technology could become a chance for consumers to be empowered and further liberalized in energy systems [27]. Blockchain properties were described that challenged the need for utilities and described more than 90 potential use cases in the energy sector [28, 29].

Scientific articles with blockchain use cases in energy-related applications were first published in 2013 by Dimitriou and Karame proposing to use Bitcoins to reward participants in a smart grid for the execution of certain tasks [24]. Bitcoins refer to the inherent digital currency of the first blockchain network implementation of the same name. A year later, Mihaylov et al. suggested to use a similar blockchain protocol to reward the feed-in of VRE with digital coins and to trade them in smart grids [26]. Similarly, Al Kawasmi et al. came up with the idea to use the Bitcoin protocol and its digital currency to trade CO_2-emission certificates [23]. Although these articles represent innovative and visionary ideas at that time, blockchain technology attracted significantly more attention among energy researchers and experts after the introduction of the Ethereum blockchain in 2015. For the first time, the Ethereum blockchain allowed to deploy programmable scripts on a blockchain, permitting to modify the state of a blockchain in a more sophisticated fashion [75].

Since the introduction of smart contracts in 2015, the number of scientific publications investigating blockchain use cases in the energy sector grew annually [76, 77, 78]. Scientific papers discussing LEMs and blockchains focus on demonstrating the feasibility with a variety of blockchain protocols such as Tendermint [79], Ethereum [80, 81], Hyperledger [82], or proprietary blockchains [83]. Other articles present comparisons with a variety of consensus mechanisms [84, 85] or implemented the functionality off-chain and used the blockchain to represent monetary values or to store market results [86, 87, 88, 89].

Only few articles include community-based LEMs on a blockchain and performance or scalability analyses. Han et al. and Son et al. present a brief analysis of a blockchain setup and visualize the throughput, latency, and computational expenses of the market clearing [90, 91]. Vieira et al. and Tsaousoglou et al. present an analysis of varying market clearing algorithms on a blockchain but do not assess the added value of the technology itself [92, 93]. Other papers conduct economic analyses of their implementations [88, 94].

In summary, the literature so far lacks an objective evaluation based on technology-independent infrastructure requirements of the added value of blockchain-based LEM implementations compared to centralized setups. Hence, the hypothesis that blockchain technology could be a chance for consumers and prosumers and can empower them in the context of LEMs has so far not been investigated.

Contribution

The article presented in this section analyzes whether the blockchain technology can empower and further liberalize consumers and prosumers by enabling them to host their own community-based LEM applications.

For a comparative evaluation, the developed library of market clearing algorithms introduced in section 2.1 is used as a central reference implementation. Additionally, the same functionality of the market clearing and settlement for a PDA was implemented in the form of smart contracts on an Ethereum blockchain network. To feed both systems with variable input data and to test balancing energy functions, a market bid and metering data generator was used (see figure 2.1). The code of the centralized and blockchain-based LEM implementations is publicly available as part of the open-source project *lemlab* [32]. Furthermore, the article contains technology-independent LEM-specific infrastructure requirements that are used to objectively compare essential features of a LEM such as data privacy and scalability.

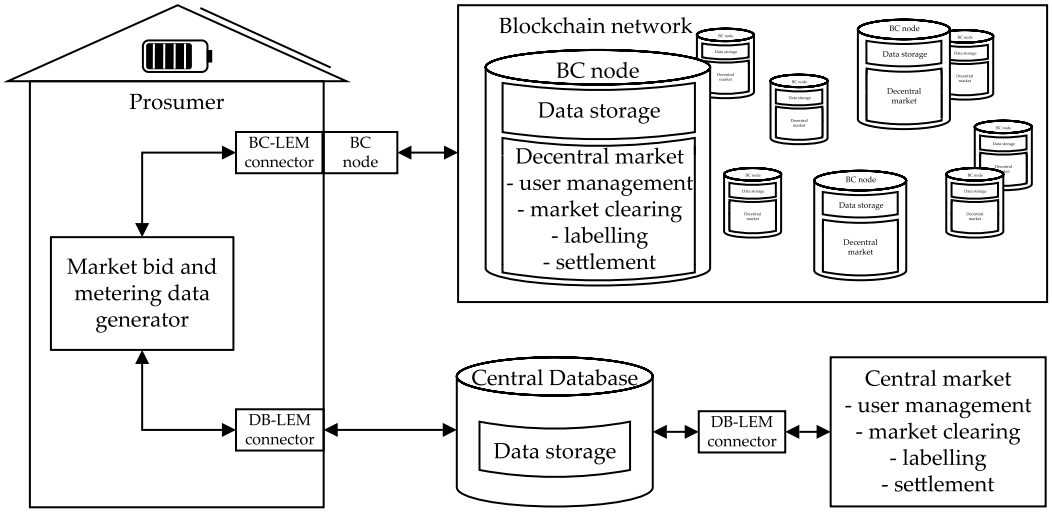

Figure 2.1: Schematic of the experimental test setup for the blockchain-based and centralized LEM implementation. Figure was taken from [95] and graphically edited.

To evaluate the performance of both systems, we designed and implemented a comparative performance analysis for the centralized and blockchain-based LEM implementation. We inserted an increasing number of market bids into both implementations and measured the execution time of each market function. Market functions refer in this context to the posting of bids, clearing, logging of meter readings, and settlement. Furthermore, we qualitatively evaluated the technology-independent LEM-specific infrastructure requirements.

The results presented in the paper show that blockchain promises of a decentralized and transparently managed infrastructure can only be realized to a limited extent for

community-based LEMs. The presented blockchain-based implementation is reliable, but requires more than 140 times the computation time compared to a centralized implementation, and cannot fulfill data security requirements such as closed-order books and protect personal metering data. Only the tamper resistance, which is a consequence of the consensus mechanism, represents a significant added value that comparable centralized implementations cannot similarly provide. In conclusion, blockchain technology at its current stage of development does not add sufficient value to LEMs that could empower consumers and prosumers to host their own energy trading application.

Publication #2: Evaluating the added value of blockchains to local energy markets –- Comparing the performance of blockchain-based and centralised implementations

Authors Michel Zade, Marcello Feroce, Arturo Guridi, Sebastian Dirk Lumpp, Peter Tzscheutschler

Publication medium IET Smart Grid

Digital object identifier https://doi.org/10.1049/stg2.12058

Open-source repository the data and models that support the findings of this study are openly available in *lemlab* [32].

Author contributions

Michel Zade:	45 %	Conceptualization, Formal analysis, Funding acquisition, Investigation, Methodology, Project administration, Software, Visualization, Writing – original draft, Writing – review & editing.
Marcello Feroce:	20 %	Software, Writing – review & editing.
Arturo Guridi:	15 %	Software, Writing – review & editing.
Sebastian Dirk Lumpp:	10 %	Conceptualization, Formal analysis, Resources, Software, Writing – review & editing.
Peter Tzscheutschler:	10 %	Conceptualization, Funding acquisition, Project administration, Resources, Supervision, Writing – review & editing.

Received: 21 December 2021 | Revised: 19 January 2022 | Accepted: 29 January 2022

IET Smart Grid

DOI: 10.1049/stg2.12058

ORIGINAL RESEARCH

Evaluating the added value of blockchains to local energy markets—Comparing the performance of blockchain-based and centralised implementations

Michel Zade | **Marcello Feroce** | **Arturo Guridi** | **Sebastian Dirk Lumpp** | **Peter Tzscheutschler**

School of Engineering and Design, Technical University of Munich, Munich, Germany

Correspondence

Michel Zade, School of Engineering and Design, Technical University of Munich, Arcisstrasse 21, 80333 Munich, Germany.
Email: michel.zade@tum.de

Funding information

Bayerisches Staatsministerium für Wirtschaft, Landesentwicklung und Energie, Grant/Award Number: IUK589/001
Open Access funding enabled and organised by Projekt DEAL

Abstract

The continuous decentralisation of the energy system due to the expansion of renewable energies requires new coordination mechanisms such as Local Energy Markets (LEMs) that are capable of integrating millions of prosumers as active participants. Since the end of the 2010s, the blockchain technology has been discussed as a potential infrastructure for LEMs and as a potential game-changer in the energy industry. In this work, the authors introduce LEM specific technology-independent infrastructure requirements, present a Solidity and Python toolbox that allows to compute a comparative performance analysis between a blockchain-based and a central LEM and evaluate the added value of a blockchain-based implementation compared to a conventional reference implementation. Simulations of a LEM with a periodic double auction and settlement showed that a blockchain-based LEM operation requires more than 140 times the computation time compared to a centralised implementation and cannot fulfil data security requirements. Thus, the authors find that blockchain technology in its current state of development does not add significant value to LEMs. All implemented programmes are published in the open-source project *lemlab* as part of the research project *RegHEE*.

1 | INTRODUCTION

Our energy system is continuously transforming from a formerly centralised system with few fossil-fuelled and nuclear power plants to a renewable, distributed, and volatile energy system consisting of millions of participants [1]. Consumers become prosumers and legislation empowers individual households to become an active part of the energy transition [2].

However, the conventional coordination mechanisms used to manage a relatively small number of fossil-fuelled power plants are not-transferable to millions of non-professional prosumer households [3]. Therefore, we need new coordination mechanisms that are capable of integrating millions of prosumers as active participants into our energy system. Recent research has investigated ideas such as aggregating single households and marketing their surplus or deficits on wholesale markets, operating them as Virtual Power Plant (VPP), letting prosumers trade among each other in Peer-to-Peer (P2P) or coordinated Local Energy Markets (LEMs), or centrally optimising their control. As nations realise the necessity for new ways of coordination, they start to incentivise, enable, or fund various variants of the aforementioned ideas [2, 4]. In this work, we focus on auction-based LEMs. LEMs allow prosumers to trade their energy surpluses and deficits locally, to react to external signals such as prices, thereby making them an active part of the energy system [5]. At the same time, LEMs do not necessarily require prosumers to disclose too much personal data and can enable grid operators to maintain grid stability [6].

Towards the end of the 2010s, researchers and the energy industry started to discuss whether the blockchain technology could provide significant benefits to LEMs while at the same time being transparent, automated, and completely decentralised [7]. Immediately following the launch of the Ethereum

blockchain in 2015 and the introduction of smart contracts, a study was published by PricewaterhouseCoopers summarising the potential opportunities of lower transaction costs, transparency, and the ability to become electricity or service providers for prosumers and consumers [8]. In the same year, the German energy agency Dena conducted a survey among managers of the energy industry and found that half of the 70 managers interviewed were already experimenting with blockchains or planning to and 21% said that blockchain would become a 'game changer' in the energy industry [9]. In 2018, the Forschungsstelle für Energiewirtschaft characterised blockchain as tamper proof, reliable, transparent, highly automatable, and easily accessible and identified 91 potential use cases in the energy sector [10]. The first scientific papers on blockchains from an energy perspective investigated the potential in microgrid exchanges [11], P2P electricity trading among hybrid electric vehicles [12], and among neighbours [13, 14]. The number of scientific publications has since increased year by year [15–17]. For a detailed description of blockchain technology, see section Blockchain technology of the appendix.

Most papers investigating auction-based LEMs in a blockchain network demonstrated their feasibility on different kinds of blockchains such as Tendermint [18], Ethereum [19, 20], Hyperledger [21], proprietary blockchains [22], or compared different consensus mechanisms [23, 24]. Other papers described off-chain market-clearing algorithms, using the blockchain only to represent monetary values or to store market results [25–28]. Off-chain refers to a centralised system hosted by a single entity that retrieves data from the blockchain (on-chain), processes it on its own system, and then returns the results to the blockchain in order to reduce the computational complexity on-chain. Troncia et al. implemented different variants of LEMs on a blockchain that considered network constraints and compared them to an optimal power flow result [29]. Meeuw et al. compared and evaluated smart grid communication technologies for blockchain applications [30] and Christidis et al. analysed how market positions are efficiently encrypted on a blockchain so that closed-order book LEMs are possible [31].

Narrowing the search to papers that include an auction-based LEM on a blockchain and a performance or scalability analysis, we find papers such as Han et al. that present the throughput, latency, and computational expenses of a single setup [32, 33] or of functionally differing algorithms [34, 35]. Other papers conduct economic analyses of their implementations [27, 36]. However, no publication was found that includes an auction-based LEM on a blockchain, compares its performance to a centralised system, and assesses the actual added value of blockchains to LEMs based on application-specific infrastructure requirements.

Therefore, this paper addresses the above-mentioned research gap by investigating whether a blockchain-based implementation adds significant value to auction-based LEMs in comparison to a centralised implementation. Within this paper, we introduce application-specific infrastructure requirements for LEMs, present an open-source evaluation toolbox for centralised and blockchain-based LEM applications, discuss the results of a comparative performance analysis, and evaluate whether the implementations under investigation can fulfil the introduced requirements.

The paper is structured as follows. Section 2 introduces the application-specific infrastructure requirements for LEMs while section 3 describes the experimental setup of the evaluation toolbox with the blockchain-based and centralised LEM implementations. Section 4 presents the results of the comparative performance analysis, which are discussed in section 5. Finally, section 6 puts the findings of this paper into a broader perspective.

2 | INFRASTRUCTURE REQUIREMENTS FOR LOCAL ENERGY MARKETS

Recent technological advancements such as the blockchain technology, machine learning, Internet of things, or artificial intelligence allow us to design new systems or re-implement existing systems in new ways. Despite these new possibilities, we must define requirements for LEMs that need to be fulfiled by any infrastructure or algorithm that handles personal data and is connected to our energy system (see [35, 37, 38]). We summarise technology-independent infrastructure requirements that are in our opinion essential for LEMs in the following paragraphs.

2.1 | Reliability

A reliable software can be described by the probability of failure-free operation [39]. Applied to a LEM, we can define a 'failure-free' operation as the availability of the LEM for prosumers, grid and market operators, as well as the correct processing of data.

2.2 | Scalability

A scalable system ensures that a given quality of service is maintained as data input increases [40]. A LEM, for example, must fulfil temporal requirements such as a 15 min market interval. In addition, a scalable infrastructure must provide developers with the ability to implement the necessary functions has an only open-source community that improves and documents functionalities and bottlenecks, and, ideally, provides pre-built libraries for efficient implementations.

2.3 | Data security

An executing infrastructure must comply with existing data protection regulations, depending on the data processed. In the case of a LEM, we process personal data in the form of account balances, market positions, and meter readings, which requires the infrastructure to comply, for example, in Europe

with the General Data Protection Regulation (GDPR). Market positions refer to a tuple of quantity and price placed by prosumers on LEMs in order to express their willingness to buy or sell energy. In addition, closed-order book auctions such as a Periodic Double Auction (PDA) require that market positions must be kept concealed in order to prevent gaming. Gaming refers to agent strategies that depend on the expected decisions of other agents [41] and potentially manipulate a market.

2.4 | Tamper resistance

The infrastructure must ensure that stored data cannot be manipulated, is trustworthy and should automatically detect manipulations [37]. Optimally, the validity of the data can be confirmed by anyone.

2.5 | Low operating costs

When considering LEMs for prosumers that trade on an hourly or quarter-hourly basis with traded volumes of a few 100 Wh, it is important that the operating costs of the platform do not significantly influence the incentive to participate in LEMs.

3 | EVALUATION TOOLBOX

In order to objectively compare a blockchain-based and centralised LEM, we built the comparative performance analysis toolbox for *lemlab*. The functional and implemented software components of the toolbox are described in the following subsections. Figure 1 visualises the functional components of the evaluation toolbox. The toolbox consists of a prosumer simulation, a blockchain-based, and a centralised LEM implementation. The performance analysis module is not visualised but accesses the results on the blockchain and the centralised database. The following subsections describe the functional LEM modules, implemented connector classes, used blockchain and central database configuration, and prosumer simulation.

3.1 | Local energy market functions

This section describes the main functions of the LEM from user management to market clearing and settlement. This description is technology independent since it has been mirrored on both systems.

3.1.1 | User and meter management

Before a user can participate in a LEM, a user account needs to be created, labelled, and linked to corresponding meters and their Home Energy Management Systems (HEMSs). HEMSs refer to a smart home device that collects data from the household, retrieves forecasts, has a web interface to the user, optimises operating strategies, acts on a LEM on behalf of the household, and controls the household devices accordingly. During operation it may be necessary to add new users or meters, to edit, or delete existing ones. Additionally, users and market operators must

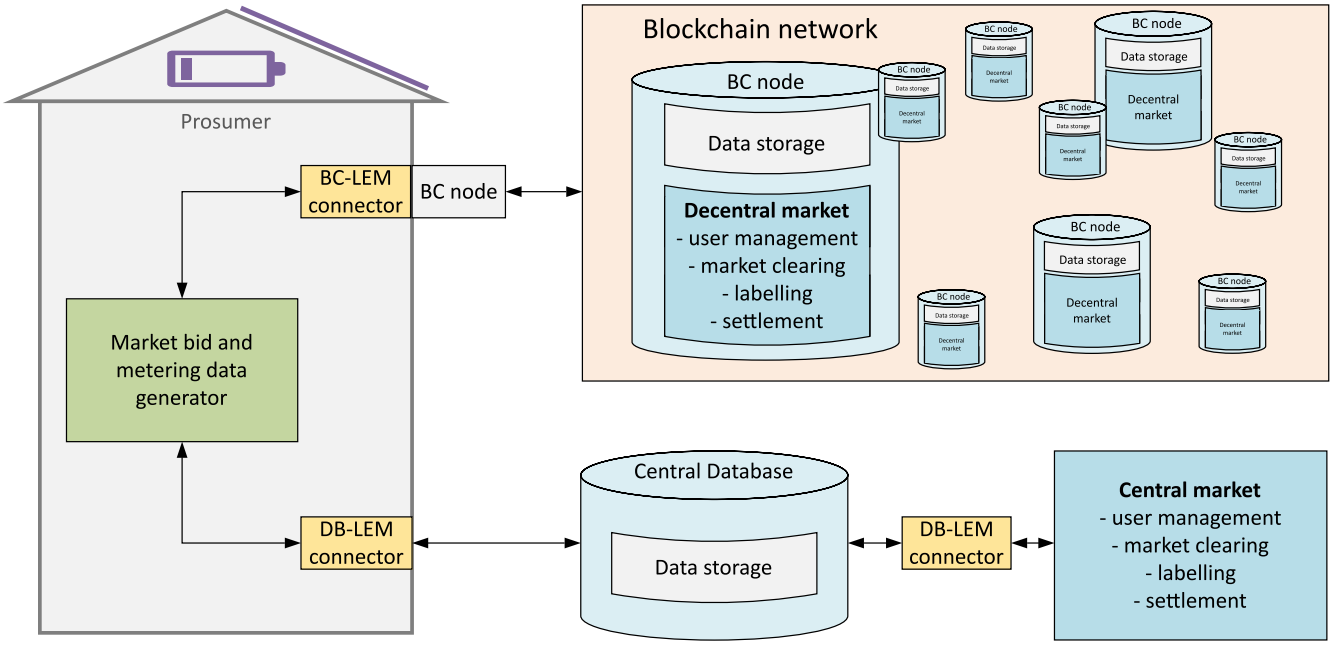

FIGURE 1 Schematic of the evaluation toolbox to analyse the performances of a blockchain-based and central Local Energy Market (LEM). The abbreviations BC refers to a blockchain module and DB to a centralised database module. The performance analysis module is not visualised in the functional overview of the toolbox but accesses the results on the blockchain and the central database

be able to access and alter their data on the LEM. The functions that manage user accounts and meters are normally executed only when a user is added or if unexpected events happen that influence user accounts (e.g. a replaced meter).

3.1.2 | Market clearing

The main goal of a LEM is to match supply and demand energy locally between prosumers. However, different approaches exist which differ greatly and can be distinguished by their market-clearing time. If a LEM is cleared before the energy is exchanged between LEM participants, we talk about an ex-ante clearing. For an ex-ante clearing, we need feed-in and consumption forecasts and a settlement that calculates differences between market results and meter readings. A LEM that clears energy after it has been exchanged is called an ex-post clearing and does not require any forecasts. In this context, we will often talk about the time of delivery that refers to the starting point of the energy exchange period. The toolbox presented in this paper contains an ex-ante clearing but can be easily extended to incorporate ex-post clearings.

Market-clearing algorithms can be further distinguished by the clearing mechanism. In the literature, we often find a Continuous Double Auction (CDA) that clears the market whenever new market positions are placed on the LEM or a PDA that clears the market at pre-defined intervals [42]. Since CDAs discriminate prosumers with slower internet connections and motivate high-frequency trading [43], we implemented a standard PDA in the LEM toolbox that clears in quarter-hourly intervals market positions based on their quantity and price. Market positions are placed by market agents that trade energy on LEMs on behalf of prosumer households.

In summary, the market-clearing functions read stored market positions, compute a sorted ascending supply and a descending demand curve, find the intersection of the two, calculate a uniform clearing price, label cleared positions, and store them.

3.1.3 | Settlement

After the ex-ante market clearing and the exchange of energy took place for a specific time of delivery, the LEM needs to be settled. Settling a market refers to functions that are executed after meter readings are transferred to the LEM. After the arrival of meter readings, balancing energies can be calculated for each user. Balancing energy refers to the differences between market results and measured energy consumption and feed-in. Based on balancing energies user accounts are credited or debited by the appropriate amounts. Finally, price components such as grid fees and taxes are applied.

3.1.4 | Labelling

Labels in a LEM offer prosumers information about the origin of their consumed electricity and ideally motivate consumers to consume more climate-neutral and less fossil-fuelled energy (see [44]). In the evaluation toolbox presented in this paper, the labelling of energy quantities is implemented in all of the aforementioned LEM functions as pre-defined energy qualities. Energy qualities refer to labels such as green, local, or local-green electricity but can be easily replaced by any other label type.

During a user registration, each meter that measures energy feed-in is labelled with a specific energy quality. Whenever prosumers wish to sell energy from or to the LEM, market agents on behalf of their prosumer households place ask positions with the quality labels of their meters on the LEM. After the PDA, cleared energy qualities can then be labelled based on the shares of the cleared ask positions. Finally, settlement functions label balancing energies based on the actual shares exchanged in the LEM or as an unknown energy quality.

3.2 | Local energy market connectors

In order to interact with the central database and the blockchain infrastructure, we implemented two Python classes that abstract all interactions with the two database infrastructures for the LEM user. These connectors retrieve data from the databases, trigger functions in smart contracts, and wait for transaction receipts in order to ensure a completed execution.

3.3 | Ethereum blockchain

This subsection describes all components that are necessary to implement a LEM on a private or consortium Ethereum blockchain. The words private and consortium indicate the accessibility and operation type of the blockchain network. Private blockchains are operated and useable only by a homogeneous group such as a company, whereas consortium blockchains are operated and managed by a variety of groups or institutions [45].

As this paper focusses on the implementation of a LEM application, we used a private blockchain with a Proof-of-Authority (PoA) consensus mechanism. This setup allows us to have an insignificant energy demand, to minimise external influences, and to modify the blockchain's parameters according to our will (see [24]). We set up two Linux machines as block validators, signing blocks every 5 s. To allow LEM executions with more than a hundred market positions, we set the block gas limit to 1.5 billion gas. All connected nodes use OpenEthereum clients that establish the connection to the network.

In Ethereum, all functions are implemented in smart contracts. The following paragraphs summarise their functional scope.

ClearingExAnte: the contract contains all functions for the market clearing and stores static and dynamic user data. Static user data refer to users' identifiers on the platform and their related meters. Dynamic user data refer to their placed market positions. As for the clearing functionality, we implemented functions that sort all placed market positions, filter them by their time of delivery, calculate a market-clearing price, calculate the cleared energy qualities, and update user balances. In addition, the contract contains functions to add, edit, or remove users and meters, and to place market positions.

Settlement: functions that are executed after energy has been exchanged between LEM users and meter readings are available. In this contract, we store all meter readings, balancing energies, and settlement prices in a 'rolling horizon array' for a configurable number of timesteps. The rolling horizon approach allows us to keep the storage consumption to a minimum. Past data can be accessed via past blocks. Furthermore, this contract is linked to the *ClearingExAnte* contract at deployment in order to access market results and user data.

Sorting, *Param*, and *LEMLib*: in addition to the core modules *ClearingExAnte* and *Settlement*, we implemented a variety of reusable subcontracts that contain static LEM parameters, data structures for exchanged and stored information, sorting algorithms, and a variety of array functions, for example, finding the minimal and maximal value of an array. Especially, the sorting library with implementations of *quick_sort*, *counting_sort*, and *insertion_sort* offers a variety of different sorting algorithms in Solidity. These functions are implemented in the contracts *Sorting*, *Param*, and *LEMLib*.

3.4 | Central database

Our central reference database setup is a relational database implemented as a PostgreSQL server. On this server, we set up roles for market operators and users who have different reading and writing privileges on the different tables. Features such as composite keys and upsert statements are used in order to prevent data collisions. Multiple tables store LEM data ranging from static user and meter information to dynamic market positions and results, meter readings, balancing energies, and settlement prices. The number of tables increases if additional market-clearing variants are executed in parallel.

3.5 | Prosumer

In a real-world setting, a prosumer would need to be equipped with a HEMS that acts on the LEM on behalf of the prosumer, and a smart meter to reliably transmit verified meter readings to the platform. Such a prosumer configuration is set up in a German field trial with 17 households as part of the research project RegHEE—Local Trade of Renewable Energies and Labelling on a Blockchain Platform [46]. As the focus of this paper is not to precisely model prosumer behaviour but to analyse whether the LEM requirements can be fulfiled by a blockchain-based LEM and a centralised approach, we simulated prosumer inputs in a data generator arbitrarily (see Figure 1).

During market initialisation, we generate a pre-defined number of user accounts and associated smart meters and register them on the two LEM platforms. Afterwards, the bid generator creates a random set of market positions based on parameter ranges given in Table 1 and pushes them into the two LEMs. After the ex-ante market clearing is completed, the data generator retrieves the market-clearing results from the LEM platforms, adds or subtracts an arbitrary value from the market results and reinserts these values as meter readings to the platform. The arbitrary values simulate deviations from the market results. In order to generate independent and identically distributed (i.i.d.) random data samples, we used the numpy package *random*.

4 | COMPARATIVE PERFORMANCE ANALYSIS

This section presents a quantitative performance evaluation of the decentral blockchain-based LEM and the central database LEM. After briefly describing the setup of the analysis, we will present the results of the analysis in three parts: an equality check, a time complexity analysis, and a computational effort analysis of the blockchain-based LEM. The script to conduct this or similar analyses is publicly available in the open-source project *lemlab* [47].

4.1 | Configuration

For this performance analysis, we implemented automated test cases that insert a random set of market bids, clear the centralised and blockchain-based LEM using the same market positions, simulate meter readings with arbitrary deviations from the market results, and settle the central and blockchain-based LEMs according to the meter readings. These test cases were executed for 50 to 550 market positions with an increment of 50. The maximum number of 550 inserted market positions is a direct consequence of the set block gas limit of 1.5 billion gas. The block gas limit refers to the maximum number of operations, measured in Ethereum's own computational currency gas, that can be inserted into a block to ensure a decentralised consensus mechanism. In each test, we measure the execution time for position placement, market clearing, logging of meter readings, and market settlement. Additionally, we measure the gas consumption and compare

TABLE 1 Parameters used in the comparative performance analysis to simulate prosumer buy and ask bids on the LEM

Parameter	Value range	Unit
type	{buy, sell}	-
qty	U(1, 1000)	Wh
price	U(0.2, 0.1)	€/kWh

whether the results of the two markets are equivalent. All test cases and market position placements are executed from a single computer that is connected to the institute's Local Area Network (LAN). The two blockchain authorities and the central database server are connected to the same network. In order to reduce the impact of blockchain node instabilities and network loads, we executed all test cases 10 times and restart a test in case of connection problems. Hence, a total of 110 simulations in approximately 22 h were executed for this analysis.

4.2 | Equivalence analysis

Before we compare the computation time of the blockchain-based and central LEM, we need to ensure that both implementations computed equivalent results. However, equivalent results must be defined first. Since the PDA only sorts market positions by price, it is possible that positions from different users but of the same type and price lead to different results on two different systems because the sorting might place one position before the other. Even though, the results are not equal they can be considered equivalent and valid as long as they maximise social welfare and ensure individual rationality. Therefore, we considered market results equivalent if they cleared an equal social welfare. Social welfare is defined as the area enclosed by the supply and demand curve and the y-axis [48]. All 110 simulated test cases resulted in equivalent market-clearing results. Thus, we have demonstrated that a blockchain-based LEM is capable of computing equivalent results to a centralised implementation.

4.3 | Time complexity analysis

In this subsection, we present the results of the time complexity analysis. In a time complexity analysis, we insert an increasing amount of data into our function under investigation and measure the times basic operations are executed or the wall clock time the algorithm under investigation requires to process inserted data. In a blockchain setup, we need to consider a significant amount of time to wait for transaction receipts that ensure the correct processing of the data. Therefore, a pure consideration of the basic operations would be insufficient. Hence, we assume wall clock measurements of a time complexity analysis with 10 simulations of the same experimental setup and visualising the distribution of those measurements as a reasonably accurate approach to evaluate and compare the performance of the centralised and blockchain-based LEM. We acknowledge that wall clock measurements are dependent on the network load and the executing machine. Therefore, we limited the blockchain network load as much as possible by only executing LEM-related transactions during the experiment. These measurements are then used to evaluate the performance and scalability of the two LEM implementations.

Figure 2 shows the computation time of the centralised and blockchain-based LEM. The measurements include the time to post the market positions on the LEM, calculate a market-clearing price, log meter readings, and settle the LEM. Additionally, we calculated the ratio of the means of the computation times for each number of inserted positions. All shown data points were fitted with polynomials from the numpy *polyfit* library. Coefficients and residuals for the fitting curves are summarised in Table A1.

Since both versions of LEM are triggered and run on the same computer, the results depend on the computer's performance. As the simulations ran for approximately 22 h inside the institute's internal network, we were not able to exclude all peripheral network load effects. However, the spreads of results across the 10 samples in Figure 2 show that most peripheral network load effects were within insignificant ranges and allow us to use our timing results as reasonable comparative parameters. The centralised LEM takes 0.65 s to process 50 and 2.3 s for 550 market bids. The green dotted curve represents a second-order polynomial.

The blockchain-based LEM processes 50 bids in 94 s and 550 bids in 1343 s on average. The blue dotted curve is a second-order polynomial. Diamond markers in Figure 2 visualise the ratio between the mean blockchain-based and centralised LEM computation times and allow us to quantify the performance of the two algorithms independent of the executing machine's performance. We see that the computation time for 50 bids is 144 times and, for 550 bids, it is 583 times larger than on the blockchain-based LEM.

Since the calculation time for 450 entered market positions already exceeds a 15 min market interval, we consider the entered number of market positions to be sufficient to evaluate the usability of a blockchain-based LEM in a realistic environment.

Furthermore, we analysed which functions require the most computation time and visualised the percentage of computation time for the centralised and blockchain-based LEM in Figure 3. In the case of the central LEM, the computation shares stay almost constant from 50 to 550 inserted bids. Posting bids consumes from 2.6% to 5.5%, logging meter readings less than 1%, clearing the market 41%–44%, and settling the market 52%–56% of the computation time on the central LEM. On the blockchain-based LEM, the shares shift from the lowest to the highest amount of inserted bids significantly. The share for market clearing increases from 38% for 50 inserted bids to 58% for 550 bids. At the same time, the share for the market settlement decreases from 53% for 50 bids inserted to 37% for 550 bids. Posting bids and logging meter readings stay in the ranges from 5% to 1% of the computation time.

Based on these results, the blockchain-based market-clearing algorithm should be the first to be investigated in terms of its optimisation potential. The appendix contains the results of the Ethereum-specific gas consumption (see Figure A1).

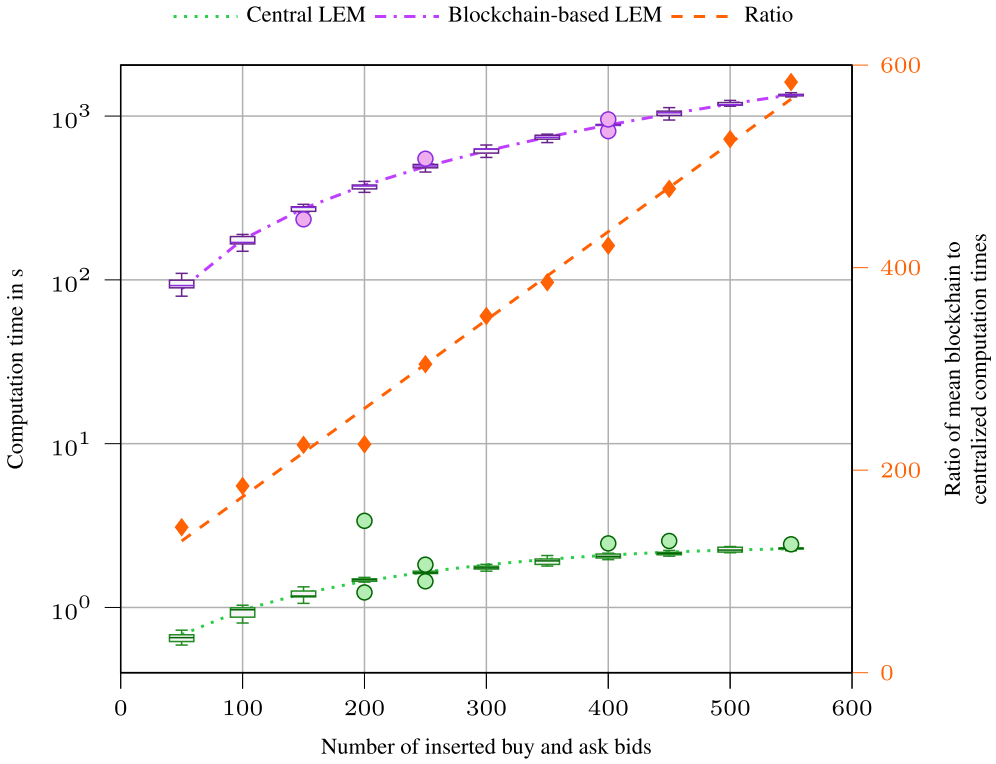

FIGURE 2 Purple and green box plots show the computation time in seconds on the left *y* axis. Outliers are marked as circles. Boxes indicate the first and third quartile, and whiskers 1.5 of the inter-quartile range (between first and third quartile). Orange markers indicate the ratios of mean blockchain to centralised Local Energy Market (LEM) computation times as a scatter plot on the right *y* axis. Coefficients for the polynomial fitting curves are summarised in Table A1

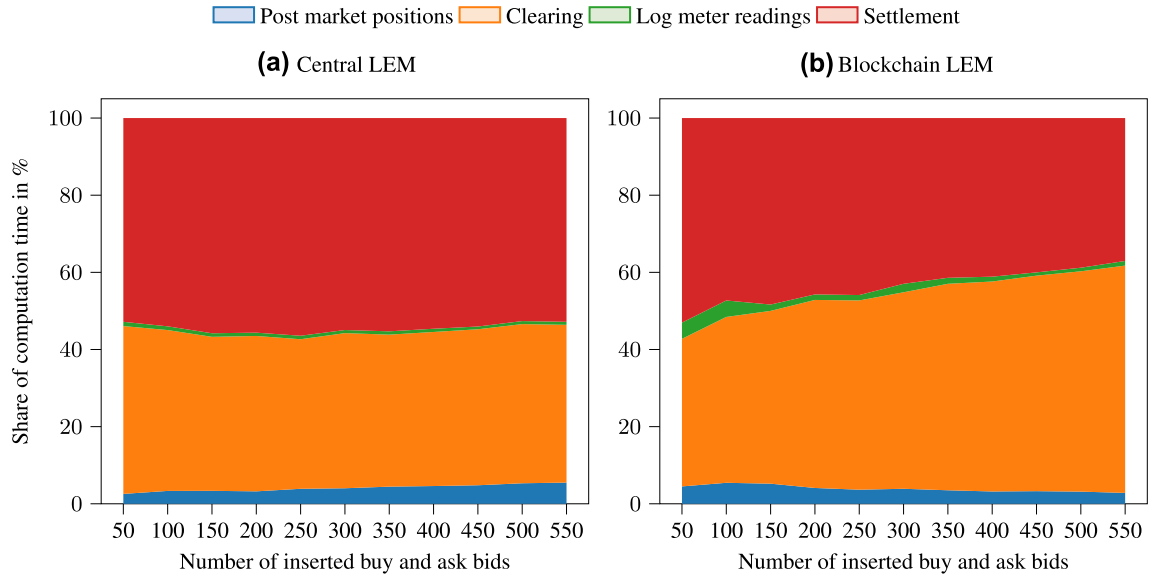

FIGURE 3 Share of computation time used for the main Local Energy Market (LEM) functions: posting bids, market clearing, meter reading logging, and market settlement in the blockchain-based and central LEM

5 | DISCUSSION

We will first discuss whether both implementations meet the LEM specific infrastructure requirements introduced in section 2 before putting the results in a broader perspective.

As mentioned in section 4.2, we were able to compute equivalent results on the blockchain-based and central LEM. Hence, we conclude that both implementations are reliable in terms of correct data processing. It is worth mentioning that this correct data processing was only possible with the help of

waiting periods for transaction receipts that increased the overall computation time extensively and made the wall time measurements necessary for the time complexity analysis. In addition, the blockchain-based LEM did not prove to be continuously available during the analysis because the blockchain node lost frequently the connection to the network and needed to be restarted due to unidentifiable synchronisation problems. On the other hand, the central LEM did not cause any connection problems during our analysis. Hence, we conclude that the blockchain-based LEM is less reliable for a continuous operation compared to a centralised implementation.

As the open-source project *lemlab* shows, a LEM is programmable and deployable on an Ethereum blockchain network. The results of the performance analysis indicate that the implemented blockchain-based LEM is scalable up to 400 bids in a time of less than 900 s, which would correspond to a 15-min market interval. Further improvements in the code can potentially increase the number of processable market positions in both implementations but we do not expect the relative difference of computation times to be significantly affected. Therefore, we conclude that the blockchain-based LEM is limited in its scalability and would likely not allow the use of advanced market-clearing algorithms such as optimisation functions. The central LEM processed 550 market positions in less than 3 s and single experiments showed that 10,000 market positions can be processed in less than 5 min. Noteworthy are the necessary modifications of the blockchain parameters such as gas floor target, transaction gas limit, and gas capacity to 1.5 billion gas in order to insert transactions for the market clearing with more than 1 billion gas. If we would have kept them at their default with an average of 15 million gas, we would not have been able to process 50 bids on the LEM and would have needed to split the functionality further apart.

In addition, we want to point out major challenges that hindered an efficient implementation: basic libraries for sorting and filtering data on blockchains are not available, variable size arrays could not be initialised, debugging Solidity code is still a major obstacle and slows down development due to missing integrated development environments for larger code projects, and the stability of blockchain nodes on Windows machines was insufficient for development but could potentially be fixed with additional blockchain authorities running on Windows machines.

Whether our implementation is GDPR compliant and a pseudonym for users is sufficient to anonymise personal data is a matter of legal assessment and is likely to vary from country to country. What we can say with certainty is that all market positions and meter readings are transmitted to the blockchain network as unencrypted transactions. However, the blockchain-based LEM can be gamed as long as the positions are written unencrypted to the blockchain. Christidis et al. presented three variants of encrypting positions in a first phase and sending a key for their decryption in a second phase that potentially can avoid LEM gaming [31]. Nevertheless, position encryption and decryption would increase computation time and would not be useful for privacy applications such as logging of meter readings. Overall, we conclude that the blockchain-based LEM implementation cannot fulfil the data security requirement. The central LEM can fulfil the requirement as long as the position and meter reading transfer can be encrypted and the access rights to the central database are carefully designed.

By nature, data that is stored in the state of the blockchain is tamper proof as long as hash functions cannot be reversed. In this context, the blockchain has a significant advantage over a centralised system that stores data on a proprietary server and can manipulate it at will. Nevertheless, we would like to emphasise that trusted entities that insert data into the blockchain are potential vulnerabilities in terms of tamper proof. If they are not completely trustworthy, the advantage of a tamper-proof blockchain is gone. In contrast, the possibilities to manipulate a central LEM are for a market operator manifold. Therefore, a tamper-resistant central LEM requires all LEM participants' trust.

In order to ensure a continuous prosumer household participation, operating costs need to be low, especially, when we consider the significantly smaller energy quantities, compared to a wholesale electricity market. Since we used an energy-efficient PoA consensus mechanism in our setup, the energy demand is insignificantly low and can be compared to a centralised setup that has redundant servers running (see section Blockchain technology). Therefore, we conclude that low operating costs are achievable with a central and a blockchain-based LEM implementation. Table 2 summarises the LEM requirement analysis.

Finally, the question remains as to how decentralised our blockchain-based LEM actually is. In our LEM, we need a market operator who adds users, maps them to their meter readings, keeps them accountable for their actions on the LEM, and triggers the market clearings periodically. Some of those functionalities could be implemented in smart contracts but would further inflate the computation time and were out of the scope of this project. Additionally, we would need to select trustworthy authorities that validate new blocks and ensure that they do not illegally collude. In summary, a decentralised blockchain-based LEM would need to be designed extremely carefully, is not readily feasible, and may need to be regulated.

TABLE 2 Qualitative comparison of Local Energy Market requirement fulfilment

LEM requirement	Central LEM	Blockchain-based LEM
Reliability	+ +	+[b]
Scalability	+ +	−[c]
Data security	+ +	− −
Tamper resistance	+[a]	+ +
Low operating costs	+ +	+ +[d]

[a]If market operator trustworthy.

[b]If we wait for transaction receipts.

[c]Up to 400 market positions for a 15 min market interval.

[d]If we use energy-efficient and not completely decentralised consensus mechanisms.

6 | CONCLUSION

This paper presents LEM specific infrastructure requirements, a modular open-source Solidity toolbox for LEMs that allows to develop applications for a blockchain-based and a central reference setup in parallel and to quantify and evaluate their performances against each other. Furthermore, we show the results of a comparative performance analysis and discuss whether the technology-independent LEM specific infrastructure requirements are met by the blockchain-based and central LEM implementations. Our results indicate that the blockchain promises of a decentrally and transparently managed infrastructure can only be realised to a limited extent in the context of LEMs, that a blockchain-based LEM implementation is reliable but requires more than 140 times the computation time compared to a centralised implementation, and cannot fulfil data security requirements. Only the tamper resistance represents a significant added value that comparable centralised implementations cannot provide to a similar degree. Thus, we conclude that blockchain technology in its current state of development is not a 'game changer' for LEMs. Nevertheless, we invite researchers to collaborate and work on the open-source LEM toolbox [47], adapt it to their needs, and send us their suggestions for improvements. The solidity toolbox for LEMs is another part in the scientific toolset to model prosumer-centric applications more precisely and evaluate the potential of blockchain implementations in the energy context. Future research should focus on the identification of optimisation potential, verifiable tamper resistance in proprietary systems, data security on blockchains and their legal assessment, and a deeper analysis of the timing complexity.

ACKNOWLEDGEMENTS

This work was funded by the Bavarian Ministry of Economic Affairs, Regional Development and Energy, Germany and supported by the Zentrum Digitalisierung.Bayern, Germany (grant number IUK589/001).

Open access funding enabled and organised by Projekt DEAL.

CONFLICT OF INTEREST

The authors have no conflicts of interest to declare that are relevant to the content of this article.

DATA AVAILABILITY STATEMENT

The data that support the findings of this study are openly available in lemlab repository at https://github.com/tum-ewk/lemlab.

ORCID

Michel Zade https://orcid.org/0000-0002-4949-9960

REFERENCES

1. Renewable capacity statistics 2021 (19.04.2021) https://www.irena.org/publications/2021/March/Renewable-Capacity-Statistics-2021
2. European Parliament, Council of the European Union. Directive (eu) 2019/944 of the european parliament and of the council of 5 june 2019 on common rules for the internal market for electricity and amending directive 2012/27/eu (recast): directive (eu) 2019/944 (06/2019) (2019). https://eur-lex.europa.eu/legal-content/EN/TXT/?uri=uriserv:OJ.L_.2019.158.01.0125.01.ENG&toc=OJ:L:2019:158:TOC
3. Khorasany, M., Mishra, Y., Ledwich, G.: Market framework for local energy trading: a review of potential designs and market clearing approaches, IET Generation. Transm. Distrib. 12(22), 5899–5908 (2018). https://doi.org/10.1049/iet-gtd.2018.5309
4. Post-2025 market design: directions paper (2021). https://esb-post2025-market-design.aemc.gov.au/32572/1609802925-p2025-january-directions-paper.pdf
5. Mengelkamp, E.M.: Engineering local electricity markets for residential communities (2019). https://doi.org/10.5445/IR/1000095229
6. Tushar, W., et al.: Peer-to-peer energy systems for connected communities: a review of recent advances and emerging challenges. Appl. Energy. 282, 116131 (2021). https://doi.org/10.1016/j.apenergy.2020.116131
7. Andoni, M., et al.: Blockchain technology in the energy sector: a systematic review of challenges and opportunities. Renew. Sustain. Energy Rev. 100, 143–174 (2019). https://doi.org/10.1016/j.rser.2018.10.014
8. von Perfall, A., et al.: Blockchain - chance für energieverbraucher? kurzstudie für die verbraucherzentrale nrw. düsseldorf (2016)
9. Burger, C., et al.: Blockchain in der energiewende (2016). https://www.esmt.org/system/files_force/dena_esmt_studie_blockchain_deutsch_0.pdf?download=1&download=1
10. Bogensperger, A., et al.: Die blockchain-technologie - chance zur transformation der energiewirtschaft? berichtsteil anwendungsfälle (2018). https://www.ffe.de/attachments/article/846/Blockchain_Teilbericht_UseCases.pdf
11. Wang, J., et al.: A novel electricity transaction mode of microgrids based on blockchain and continuous double auction. Energies. 10(12), 1971 (2017). https://doi.org/10.3390/en10121971
12. Kang, J., et al.: Enabling localized peer-to-peer electricity trading among plug-in hybrid electric vehicles using consortium blockchains. IEEE Trans. Ind. Inf. 13(6), 3154–3164 (2017). https://doi.org/10.1109/TII.2017.2709784
13. Peck, M.E., Wagman, D.: Energy trading for fun and profit buy your neighbor's rooftop solar power or sell your own-it'll all be on a blockchain. IEEE Spectrum. 54(10), 56–61 (2017). https://doi.org/10.1109/MSPEC.2017.8048842
14. Sabounchi, M., Wei, J.: Towards resilient networked microgrids: blockchain-enabled peer-to-peer electricity trading mechanism. In: IEEE conference on energy internet and energy system integration, pp. 1–5. EI2 (2017). https://doi.org/10.1109/EI2.2017.8245449
15. Ante, L., Steinmetz, F., Fiedler, I.: Blockchain and energy: a bibliometric analysis and review. Renew. Sustain. Energy Rev. 137, 110597 (2021). https://doi.org/10.1016/j.rser.2020.110597
16. Wang, Q., Li, R., Zhan, L.: Blockchain technology in the energy sector: from basic research to real world applications. Comput. Sci. Rev. 39, 100362 (2021). https://doi.org/10.1016/j.cosrev.2021.100362
17. Hasankhani, A., et al.: Blockchain technology in the future smart grids: a comprehensive review and frameworks. Int. J. Electr. Power Energy Syst. 129, 106811 (2021). https://doi.org/10.1016/j.ijepes.2021.106811
18. Brousmichc, K.-L., et al.: Blockchain energy market place evaluation: an agent-based approach. In: IEEE 9th annual information technology, electronics and mobile communication conference (IEMCON), pp. 321–327. IEEE (2018). https://doi.org/10.1109/IEMCON.2018.8614924. 01.11.2018 - 03.11.2018
19. Okwuibe, G.C., et al.: A blockchain-based double-sided auction peer-to-peer electricity market framework. In: IEEE electric power and energy conference (EPEC), pp. 1–8. IEEE (2020). https://doi.org/10.1109/EPEC48502.2020.9320030. 09.11.2020 - 10.11.2020
20. Zhang, C., Yang, T., Wang, Y.: Peer-to-peer energy trading in a microgrid based on iterative double auction and blockchain. Sustainable Energy,

Grids and Networks. 27, 100524 (2021). https://doi.org/10.1016/j.segan.2021.100524
21. Doan, H.T., Cho, J., Kim, D.: Peer-to-peer energy trading in smart grid through blockchain: a double auction-based game theoretic approach. IEEE ACCESS. 9, 49206–49218 (2021). https://doi.org/10.1109/ACCESS.2021.3068730
22. Chen, S., et al.: A trusted energy trading framework by marrying blockchain and optimization. Adv. Appl. Energy. 2, 100029 (2021). https://doi.org/10.1016/j.adapen.2021.100029
23. Heck, K., Mengelkamp, E., Weinhardt, C.: Blockchain-based local energy markets: decentralized trading on single-board computers. Energy Systems. 12(3), 603–618 (2021). https://doi.org/10.1007/s12667-020-00399-4
24. Machacek, T., Biswal, M., Misra, S.: Proof of x: experimental insights on blockchain consensus algorithms in energy markets. In: IEEE power & energy society innovative smart grid technologies conference (ISGT), pp. 1–5. IEEE (2021). https://doi.org/10.1109/ISGT49243.2021.9372194. 16.02.2021–18.02.2021
25. Blom, F., Farahmand, H.: On the scalability of blockchain-supported local energy markets. In: International conference on smart energy systems and technologies (SEST), pp. 1–6. IEEE (2018). https://doi.org/10.1109/SEST.2018.8495882. 10.09.2018–12.09.2018
26. Liu, S., et al.: A high-performance local energy trading cyber-physical system based on blockchain technology. IOP Conf. Ser. Earth Environ. Sci. 227, 032009 (2019). https://doi.org/10.1088/1755-1315/227/3/032009
27. Foti, M., Vavalis, M.: Blockchain based uniform price double auctions for energy markets. Appl. Energy. 254, 113604 (2019). https://doi.org/10.1016/j.apenergy.2019.113604
28. Esmat, A., et al.: A novel decentralized platform for peer-to-peer energy trading market with blockchain technology. Appl. Energy. 282, 116123 (2021). https://doi.org/10.1016/j.apenergy.2020.116123
29. Troncia, M., et al.: Distributed ledger technologies for peer-to-peer local markets in distribution networks. Energies. 12(17) (2019). https://doi.org/10.3390/en12173249
30. Meeuw, A., Schopfer, S., Wortmann, F.: Experimental bandwidth benchmarking for p2p markets in blockchain managed microgrids. Energy Proc. 159, 370–375 (2019). https://doi.org/10.1016/j.egypro.2018.12.074
31. Christidis, K., et al.: A framework for designing and evaluating realistic blockchain-based local energy markets. Appl. Energy. 281, 115963 (2021). https://doi.org/10.1016/j.apenergy.2020.115963
32. Han, D., et al.: Smart contract architecture for decentralized energy trading and management based on blockchains. Energy. 199, 117417 (2020). https://doi.org/10.1016/j.energy.2020.117417
33. Son, D., Al Zahr, S., Memmi, G.: Performance analysis of an energy trading platform using the ethereum blockchain. In: 2021 IEEE international conference on blockchain and cryptocurrency (ICBC), pp. 1–3. IEEE (2021). https://doi.org/10.1109/ICBC51069.2021.9461115. 03.05.2021 - 06.05.2021
34. Vieira, G., Zhang, J.: Peer-to-peer energy trading in a microgrid leveraged by smart contracts. Renew. Sustain. Energy Rev. 143, 110900 (2021). https://doi.org/10.1016/j.rser.2021.110900
35. Tsaousoglou, G., et al.: Truthful, practical and privacy-aware demand response in the smart grid via a distributed and optimal mechanism. IEEE Trans. Smart Grid. 11(4), 3119–3130 (2020). https://doi.org/10.1109/TSG.2020.2965221
36. Oprea, S.V., Bara, A., Andreescu, A.I.: Two novel blockchain-based market settlement mechanisms embedded into smart contracts for securely trading renewable energy. IEEE ACCESS. 8, 212548–212556 (2020). https://doi.org/10.1109/ACCESS.2020.3040764
37. Muzumdar, A., et al.: A trustworthy and incentivized smart grid energy trading framework using distributed ledger and smart contracts. J. Netw. Comput. Appl. 183-184, 103074 (2021). https://doi.org/10.1016/j.jnca.2021.103074
38. Tushar, W., et al.: Peer-to-peer trading in electricity networks: an overview. IEEE Trans. Smart Grid. 11(4), 3185–3200 (2020). https://doi.org/10.1109/TSG.2020.2969657
39. Iannino, A., Musa, J.D.: Software reliability Advances in Computers Volume 30, pp. 85–170. Elsevier (1990). https://doi.org/10.1016/S0065-2458(08)60299-5
40. Steed, A., Oliveira, M.F.: Scalability. In: Networked graphics, pp. 393–458. Elsevier (2010). https://doi.org/10.1016/B978-0-12-374423-4.00012-4
41. Fudenberg, D., Tirole, J.: Game theory, 6th ed. MIT Press, Cambridge (1998)
42. Shoham, Y., Leyton-Brown, K.: Multiagent systems: algorithmic, game-theoretic, and logical foundations. Cambridge University Press, Cambridge (2009). https://doi.org/10.1017/CBO9780511811654
43. Wah, E., Hurd, D., Wellman, M.: Strategic market choice: frequent call markets vs. continuous double auctions for fast and slow traders. In: Proceedings of the the third conference on auctions, market mechanisms and their applications. ACM (2015). https://doi.org/10.4108/eai.8-8-2015.2260356
44. Harrington, L., Waide, P.: Labels and standards for energy. In: Encyclopedia of energy, pp. 599–611. Elsevier (2004). https://doi.org/10.1016/B0-12-176480-X/00471-X
45. Song, Z., Zhang, X., Liang, M.: Reliable reputation review and secure energy transaction of microgrid community based on hybrid blockchain. Wireless Commun. Mobile Comput. 2021, 1–17 (2021). https://doi.org/10.1155/2021/9916735
46. Zade, M., Lumpp, S.D., Sperling, U.: Reghee - regionaler handel und stromkennzeichnung von erneuerbaren energien über eine blockchain-plattform (2021). https://reghee.de/
47. Lumpp, S.D., et al.: An open-source tool for the agent-based development and testing of local energy market applications (2021). https://github.com/tum-ewk/lemlab
48. Zade, M., et al.: Satisfying user preferences in community-based local energy markets — auction-based clearing approaches. Appl. Energy. 306, 118004 (2022). https://doi.org/10.1016/j.apenergy.2021.118004
49. Edgar, T.W., Manz, D.O.: Science and cyber security. In: Research methods for cyber security, pp. 33–62. Elsevier (2017). https://doi.org/10.1016/B978-0-12-805349-2.00002-9
50. Wood, G.: Ethereum: a secure decentralized generlised transaction ledger berlin version (2021). https://ethereum.github.io/yellowpaper/paper.pdf
51. N. Alzahrani, N. Bulusu, Towards true decentralization: a blockchain consensus protocol based on game theory and randomness, In: L. Bushnell, R. Poovendran, T. Başar (Eds.), Decision and Game Theory for Security, Volume. 11199 of Lecture Notes in Computer Science, Springer International Publishing, Cham, 2018, pp. 465–485. https://doi.org/10.1007/978-3-030-01554-1_27
52. Rauchs, M., Dek, A., Blandin, A.: Cambridge bitcoin electricity consumption index (2021). https://ccaf.io/cbeci/index
53. Zade, M., et al.: Is bitcoin the only problem? a scenario model for the power demand of blockchains. Front. Energy Res. 7 (2019). https://doi.org/10.3389/fenrg.2019.00021
54. Oyinloye, D.P., et al.: Blockchain consensus: an overview of alternative protocols. Symmetry. 13(8), 1363 (2021). https://doi.org/10.3390/sym13081363

How to cite this article: Zade, M., et al.: Evaluating the added value of blockchains to local energy markets—Comparing the performance of blockchain-based and centralised implementations. IET Smart Grid. 1–12 (2022). https://doi.org/10.1049/stg2.12058

APPENDICES

Acronyms

BC	Blockchain
CDA	Continuous Double Auction
DB	Database
GDPR	General Data Protection Regulation
HEMS	Home Energy Management System
LAN	Local Area Network
LEM	Local Energy Market
P2P	Peer-to-Peer
PDA	Periodic Double Auction
PoA	Proof-of-Authority
PoW	Proof-of-Work
VPP	Virtual Power Plant

Blockchain technology

Blockchains are virtual state machines that store data on distributed nodes. The data inserted into a blockchain becomes part of the blockchain's state and is stored as a hashed value in discrete blocks. Hash values refer to outputs of one-way mathematical functions that compute a unique value of a pre-defined length for any kind of input data but make it very difficult to reproduce the input data based on a hash value [49]. Blocks contain the current state and all requested state changes in the form of transactions [50]. When we talk about a chain of blocks, we are referring to each new block that contains a hash value of the previously added block. Advanced blockchains such as Ethereum allow us to deploy code on a blockchain and process data in a programmable manner. These scripts are informally known as smart contracts [50].

In order to decide what state changes are valid, so-called consensus mechanisms were developed for blockchains. Consensus mechanisms refer to network protocols that define how a network of equal and independent nodes can agree on the validity of current and historical states of the shared data [51]. The most prominent consensus mechanism is Proof-of-Work (PoW). PoW allows all nodes in a network to add new blocks to the chain as long as they provide a proof of their 'work' in the form of a hash value that contains all inserted transactions and fulfils a certain condition. This condition could be a certain number of leading zeros. Nodes are motivated to prove their work to the network because they are rewarded with coins in the blockchain's own currency if they are the first ones that compute a hash value that fulfils the aforementioned conditions. The outcome of a hashing function cannot be foreseen with today's computers and therefore must be computed by trial and error. This process is energy intensive and therefore widely criticised [52, 53]. To avoid the high energy demand in blockchains, the PoA consensus mechanism was introduced [54]. As the name indicates, selected authorities are allowed to validate blocks and append them to the blockchain. This reduces the energy demand of the blockchain significantly but at the same time does not provide a similarly decentralised structure as the PoW consensus mechanism. Over the past years, a variety of other consensus mechanisms were proposed to tackle these challenges [54].

Polynomial fitting functions and residuals

Table A1 lists all polynomial coefficients used to fit the data in Figure 2 and residuals.

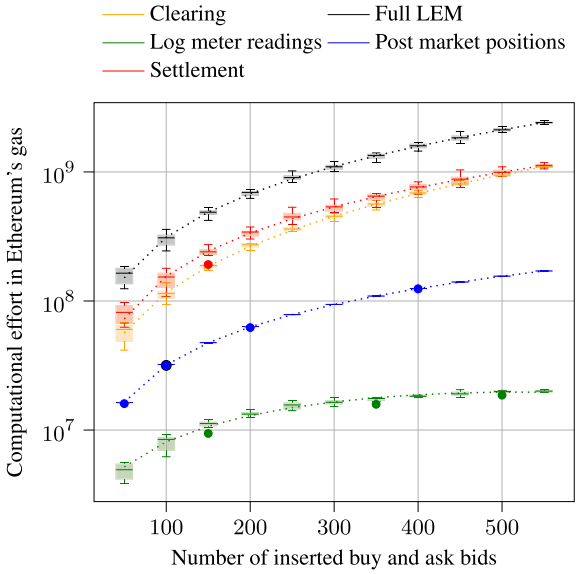

FIGURE A1 Computation effort in Ethereum's gas as box plots. Outliers are shown as circles

TABLE A1 Coefficients and residuals of polynomial fitting curves

	Computation time Central LEM	Blockchain-based LEM	Ratio of mean Computation times
a	$-5.5*10^{-6}$	$1.7*10^{-3}$	$8.7*10^{-1}$
b	$6.5*10^{-3}$	1.5	86.4
c	$3.7*10^{-1}$	8.2	
Residuals	$4.8*10^{-2}$	313	2156.3

Gas analysis

Figure A1 shows the computational effort for the different main functions of the blockchain-based LEM in Ethereum's own computation currency 'gas'. The clearing and settlement of the LEM consume most of the gas. Settling the market consumes slightly more gas than clearing the market up until 500 inserted bids and seems to reach a tipping point at 550 bids. Noteworthy is that the settlement is split up into four separate transactions while the clearing of the market is initiated with a single transaction. Hence, we assume the additional gas consumption from 50 to 500 bids is due to transaction overheads.

2.3 Digression: Power demand of Bitcoin and Ethereum

In parallel to the rising interest in energy-related use cases with blockchain technology, researchers questioned and investigated the power demand of blockchain protocols and the underlying consensus mechanism [96, 97, 98, 99]. Consensus mechanisms are network protocols that define how a network of independent and equal blockchain nodes agrees what past and current state transitions are valid [100]. As part of a preparatory investigation of the blockchain technology, I conducted a scenario analysis with a power demand model published by Malone and O'Dwyer [97] and investigated parameters influencing the power demand of Bitcoin and Ethereum.

Based on mining hardware data [101], the Bitcoin and Ethereum blockchain protocol, and publicly available historical blockchain parameter data, the analysis presented scenarios for potential power demands up until 2025. The results indicated that the average power demands were 3.9 GW for the Bitcoin and 1 GW for the Ethereum network in 2018. Furthermore, the scenarios showed that more efficient mining hardware would have only a limited impact on future power demands as long as the block difficulty of the mining process grows exponentially as was the case from 2016 to 2018.

The results of the analysis are published in a peer-reviewed article and included in this dissertation in appendix B. Based on a variety of energy consumption models including ours, the Cambridge Bitcoin Electricity Consumption Index provides a live visualization of the power demand of the Bitcoin blockchain.

Even though the results presented in this article describe power demands for the operation of blockchain networks that are comparable to entire countries such as Ecuador, alternative and more energy efficient consensus mechanisms allow to reasonably consider energy-related applications on a blockchain [102].

Chapter 3

Flexumers' market-based flexibility

Scientific context

By 2050, more than 30 TW of renewable generation capacity will be installed globally to supply more than 50 % of the final energy demand with electricity [5, 2]. VRE will be used in the transportation and heating sectors [14] and will cause grid congestions that cannot completely be prevented due to lengthy administrative processes, economic reasons, and acceptance problems of grid expansions [49, 2]. Therefore, to integrate the projected and increasing quantities of VRE into energy systems, power grids need to be expanded and grid congestion management measures enhanced.

In the 2010s, large-scale power plants with more than 10 MW capacity were asked to provide countermeasures for grid congestion management with rule-based frameworks such as redispatch in Germany [103]. Since 2017, grid congestion management in Germany cost on average more than 1.4 B€ annually (see figure 1.1). As of 2021, power plants with generation capacities of more than 100 kW have to provide redispatch services in a rule-based setting in Germany [104]. This development raises the question whether flexumers are technically feasible, can provide a cost-effective alternative to existing countermeasures, and can reduce grid management costs [105, 2, 106].

Currently discussed grid congestion management measures can be divided into two categories: dispatch and flexibility [49]. Dispatch measures refer to mechanisms that consider potential grid congestions already during dispatching processes on energy markets with nodal pricing, zonal bidding, or load-variable grid fees. Flexibility measures are procured by grid operators after the dispatching process has been completed on flexibility markets or on the basis of regulatory frameworks. In this chapter, I focus on market-based procurement of flexibility, which was the subject of extensive research in recent years [22, 107, 108, 109, 110] and is currently considered by the EU to be the most efficient method to transparently and non-discriminatory prevent congestions in distribution grids [15].

According to the European Clean Energy Package, market-based flexibility procurement allows grid operators to trade flexibility bilaterally or in an organized market with active network participants directly or through third parties that act on their behalf [105]. Active network participants refer in this chapter to flexumers that are able to offer their flexibility to grid operators [15]. Since grid congestion management measures are monopolistic, close regulatory oversight is necessary [105].

In this context, the following section presents a model for quantifying and pricing flexibility, through which consumers and prosumers become flexumers that help ensure security of supply while the energy system becomes carbon-neutral and volatile. A case study in the second section quantifies how much and at what time flexibility from EVs can be expected in the future with realistic Californian and German mobility behavior, charging strategies, and electricity pricing tariffs.

3.1 Quantifying and pricing flexibility

Contribution

Consumers and prosumers install generation units on their premises, buy EVs, optimize their own consumption, and in the future potentially participate in a certain form of energy trading as described in chapter 2. However, their market-based flexibility has so far not been used to prevent grid congestions. The EU directive 2019/944 lays the regulatory groundwork to transform consumers and prosumers into flexumers by explicitly mentioning their role and declaring them as essential participants of a renewable and carbon neutral energy system [15]. When the paper of this section was published in 2018, no prior work could be found quantifying and pricing flexumers' market-based flexibility.

Therefore, the paper referred to in this section introduces a flexibility quantification and pricing model for consumers, prosumers, and their controllable assets. A schematic of the model is visualized in figure 3.1.

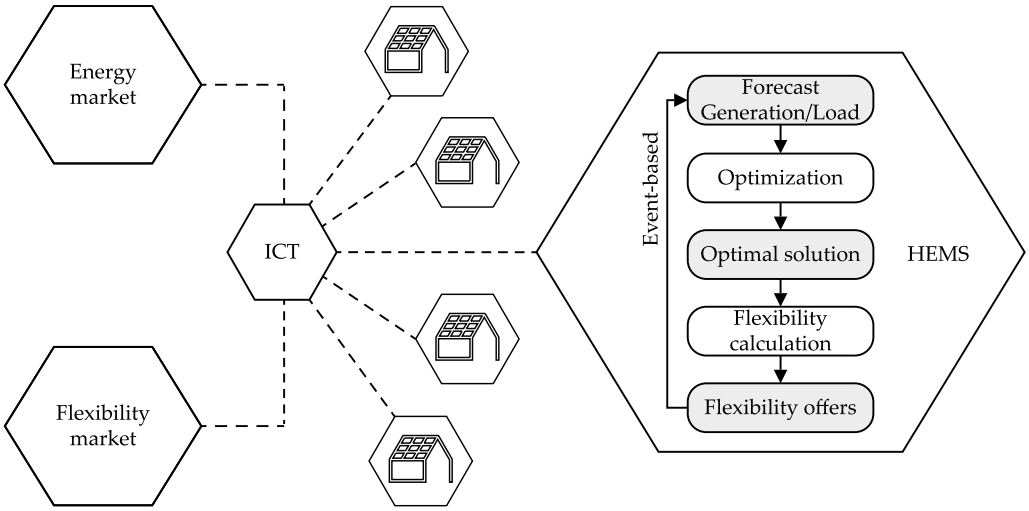

Figure 3.1: Schematic of a HEMS for a flexumer and its connections to energy and flexibility markets. Within the HEMS, gray boxes show data in- and outputs and white boxes the implemented functionality. Figure was taken from [101] and graphically edited © 2018 IEEE.

The model can be subdivided into two main steps: First, the operation of controllable household appliances are optimized with a mixed-integer linear programming model.

Based on the outcome of the optimization, a market agent buys or sells energy quantities on an energy market on behalf of the household. In the second step, the flexibility potential for each controllable household appliance is quantified and priced separately based on electricity price forecasts, appliance availability, and user comfort. These flexibility potentials are then offered by a market agent on a flexibility platform, which allows grid operators to prevent grid congestions cost-efficiently. The entire process will start over if the grid operator calls the household's flexibility. In the future, such a method can be integrated into HEMSs that have interfaces to all controllable household appliances, have the computational capacity either on-site or in the backend and control the household appliances' operations.

The following article describes the model using the example of an EV, explains why EV owners will pay in the future to provide flexibility, proposes a format for flexibility offers, and shows how HEMSs re-optimize the operation schedules of the appliances once flexibility has been called. The article was submitted to the 2nd IEEE Conference on Energy Internet and Energy System Integration (EI2), received one of the best paper awards, and the model is publicly available in the open-source repository *OpenTUMFlex* [33].

The article presented in this section described the method for EVs, however, other household appliances such as HPs, combined heat and power, and photovoltaic systems were complemented by colleagues at the institute of Energy Economy and Application Technology of the Technical University of Munich and integrated into the open-source project *OpenTUMFlex* [111, 112, 113].

Publication #3: Prosumer Integration in Flexibility Markets: A Bid Development and Pricing Model

Authors Michel Zade, Yasin Incedag, Wessam El-Baz, Peter Tzscheutschler, Ulrich Wagner

Publication medium 2018 2nd IEEE Conference on Energy Internet and Energy System Integration (EI2)

Digital object identifier https://doi.org/10.1109/EI2.2018.8582022

Open-source repository the data and models that support the findings of this study are openly available in *OpenTUMFlex* [33].

Author contributions

Michel Zade:	55 %	Conceptualization, Methodology, Software, Formal analysis, Writing - Original Draft, Writing - Review & Editing, Visualization.
Yasin Incedag:	15 %	Conceptualization, Methodology, Writing - Original Draft, Writing - Review & Editing.
Wessam El-Baz:	10 %	Writing - Review & Editing, Project administration, Funding acquisition.
Peter Tzscheutschler:	15 %	Conceptualization, Methodology, Resources, Writing - Review & Editing, Supervision, Project administration, Funding acquisition.
Ulrich Wagner:	5 %	Resources, Writing - Review & Editing, Supervision, Funding acquisition.

Prosumer Integration in Flexibility Markets: A Bid Development and Pricing Model

Michel Zade
Chair of Energy Economy and Application Technology
Technical University of Munich
Munich, Germany
michel.zade@tum.de

Yasin Incedag
Chair of Energy Economy and Application Technology
Technical University of Munich
Munich, Germany
yasin.incedag@tum.de

Wessam El-Baz
Chair of Energy Economy and Application Technology
Technical University of Munich
Munich, Germany
wessam.elbaz@tum.de

Peter Tzscheutschler
Chair of Energy Economy and Application Technology
Technical University of Munich
Munich, Germany
ptzscheu@tum.de

Ulrich Wagner
Chair of Energy Economy and Application Technology
Technical University of Munich
Munich, Germany
uwagner@tum.de

***Abstract*— The impact of renewable energies on the power grid is continuously increasing. Besides the emission-free power generation, the renewable energies often are the cause for congested grids, component failure and costly interventions by the distribution system operators (DSO) and transmission system operators (TSO) in order to maintain grid stability. The scientific community discusses in recent years the usability of distributed energy resources (DER) as flexible devices. However, no approach can be found that actually quantifies the potential flexibility and sets a price to it. The model presented in this paper optimizes the charging operation of an electric vehicle (EV) according to a price signal with a state of the art exhaustive search algorithm. Furthermore, this model offers all possible deviations from the optimal operation as flexibility to a corresponding market platform and sets a price to each offer, which is dependent on the future price level of the energy. With this model, it is possible to offer positive and negative prices for flexibility. The proposed model shows that an exhaustive enumeration algorithm is feasible to calculate flexibility offers, prices and applicable on currently discussed platform models. The example of an EV charging schedule is successfully modelled and described in this paper.**

Keywords—flexibility platform, distributed energy resources, home energy management system, operation planning, electric vehicles, smart grids

I. INTRODUCTION

The Union of the Electricity Industry (Eurelectric) describes flexibility as "the modification of the generation injection and/or consumption patterns in reaction to an external signal (price signal or activation) in order to provide a service within the energy system. The parameters used to characterize flexibility include the amount of power modulation, the duration, the rate of change, the response time, the location, etc." [1]

In accordance to the above mentioned definition, positive flexibility describes the consumption of energy or the postponement of feeding energy into the grid at times when it was initially scheduled. Negative flexibility means the exact opposite, i.e. to refrain from consuming energy or feeding energy into the grid at times when it was not scheduled.

On a large scale (> 1 MW) flexibility measures are already common practice to maintain grid frequency and avoid grid congestion. Concepts like 'redispatch' on the supply side, as well as demand-side-management in energy intensive industries are grid ancillary services applied by transmission system operators (TSO) and distribution system operators (DSO) today [2, 3, 4]. However, in addition to already available energy markets and regulatory mechanisms, the idea of a separate, flexibility platform or market arises and is proposed more frequently in academic and industrial research [5, 6, 7, 8, 9, 10]. Proposed platforms are meant to be accessible, not only by large industrial parties, but also by small DER, such as residential heat pumps (HP), combined-heat-and-power units (CHP), electric vehicles (EV) as well as photovoltaic (PV) and battery storage units. Such a platform would provide an alternative to grid expansion, modulation of large power plants and especially curtailing renewables and therefore allow the DSO and TSO to manage grid congestions in a more cost-effective and resource-efficient manner [11, 12].

The paper at hand presents a novel home energy management system (HEMS) which provides the opportunity to participate in above mentioned flexibility market, as well as in a regular energy market. State-of-the-art HEMS are mostly known to determine the cost-optimal operation of energy generation and storage units within a household, mostly by utilizing mixed-integer-linear programming (MILP) or meta-heuristic search algorithms, such as genetic algorithm (GA) [13, 14, 15]. However, the proposed HEMS will - on top of finding the cost optimal operation strategy – find every deviation from this optimized schedule and post them as flexibility options on flexibility market platforms, by determining a price and considering user and unit specifications. This approach is considered an exhaustive enumeration method, which is often criticized for its high computational costs [16, 17].

Flexibility market concepts for residential participants are designed and discussed in various different forms by current research projects, the most prominent ones in Germany/Europe being Invade H2020, Empower H2020, Flex4Energy, Enko, and SINTEG C/sells [18, 19, 20, 21, 22]. The main distinction between an existing energy market and a potential flexibility market is that power (kW) is traded, instead of energy (kWh). The demand is given by the congestion forecasts of DSOs and TSOs. A flexibility platform that is currently developed within the project C/sells is based on the following premises:

978-1-5386-8549-5/18/$31.00 ©2018 IEEE

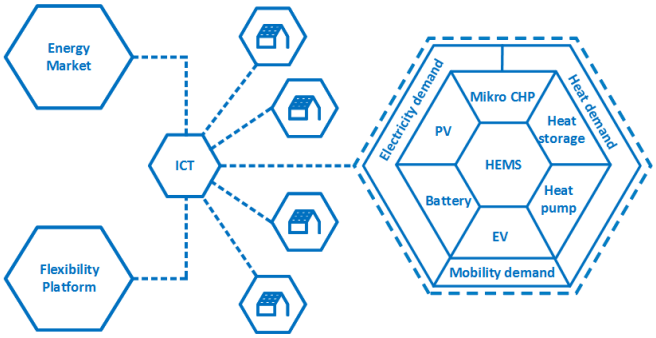

Fig. 1 Schematic of the HEMS and its connection to the energy market and to the flexibility platform

- Day-Ahead and congestion predictions are performed by DSO and TSO to generate flexibility demand
- Flexibility offers are posted for the next 24 hour in 15 minute intervals on the platform
- Every participant has direct access to the platform and can place offers
- Call and settlement will be communicated 15 minutes before delivery
- The efficiency of a flexibility measure on grid instances will be calculated by the platform itself and factored in to the given price
- A flexibility offer by a HEMS is defined by the following parameters: Time and date, negative/positive flexibility (power), available energy (negative/positive) and costs

In the following, a HEMS model for participation on a flexibility platform with above mentioned characteristics is proposed and described in detail.

II. Method

Fig. 1 visualizes the home energy management system (HEMS) as the central control unit of a property and the connected devices therein (e.g. electric vehicles (EV), heat pumps (HP), cogeneration units (CHP), heat storages and batteries). In Fig. 2 the functional overview of the HEMS is displayed. At the beginning of any optimization and calculation of flexibility offers the HEMS is supplied with input data. Afterwards, the optimization algorithm calculates an operating strategy for each device that minimizes energy costs. The coverage of the electricity, heat and mobility demand is the most important constraint and has to be fulfilled at any time. In accordance to the optimization result the HEMS will then buy or sell energy on the energy market for the operation of the connected distributed energy resources (DER). Deviations from the optimal solutions can further be offered as flexibility to a flexibility platform. The following subsections will describe the functionalities of the HEMS from Fig. 2 in detail.

A. Input Data, Generation and Consumption Forecast

In order to optimize the devices operation the HEMS depends on input data from multiple parties such as the user, weather stations, forecast provider or the DER itself. Device parameters are either set at the initial operation by setting for example an EV's battery capacity, maximum charging power etc. On the other hand, some parameters are continuously communicated when a new unit state occurs or for example certain boundaries such as the maximum SOC have been reached. The user provides general operational constraints. For example, the user sets the time when he needs to have a fully charged EV, what temperature level he would like to maintain inside his house, or at what time he might have scheduled to turn on his sauna. Besides those inputs from parties within the household the HEMS is fed with historical data and forecasts of the upcoming weather conditions and energy prices.

Based on all the described input data, the HEMS formulates constraints that limit the possibilities of the unit's operation. Below are the fundamental constraints of the model for the charging process of an EV listed.

$$t_{\text{operation}} \geq \frac{\left(SOC_{\text{Bat,desired}} - SOC_{\text{Bat}}(1)\right) \cdot E_{\text{Bat,cap}}}{P_{\text{Bat,charg,max}}} \quad (1)$$

$$P_{\text{Bat,charging}}(t) \leq P_{\text{Bat,charg,max}} \quad \forall t \in 1, \dots, end \quad (2)$$

$$SOC_{\text{Bat}}(t) \leq SOC_{\text{Bat,max}} \quad \forall t \in 1, \dots, end \quad (3)$$

$$SOC_{\text{Bat}}(t_{\text{end}}) = SOC_{\text{Bat,desired}} \quad (4)$$

The first constraint (1) covers that the operation time $t_{\text{operation}}$ is greater or equal than the time it takes to charge the battery with maximum charging power $P_{\text{Bat,charg,max}}$. $SOC_{\text{Bat,desired}}$ indicates the desired SOC of the user at the pick-up time, $SOC_{\text{Bat}}(1)$ the initial SOC and $E_{\text{Bat,cap}}$ the battery capacity in kWh. Constraints (2) and (3) limit the charging power and SOC during all time steps t. Equation (4) ensures that the desired SOC is reached at the last time step t_{end}. Non-negativity and further constraints are neglected within this brief summary.

Based on all the formulated constraints and input data the HEMS starts to forecast the energy consumption and generation of the entire household and the devices therein.

B. Optimization Approach

A fundamental difference between the approaches discussed in section I is the usage of an exhaustive search method to find the connected devices' optimal cost operation. Because only if all possibilities are available, the model offers the entire solution space as flexibility and likewise calculates its costs. The brute-force method is often criticized for its high computational cost [16, 17]. However, in the case of a HEMS the presented model finds the cheapest operation plan for the case of an EV charging optimization within less than 1 second on a state-of-the-art personal computer. Prerequisites are accurate thermal and electric demand forecasts, a temporal resolution of 15 minutes and that the number of possibilities is furtherly reduced by constraints. The model's temporal resolution is set in accordance to common forecasting and data acquisition models, the European energy market, and the flexibility platforms developed in current research projects [22]. Therefore, this method is used in this model to calculate the cheapest operation plan.

Once all constraints are formulated, all possible operation plans of the unit can be extracted. Operation plans that do not fulfill the aforementioned constraints are disregarded. The next step is to calculate the operation plan's cost by summing up the consumption at each time step and multiplying it by the energy prices which are given as a price forecast to the HEMS. Based on the calculated costs of each operation plan the cost optimal solution can be determined.

Finding the cost optimal solution for the charging process of an EV follows the above mentioned method. First, the necessary time to charge the EV with maximum power $t_{\mathrm{min,Bat,charg}}$ is calculated in (5).

$$t_{\mathrm{min,Bat,charg}} = \frac{\left(SOC_{\mathrm{Bat,desired}} - SOC_{\mathrm{Bat}}(t_1)\right) \cdot E_{\mathrm{Bat,cap}}}{P_{\mathrm{Bat,charg,max}}} \quad (5)$$

Equation (6) divides $t_{\mathrm{min,Bat,charg}}$ by the HEMS' temporal resolution to calculate the necessary time steps $n_{\mathrm{tSteps,min,Bat,charg}}$ for charging the EV.

$$n_{\mathrm{tSteps,min,Bat,charg}} = \frac{t_{\mathrm{min,Bat,charg}}}{n_{\mathrm{minutes/timeslot}}} \quad (6)$$

Next, the model sorts the time table by price forecast in ascending order. The cost optimal charging plan is then, to charge the EV at the $n_{\mathrm{tSteps,min,Bat,charg}}$ first time steps of the sorted price forecast with maximum power.

After determining the cost optimal solution of the DER the HEMS interacts with the day-ahead energy market, buys energy and communicates the charging plan to the unit control. The next subsection will discuss how the HEMS will determine the flexibility offers of the DER.

C. Flexibility Offers

The DSO is interested in the information of how much power the DER can offer as flexibility, for how long, at what location in the grid, and at what price. Therefore, a HEMS that offers flexibility must answer all of the mentioned characteristics. As described in section I, flexibility is defined as the "modification of generation injection and/or consumption" [1]. Hence, it is essential to analyze the 'normal', in the presented model the cost optimal, operation, in order to determine possible 'modifications' of the operation plan and offer those to a flexibility platform.

1) Location, Positive, and Negative Flexibility

The location of DER is a constant and therefore, can be set just once. For the German grid the description of the location can be described by the accounting grid, grid area and an identification number of the DER set by the DSO or TSO.

Positive flexibility in terms of consuming energy can be summarized as charging an EV, a battery or operating a HP. From the perspective of a CHP unit, positive flexibility can be offered by stopping the operation of the unit or feeding electrical energy into a local battery instead of the grid. Negative flexibility can be offered by the same DER by stopping the charging operation of an EV or the operation of a HP, starting to feed electrical energy into the grid with the CHP, PV unit or the battery. Therefore, with all above mentioned units positive and negative flexibility can be offered.

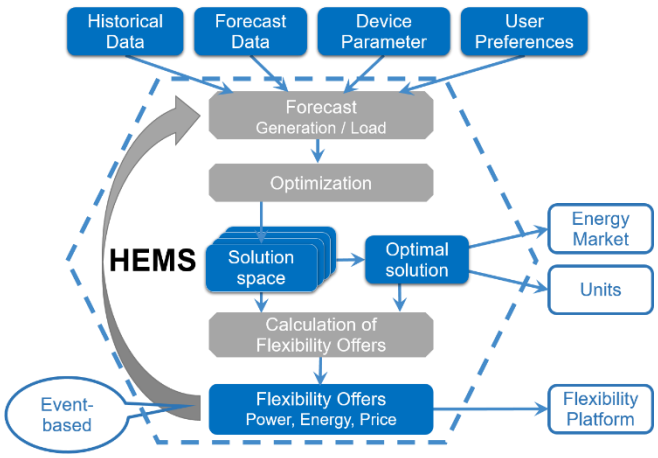

Fig. 2 Functional overview of the HEMS

For the example of an EV, the decision whether it can offer positive or negative flexibility is dependent on the charging plan. Is the EV currently not charging and not fully charged, positive flexibility can be offered. On the other hand if the EV is scheduled to be charged, negative flexibility can be offered.

After determining the direction of the flexibility and at which location it can be offered it is important to quantify the power and energy to be offered.

2) Power, Duration and Energy

The DER's operating power is mostly limited by design and only in a few cases dependent on the unit's current state. Therefore, the presented model uses the maximum power as the power with which it can offer flexibility. In the case of a HP and positive flexibility it is the maximum operating power or in the case of negative flexibility the planned operating power.

The duration for which the flexibility $t_{\mathrm{Flex,offer}}$ can be offered is calculated in (7). $E_{\mathrm{Flex,offer}}$ sets the amount of energy $E_{\mathrm{Flex,offer}}$ that can be consumed, restrained or generated and the offered power $P_{\mathrm{Flex,offer}}$ is set as above mentioned.

$$E_{\mathrm{Flex,offer}} = P_{\mathrm{Flex,offer}} \cdot t_{\mathrm{Flex,offer}} \quad (7)$$

The amount of energy is always dependent on the unit's current state. Using the example of a battery storage the flexibility that can be offered depends on its SOC. Similarly, the CHP and HP's flexibility depends on the SOC of the heat storages that are connected to them and the load that is consuming energy. If no heat storages are installed the flexible energy will depend on the heat storage capacity of the supplied building and its current state.

Coming back to the example of an EV, the offered flexible power is equal to the maximum charging power as positive flexibility and the planned charging power as negative flexibility. In the case of an initial SOC of 50 % and a battery capacity of 80 kWh the flexible energy can be ±40 kWh.

3) Price of the flexibility

After determining all technical characteristics of a flexibility offer, the final step is to calculate a reasonable price that ensures the reimbursement of additional effort, considers a financial risk on the energy market, and creates a high probability of being called. In order to fulfill those requirements (8) to (10) were developed.

In (9) the cost for a kWh of positive flexibility is calculated. Meaning, the unit's offered flexibility price when the HEMS already bought the energy on the day-ahead market for a later operation but it is being called up for operation ahead of time. Hence, when a flexibility call occurs, the HEMS can sell the pre-bought energy on the intra-day market and even offer negative prices for positive flexibility. Negative prices mean that the HEMS pays money to be called up for flexibility. Similar to (7), (8) calculates the number of offered flexibility time steps $n_{\mathrm{off,Flex,tSteps}}$ by dividing the offered energy by the power at time step i and the number of time steps per

hour $n_{\mathrm{tSteps/hour}}$. In (9) the average of the $n_{\mathrm{off,Flex,tSteps}}$ minimal prices is multiplied by a factor consisting of the risk margin R_{margin} from which minus 1 is subtracted. The risk margin can be in the range of 0 to 1. Zero indicating a very low risk and the expectancy to sell energy at the buy-in price and one expecting high fluctuations on the intra-day market.

$$n_{\mathrm{off,Flex,tSteps}} = \frac{E_{\mathrm{Flex,offer}}(i)}{P_{\mathrm{Flex,offer}}(i) \cdot n_{\mathrm{tSteps/hour}}} \tag{8}$$

$$c_{\mathrm{pos.,Flex}} = mean\left(mink\left(c_{Forecast}(i\colon i_{\mathrm{end}}), n_{\mathrm{off,Flex,tSteps}}\right)\right) \cdot (R_{\mathrm{margin}} - 1) \tag{9}$$

The cost for negative flexibility can be calculated by assuming the scenario of a HEMS that has pre-bought energy on the day-ahead market for charging an EV at a certain point in time. Negative flexibility for this exact moment is being called, meaning that the HEMS will send appropriate signals to the charging station to stop the charging process of an EV. In this scenario the refrained energy must be caught up at a later point in time. The HEMS must therefore buy the energy on the intra-day market, which can result in much higher prices than the pre-bought energy. Therefore the prices will be positive, indicating that the HEMS will receive money for offering negative flexibility.

In (10) the average of the $n_{\mathrm{off,Flex,tSteps}}$ minimal prices in which no operation was initially scheduled $i_{non-operational}$ by the HEMS and past the flex offer is multiplied with a factor consisting of a risk margin to which 1 is added to.

$$c_{\mathrm{pos.,Flex}} = mean\left(mink\left(c_{Forecast}(i + i_{non-operational}\colon end), n_{\mathrm{off,Flex,tSteps}}\right)\right) \cdot \left(R_{\mathrm{margin}} + 1\right) \tag{10}$$

The accumulation of the aforementioned characteristics of flexibility offers are then communicated as a table to a flexibility platform. In the event of a forecasting error, new input data, a flexibility call, or an unexpected user behavior the HEMS restarts the optimization process.

III. Results

Within this section the results of the above described model for offering flexibility with an EV that requires a total energy of 80 kWh, can be charged with a maximum power of 20 kW and is available for operation in the time period from 04:30 to 18:30 are presented. Fig. 3 shows the cost optimal charging plan (black line), all placed flexibility offers (color map, from orange to purple), a simulated flexibility call (red line) and the new optimization results (grey line) after a flexibility call. The x-axis shows the time of a day and the y-axis the cumulated energy. The calculated cost optimal operation shows multiple charging periods over the period of the day. When the EV is not available for operation, the HEMS cannot offer any flexibility and therefore, shows only dots in the period from 00:00 until 4:00 and in the late evening. Once the EV is available for operation the flexibility offers are visible as colored lines, that start on the line of the cost optimal operation plan, either start to rise with a constant gradient and end at a certain energy level. The starting point of each flexibility line is equal to the time step at which the flexibility is offered. The gradient of the offers is dependent on the offered power. In the case of positive flexibility the gradient will be proportional to the charging power of 20 kW and for negative flexibility equal to zero, since the HEMS will refrain from charging the EV in those time steps. The offered flexible energy is for positive flexibility the difference between the energy levels (from starting to end point) of each flexibility offer. Is negative flexibility offered, the energy is equal to the difference between the end point of the flexibility offer and the energy level of the cost optimal operation plan at the same time step.

At time step 10:00 Fig. 3 shows the simulated call for positive flexibility. The total offered flexibility at this time is according to Table 1 40 kWh but only 25 kWh are called, indicated by the red line. The power of the flexibility offer is completely retrieved, indicated by the congruence of the flexibility retrieval with the offer. After the flexibility retrieval ends the HEMS calculates a new cost optimal operation plan for the remaining energy. Because in the presented model the price forecast was not altered between the initial optimization and the simulated flexibility retrieval the new optimal operating strategy is only slightly different than the initial strategy.

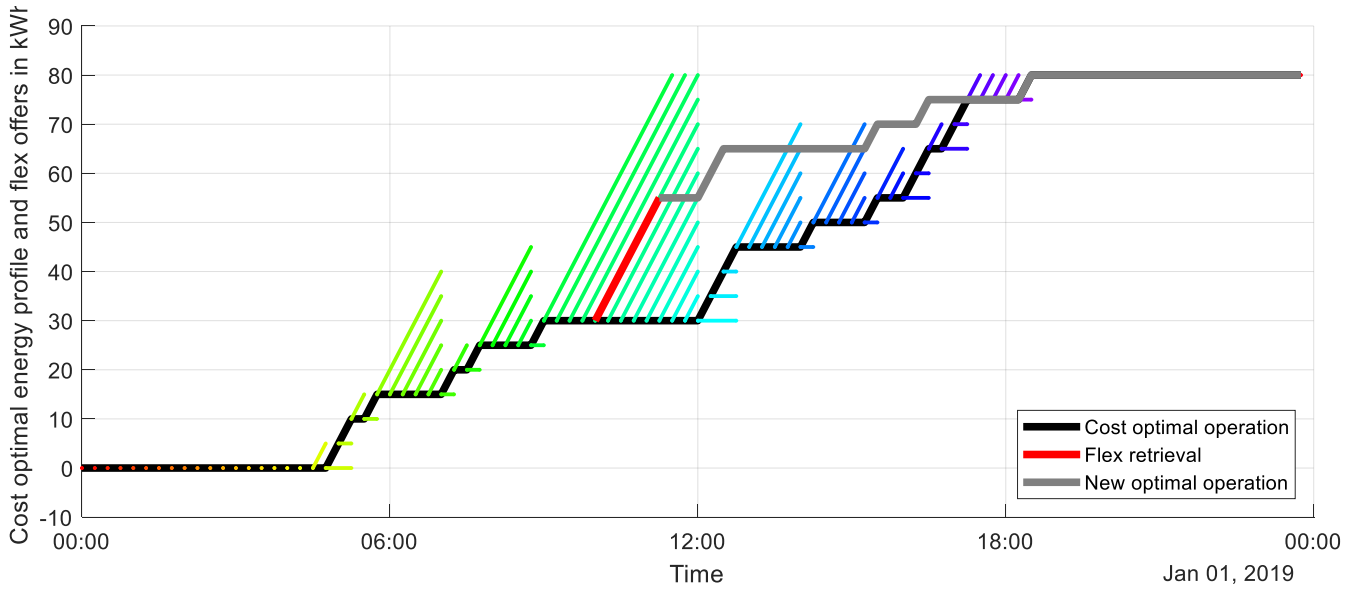

Fig. 3 Flexibility model of an EV with, cost optimal operation plan, simulated flexibility call and re-optimization results

Table 1 Flexibility offers from 9:45 to 12:45 with the scheduled power, negative and positive power, energy, and prices

Time	Scheduled Power in kW	Neg. Power in kW	Pos. Power in kW	Neg. Energy in kWh	Pos. Energy in kWh	Neg. Price in €/kWh	Pos. Price in €/kWh
01.01.2019 09:45	0	0	20	0	45	0,000	-0,182
01.01.2019 10:00	0	0	20	0	40	0,000	-0,181
01.01.2019 10:15	0	0	20	0	35	0,000	-0,180
01.01.2019 10:30	0	0	20	0	30	0,000	-0,180
01.01.2019 10:45	0	0	20	0	25	0,000	-0,179
01.01.2019 11:00	0	0	20	0	20	0,000	-0,178
01.01.2019 11:15	0	0	20	0	15	0,000	-0,177
01.01.2019 11:30	0	0	20	0	10	0,000	-0,177
01.01.2019 11:45	0	0	20	0	5	0,000	-0,176
01.01.2019 12:00	20	-20	0	-15	0	0,379	0,000
01.01.2019 12:15	20	-20	0	-10	0	0,375	0,000
01.01.2019 12:30	20	-20	0	-5	0	0,366	0,000
01.01.2019 12:45	0	0	20	0	25	0,000	-0,180

After discussing the technical characteristics of the flexibility offers, Table 1 is an excerpt of the flexibility offers in a tabular form and Fig. 4 shows the offered flexibility prices and the power over one day. The flexibility power is constant at a level of ± 20 kW for either positive or negative flexibility and corresponds to the maximum charging power of the EV. The subplot below, shows the offered flexibility prices in €/kWh. The HEMS calculates for positive flexibility negative prices and for negative flexibility positive prices.

The prices for negative flexibility rise towards the end of the day because the energy must be caught up at a later point in time and the number of possible operation time steps decreases. The prices at 12:00 temporarily decrease for negative flexibility due to the fact, that the offered energy is decreasing over time and therefore more options to catch up the energy are available. The prices for positive flexibility slightly decrease with the amount of offered energy. Only at the last block of positive offers the costs stay constant. This behavior of the model can be explained with (9) in which the average of the minimum prices for the required energy is calculated. When the amount of offered energy is high, more time steps must be considered, indicating a higher risk on the energy market and therefore resulting in a higher energy price. The constant prices for the last block of negative prices (time period 17:15 to 18:00) is caused by the constant amount of offered energy of 5 kWh (see Fig. 3).

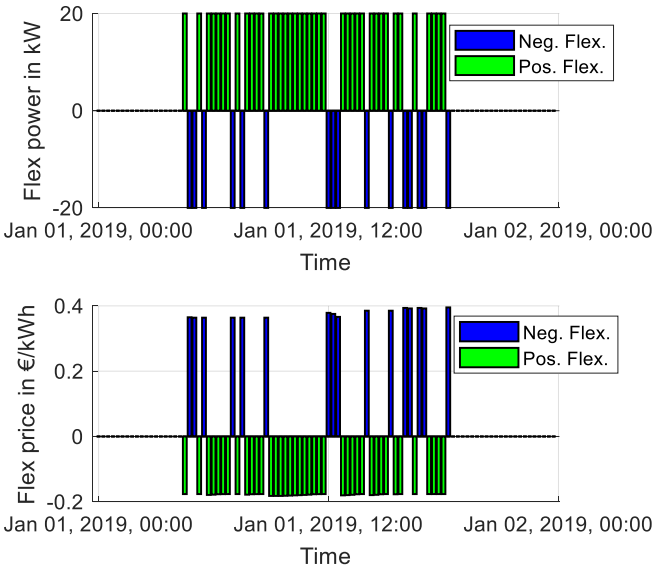

Fig. 4 Offered flexible power and prices for flexibility in €/kWh

The presented results verify the models structure described in section II. The next section will summarize the possible applications and limitations of the presented model.

IV. Discussion

The model presented in this paper is capable of processing user preferences, historical data, unit parameters, energy price and weather forecasts, calculating cost optimal operating strategies and flexibility offers. The results of the model show the compatibility to flexibility platforms described in section I and developed in current research projects [22]. A simulation of a unidirectional EV model verified the functionalities of the proposed HEMS. The implementation of HEMS models for further DER shall verify the applicability of the presented method to HP, CHP, PV units and connected battery and heat storages.

The general criticism regarding exhaustive enumeration methods of consuming too much computational costs [16, 17] could not be confirmed by the results of the presented model. The model shows rather that for a discrete model with a time horizon of 24 h and a temporal resolution of 15 minutes, the exhaustive enumeration approach can calculate an optimal operating strategy and the respective flexibility offers in less than 1 second on a personal state-of-the-art computer. Moreover, this technique offered a simple approach to investigate all possible deviations from the cost optimal operating strategy, hence laid the foundation of the flexibility calculations.

V. Conclusion and Outlook

Within this paper, a novel HEMS model is presented, which processes input data from multiple parties, optimizes the DER's operation strategy and calculates offers for a flexibility market platform. The results of the EV simulation are presented in this paper. It is verified that the proposed model

shows the expected functionality and enhances the economic opportunities for DER's and prosumers, by participating on a flexibility platform. The quantification of the offerable flexibility by DER and their pricing, which so far cannot be found in the literature, represents a novelty to the scientific community.

In future research, the transferability to other DER units will be demonstrated and more complex systems of multiple market participants will be investigated. Within the scope of the SINTEG project c/sells, where more than 50 partners from German academic and industrial research institutions, including multiple DSOs and TSOs participate in discussions and the development of different local flexibility platforms, the opportunity for in-depth analysis and validation of the concept is given. The next step will be the application of the presented method to a PV and battery storage combination and HP/CHP unit and heat storage combination. Laboratory testing in a Hardware-in-the-Loop environment as well as testing in the field will be conducted in near future. Another field of research is the investigation of alternative cost functions, such as minimizing CO_2-emmissions or maximizing the level of autarky.

ACKNOWLEDGMENT

This contribution is supported by the Federal Ministry for Economic Affairs and Energy, Bundesministerium für Wirtschaft und Energie, as a part of the SINTEG project C/sells. Responsibility for the content of this publication lies with the authors.

REFERENCES

[1] D. Trebolle und R. Otter, „Flexibility and Aggregation," 2014. [Online]. Available: https://www.usef.energy/app/uploads/2016/12/EURELECTRIC-Flexibility-and-Aggregation-jan-2014.pdf. [Zugriff am 16 9 2018].

[2] M. Paulus und F. Borggrefe, „The potential of demand-side management in energy-intensive industries for electricity markets in Germany," *Applied Energy,* Bd. 88, Nr. 2, p. 432–441, 2011.

[3] G. Strbac, „Demand side management: Benefits and challenges," *Energy Policy,* Bd. 36, Nr. 12, p. 4419–4426, 2008.

[4] K. Zhou und S. Yang, „Demand side management in China: The context of China's power industry reform," *Renewable and Sustainable Energy Reviews,* Bd. 47, p. 954–965, 2015.

[5] P. Olivella-Rosell, E. Bullich-Massague, M. Aragues-Penalba, A. Sumper, S. O. Ottesen, J.-A. Vidal-Clos und R. Villafafila-Robles, „Optimization problem for meeting distribution system operator requests in local flexibility markets with distributed energy resources," *Applied Energy,* Bd. 210, p. 881–895, 2018.

[6] P. Olivella-Rosell, P. Lloret-Gallego, I. Munne-Collado, R. Villafafila-Robles, A. Sumper, S. O. Ottessen, J. Rajasekharan und B. A. Bremdal, „Local Flexibility Market Design for Aggregators Providing Multiple Flexibility Services at Distribution Network Level," *Energies,* Bd. 11, Nr. 4, 2018.

[7] C. Eid, P. Codani, Y. Perez, J. Reneses und R. Hakvoort, „Managing electric flexibility from Distributed Energy Resources," *Renewable and Sustainable Energy Reviews,* Bd. 64, p. 237–247, 2016.

[8] E. Amicarelli, T. Q. Tran und S. Bacha, „Flexibility Service Market for Active Congestion Management of Distribution Networks using Flexible Energy Resources of Microgrids," *2017 IEEE Pes Innovative Smart Grid Technologies Conference Europe (Isgt-Europe),* 2017.

[9] C. Zhang, Y. Ding, N. C. Nordentoft, P. Pinson und J. Ostergaard, „FLECH: A Danish market solution for DSO congestion management through DER flexibility services," *Journal of Modern Power Systems and Clean Energy,* Bd. 2, Nr. 2, p. 126–133, 2014.

[10] S. S. Torbaghan, N. Blaauwbroek, P. Nguyen und M. Gibescu, „Local market framework for exploiting flexibility from the end users," Piscataway, NJ, IEEE, 2016, p. 1–6.

[11] A. Pillay, S. Prabhakar Karthikeyan und D. P. Kothari, „Congestion management in power systems – A review," *International Journal of Electrical Power & Energy Systems,* Bd. 70, p. 83–90, 2015.

[12] A. Kumar, S. C. Srivastava und S. N. Singh, „Congestion management in competitive power market: A bibliographical survey," *Electric Power Systems Research,* Bd. 76, Nr. 1-3, p. 153–164, 2005.

[13] A. Agnetis, G. Pascale, P. Detti und A. Vicino, „Load Scheduling for Household Energy Consumption Optimization," *Ieee Transactions on Smart Grid,* Bd. 4, Nr. 4, p. 2364–2373, 2013.

[14] J. M. Lujano-Rojas, C. Monteiro, R. Dufo-López und J. L. Bernal-Agustín, „Optimum residential load management strategy for real time pricing (RTP) demand response programs," *Energy Policy,* Bd. 45, p. 671–679, 2012.

[15] M. Beaudin und H. Zareipour, „Home energy management systems: A review of modelling and complexity," *Renewable and Sustainable Energy Reviews,* Bd. 45, p. 318–335, 2015.

[16] R. A. Lara, E. Naboni, G. Pernigotto, F. Cappelletti, Y. Zhang, F. Barzon, A. Gasparella und P. Romagnoni, „Optimization Tools for Building Energy Model Calibration," *Energy Procedia,* Bd. 111, p. 1060–1069, 2017.

[17] J. A. Martín García und A. J. Gil Mena, „Optimal distributed generation location and size using a modified teaching–learning based optimization algorithm," *International Journal of Electrical Power & Energy Systems,* Bd. 50, p. 65–75, 2013.

[18] P. L. Olivella, „Smart System of Renewable Energy Storage Based on Integrated EVs and Batteries to Empower Mobile, Distributed and Centralised Energy Storage in the Distribution Grid," 2017.

[19] C. Cordobés, „Loacl Electricity Retail Markets for Prosumer smart grid Power Services," 2016.

[20] B. Fenn, D. Petermann und K. Lerchl-Mitsch, „Abschlussbericht der ENTEGA AG für das Forschungsprojekt "Flex4Energy"," 2018.

[21] M. Boxberger und M. Grundmann, „ENKO - Das Konzept zur verbesserten Integration von Grünstrom ins Netz," 2018.

[22] A. Reuter und S. Breker, „C/sells: Netze und Märkte verbünden," 2018.

3.2 Assessing the potential of electric vehicles

Contribution

After introducing the *OpenTUMFlex* model, the question is how much flexibility can be expected from flexumer appliances such as EVs with realistic user behavior. Since the literature did not offer any approach to model flexumer behavior in a market-based setting, the following article presents a case study based on publicly available real-world vehicle field trial data that allow to estimate the flexibility potentials of EVs in the future.

The case study consists of a raw data acquisition, preprocessing, optimization and flexibility calculation, and a post-processing phase (see figure 3.2). In the first phase, mobility data from a Californian and a German field trial and three electricity pricing tariffs (RT, Time-of-Use (ToU), and Constant (Con)) were collected. Based on the collected data sets, I computed more than 15,000 vehicle availabilities, implemented controller strategies, which cause the HEMS to either charge immediately after arrival or to wait until the last possible moment to recharge, and modelled pricing tariffs for the field trial years. After the preparation stage, *OpenTUMFlex* is iteratively fed and executed to calculate optimal charging schedules and flexibility offers with varying controller strategies, pricing tariffs, and maximum charging power levels. Finally, results are aggregated and visualized for analyses.

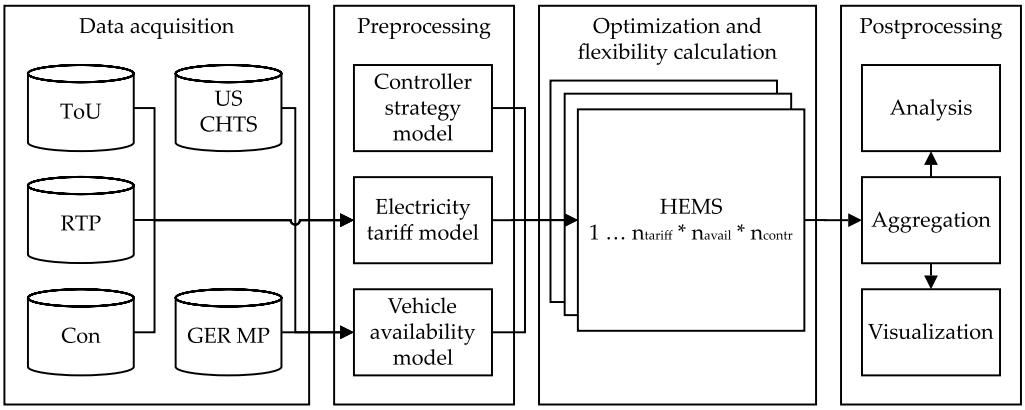

Figure 3.2: Overview of the performed flexibility case study for EVs. ToU, Con, and RT are the collected electricity pricing schemes, whereas US CHTS and GER MP mark the Californian and German mobility field trial data sets. Figure was taken from [50] and graphically edited.

The results indicate that EVs can provide

- positive flexibility mostly in the morning or evening hours depending on the controller strategies,
- negative flexibility, which follows the vehicle availability if the controller strategy is to charge as late as possible,
- no negative flexibility if a Con tariff and a charge as soon as possible strategy is used, and

– increased amounts of flexibility if the charging power levels are higher.

Furthermore, the results verify that ToU tariffs and a controller strategy that charges the vehicle as soon as possible can lead to demand peaks that are 250 % to 300 % higher compared to the other investigated pricing strategies and controllers, thereby potentially increasing grid congestions.

As part of the C/sells research project, we verified our model outputs on the flexibility platforms developed by research partners such as Forschungsstelle für Energiewirtschaft e.V. and Tennet TSO GmbH. Furthermore, the pricing results of the case study were analyzed in a student project supervised by me [114]. The presented case study was published as an add-on to the open-source project *OpenTUMFlex* [33].

This case study design allows fellow researchers, regulators, and energy industry experts to model flexumers in detail and investigate various impacts on their flexibility potential and prices.

Publication #4: Quantifying the Flexibility of Electric Vehicles in Germany and California – A Case Study

Authors Michel Zade, Zhengjie You, Babu Kumaran Nalini, Peter Tzscheutschler, Ulrich Wagner

Publication medium Energies, Volume 13

Digital object identifier https://doi.org/10.3390/en13215617

Open-source repository the data and models that support the findings of this study are openly available in *OpenTUMFlex* [33].

Author contributions

Michel Zade:	65 %	Conceptualization, Data curation, Formal analysis, Investigation, Methodology, Software, Visualization, Validation, Writing - Original draft, Writing - review and editing.
Zhengjie You:	15 %	Investigation, Methodology, Software, Writing - Original draft, Writing - review and editing.
Babu Kumaran Nalini:	5 %	Software, Writing - review and editing.
Peter Tzscheutschler:	10 %	Formal analysis, Funding acquisition, Project administration, Supervision, Writing - review and editing.
Ulrich Wagner:	5 %	Funding acquisition, Project administration, Supervision, Writing - review and editing.

energies

MDPI

Article

Quantifying the Flexibility of Electric Vehicles in Germany and California—A Case Study

Michel Zade *, Zhengjie You, Babu Kumaran Nalini, Peter Tzscheutschler and Ulrich Wagner

Chair of Energy Economy and Application Technology, TUM Department of Electrical and Computer Engineering, Technical University of Munich, 80333 Munich, Germany; zhengjie.you@tum.de (Z.Y.); babu.kumaran-nalini@tum.de (B.K.N.); ptzscheu@tum.de (P.T.); uwagner@tum.de (U.W.)

* Correspondence: michel.zade@tum.de; Tel.: +49-89-23972

Received: 9 September 2020; Accepted: 21 October 2020; Published: 27 October 2020

Abstract: The adoption of electric vehicles is incentivized by governments around the world to decarbonize the mobility sector. Simultaneously, the continuously increasing amount of renewable energy sources and electric devices such as heat pumps and electric vehicles leads to congested grids. To meet this challenge, several forms of flexibility markets are currently being researched. So far, no analysis has calculated the actual flexibility potential of electric vehicles with different operating strategies, electricity tariffs and charging power levels while taking into account realistic user behavior. Therefore, this paper presents a detailed case study of the flexibility potential of electric vehicles for fixed and dynamic prices, for three charging power levels in consideration of Californian and German user behavior. The model developed uses vehicle and mobility data that is publicly available from field trials in the USA and Germany, cost-optimizes the charging process of the vehicles, and then calculates the flexibility of each electric vehicle for every 15 min. The results show that positive flexibility is mostly available during either the evening or early morning hours. Negative flexibility follows the periodic vehicle availability at home if the user chooses to charge the vehicle as late as possible. Increased charging power levels lead to increased amounts of flexibility. Future research will focus on the integration of stochastic forecasts for vehicle availability and electricity tariffs.

Keywords: charging strategy; optimization; electricity pricing; electric vehicle; flexibility; flexibility market; home energy management system

1. Introduction

Scarcity of fossil fuels, oil price fluctuations, and increased awareness of the negative impacts caused by anthropogenic climate change have led to an increasing use of variable renewable energy (VRE) sources. With the agreed goal of limiting anthropogenic global warming to well below 2 degrees Celsius, this trend is expected to continue and even accelerate. While hydropower and biomass are, in their operational behavior comparable to conventional power plants, the power generation of photovoltaic and wind systems is variable, and generation prediction challenging and subject to uncertainty. Introducing flexibility products to the power system is one measure to cope with this variability and uncertainty.

Ma et al. define flexibility as the "the ability of a power system to cope with variability and uncertainty in both generation and demand, while maintaining a satisfactory level of reliability at a reasonable cost, over different time horizons" [1]. While this definition describes the general characteristic of flexibility, the Union of the Electricity Industry—Eurelectric—defines flexibility in a more application-oriented way, as "the modification of generation injection and/or consumption patterns in reaction to an external signal (price signal or activation) in order to provide a service

within the energy system. The parameters used to characterize flexibility include the amount of power modulation, the duration, the rate of change, the response time, the location, etc." [2].

Nowadays, large-scale flexibility products with a capacity greater than 1 MW are widely used to stabilize grid frequency. On the supply side, system operators (SO) use measures such as redispatch and feed-in management. On the demand side, they use sheddable loads and industrial demand-side-management as grid ancillary services [3–5]. While regulation and various market designs for energy trading already exist, academic and industrial research now focus on introducing unique flexibility platforms [6]. Such new platforms will allow residential consumers and prosumers to participate with their distributed energy resources (DER)—such as combined-heat-and-power units (CHP), electric vehicles (EV), residential heat pumps (HP), photovoltaic systems (PV), and battery storage units—as well as large industrial parties to offer flexibility [7–9]. In the future, SO will be able to manage grid congestions in a less resource-intensive manner and potentially avoid costly grid expansions and the curtailment of VRE [10,11]. Such flexibility platforms differ from existing energy market mechanisms in that they trade power instead of energy. SOs place their flexibility demand on the platform and are matched with residential and industrial flexibility providers.

Flexibility can be both negative and positive. Negative flexibility refers to the delay of grid feed-in or the consumption of non-scheduled energy. Positive flexibility is the delay of grid energy consumption or the non-scheduled grid feed-in.

Home energy management systems (HEMS) can quantify, price, and offer flexibility from private DER to such platforms and re-schedule devices based on the platform response. Beaudin et al. conclude that an HEMS is a demand response tool with the goal of optimizing consumption and production profiles in a house that communicates with household devices, utilities, and forecasting service provider [12]. The most important components of such a system required for calculating flexibility offers are visualized in Figure 1.

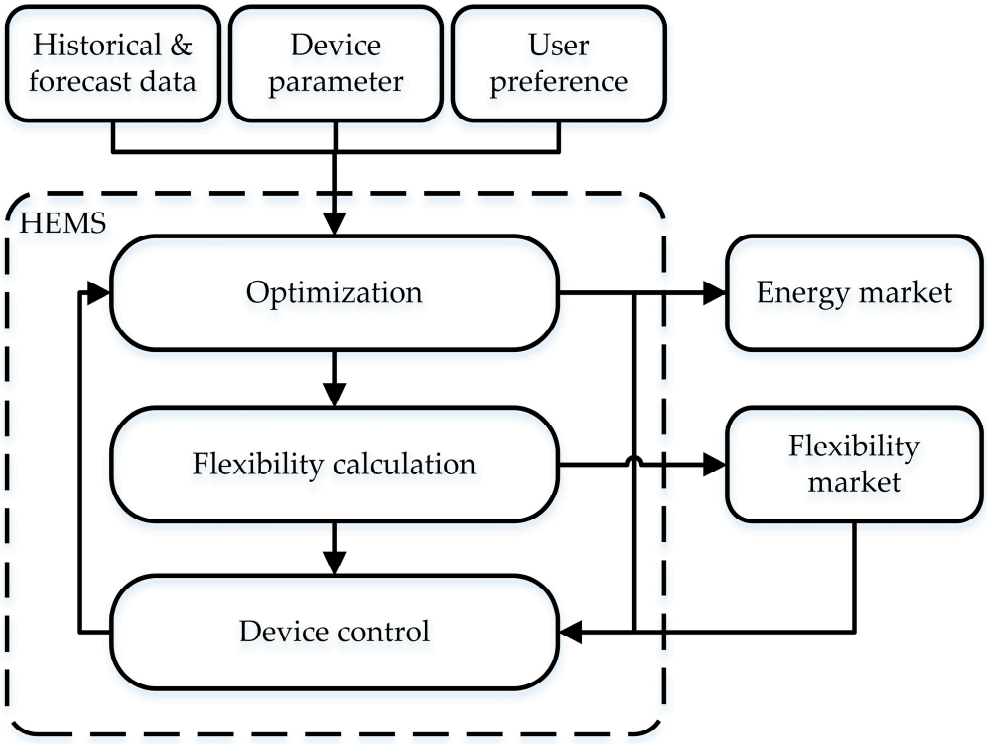

Figure 1. Generalized structure of an HEMS. Historical and forecast data refers to weather data, historical consumption and production data and expected energy prices.

A review of HEMS concluded that cost optimization is the most frequently implemented objective function [12]. Yan et al. state that price-driven demand response is an important demand response measure [13]. Therefore, the type and structure of the electricity price signal is of crucial importance for the optimization problems of HEMSs.

Eurelectric differentiates fixed-priced offers and various types of dynamic pricing [14]. Nowadays, the majority of residents in the US, for example, have a fixed-priced electricity tariff [15]. Besides fixed-priced offers, utilities offer different types of dynamic pricing: time-of-use (ToU), real-time pricing (RTP), and others, such as critical peak pricing (CPP). ToU tariffs offer static pricing schemes with pre-defined prices for specified periods and seasons. As such, ToU tariffs are easy to follow for any customer, however, for the SO they run the risk of creating demand peaks of higher magnitude than the ones caused by fixed-priced offers [13]. In RTP, prices vary over short periods and are communicated to customers one day or less in advance. California was one of the first states to introduce RTP, in 1985 [16]. Nowadays, only a few RTP programs, such as ComEd's Hourly Pricing, exist because they are technically difficult to implement and hard for customers to understand. A lot of studies have investigated the impact of different electricity tariffs on the peak demand of a distribution grid and concluded that simple ToU strategies can lead to increased peak demand [17,18]. However, the literature rarely discusses the impact of different electricity tariffs on flexibility.

Zade et al. published an HEMS model that optimizes the charging process of an electric vehicle (EV), and calculates the flexibility based on synthetic electricity prices, vehicle availabilities, and energy demands [9]. In order to analyze the realistic flexibility potential of EVs in a distribution grid, this paper describes a detailed case study conducted with vehicle field trial data from California, USA and Germany, three electricity tariffs, two controller strategies, and three charging power levels.

2. Materials and Methods

Figure 1 provides a functional overview of the generalized structure of an HEMS. As defined above, the primary objective of the HEMS is to fulfill the electricity, heat, and mobility demand of the household. For this purpose, the HEMS retrieves historical load profiles from an internal database and various other input data, e.g., user preferences, weather, and price forecasts from external sources. Then, an optimizer inside the HEMS calculates cost-optimal operating strategies for all controllable devices. Based on those operating schedules, the HEMS buys and sells energy on the energy market. Afterwards, the HEMS can offer deviations from the cost-optimal operating strategy as flexibility to SOs via a flexibility platform.

2.1. Input Data, Generation, and Consumption Forecast

The HEMS receives data from various parties, e.g., household inhabitants, forecast providers and weather stations. In an initial configuration step, household inhabitants insert device parameters like the charging station's maximal charging power, or EV's battery capacity, etc. More frequently, inhabitants update operational constraints, such as the daytime when an EV needs to be fully charged or the room temperature they find comfortable. Besides those user inputs, the HEMS is fed with different forecasts such as the upcoming weather conditions and expected energy prices. Finally, the optimization is triggered whenever new input data arrives or a certain amount of time has passed.

2.2. Optimization Approach

The calculation of the cost-optimal charging schedule is based on [19] but has been modified in order to incorporate constraints such as EV availabilities over time. This section describes the mixed-integer linear programming (MILP) model that has been used to calculate the cost-optimal charging schedule. In this work, it is assumed that the prosumer prefers a cost-optimized solution to the scheduling problem. Therefore, the target function in Equation (1) is formulated as a cost minimization.

$$\min\left(\sum_{t=1}^{T}(p_t^{im}\cdot c_t^{im} - p_t^{ex}\cdot c_t^{ex} + p_t^{gas}\cdot c_t^{gas})\cdot\Delta t + K\cdot\Delta SoC_t\right) \quad (1)$$

Here T is the set of time steps (t) considered throughout the scheduling horizon. Δt is the duration of each time step, p^{im} and p^{ex} are the electrical import and export power, while c^{im} and c^{ex} are the corresponding electricity costs or revenues. p^{gas} and c^{gas} denote the volume of natural gas used and its specific cost, respectively. K represents a penalty coefficient that is multiplied with the variable ΔSoC_t which is the difference between the desired final state of charge (SoC) and the actual SoC at the end of charging. This penalty term allows the optimizer to create a feasible problem even though the available time is not sufficient to charge a vehicle fully. Thereby, infeasible problems are avoided.

In addition, the energy balance and constraints for each appliance are critical to reflect a correct and realistic optimization. The constraints are as follows. The energy balance for electricity is represented by Equation (2) and for heat by Equation (3).

$$p_t^{im} + \sum_{\delta\in Flex_{el}} p_t^{\delta} - p_t^{ex} - p_t^{load} = 0 \qquad \forall t \in [1,T] \quad (2)$$

$$\sum_{\delta\in Flex_{th}} p_t^{\delta} - q_t^{load} = 0 \qquad \forall t \in [1,T] \quad (3)$$

p^{load} *and* q^{load} represent the electrical and thermal load of the household. p^{δ} is the power of one specific device, which belongs to one of the flexible appliance groups $Flex_{el} \in \{EV,\ CHP,\ HP,\ PV,\ Bat\}$ or $Flex_{th} \in \{CHP,\ HP,\ TES\}$. The group $Flex_{el}$ includes electric vehicles (EV), combined heat and power (CHP), heat pumps (HP), photovoltaic (PV), and battery systems (Bat). The group $Flex_{th}$ covers CHP, HP and thermal energy storages (TES). CHPs and HPs are classified into both groups because CHP produce electricity and heat at the same time and heat pump can convert power to heat.

For each flexible appliance and storage system, multiple constraints exist concerning their operation. Because this paper focuses on the quantification of flexibility of EVs, Equations (4)–(10) only list the constraints for EVs.

$$SoC_t = SoC_0 + \frac{1}{C_{Bat}}\sum_{s=1}^{t}\left(p_t^{EV}\cdot\eta - p_t^{cons}\right)\cdot\Delta t \qquad \forall t \in [1,T] \quad (4)$$

$$SoC_{min} \le SoC_t \le SoC_{max} \qquad \forall t \in [1,T] \quad (5)$$

$$SoC_t \ge SoC_t^e - \Delta SoC_t \qquad \forall t \in \left\{t_1^e, t_2^e, \ldots\right\} \quad (6)$$

$$SoC_t \le SoC_t^s \qquad \forall t \in \left\{t_1^s, t_2^s, \ldots\right\} \quad (7)$$

$$0 \le p_t^{EV} \le A_t\cdot P_{max}^{EV} \qquad \forall t \in [1,T] \quad (8)$$

$$A_t = \begin{cases} 1 & \forall t \in \left[t_1^s, t_1^e\right] \cup \left[t_2^s, t_2^e\right] \cup \ldots \\ 0 & \forall t \in \left[0,\ t_1^s\right) \cup \left(t_1^e, t_2^s\right] \cup \ldots \end{cases} \quad (9)$$

$$p_t^{cons} \ge 0 \qquad \forall t \in [1,T] \quad (10)$$

In Equations (4)–(7), SoC represents the SoC of the EV battery. SoC_0 denotes the initial SoC of the EV, SoC_{min} and SoC_{max} are minimal and maximal SoC. SoC_t^s refers to the SoC at time step zero and SoC_t^e represents the SoC at the last available time step. SoC_t^e may be reduced by ΔSoC_t if the time the vehicle is parked at home is not sufficient to charge the battery from start SoC to the desired end SoC. t^s and t^e refer to the start and end time of each availability period of the EV. C_{Bat} is the battery capacity, p_t^{EV} is the charging power of the EV, and η is the charging efficiency. p_t^{cons} is a variable that covers the power

demand if the EV is available for multiple periods and energy has been discharged from the battery in between.

Equations (8)–(10) describe the constraints for p_t^{EV}. A_t describes the vehicle availability for charging, which is 1 between t^s and t^e, and otherwise zero. Integrated into Equation (8), the availability does not allow the charging power to be greater than 0 if the vehicle is not available for charging. If the vehicle is available for charging, the charging power can be as high as the maximal charging power P_{max}^{EV}.

The formulated MILP model can be solved using commercial and open-source solvers, such as GLPK or Gurobi. Depending on the problem complexity, a conventional computer (e.g., Intel i7, 4 Cores, 24 GB RAM) presents a solution within a few seconds.

After optimizing the device's operating strategy, a market agent in the HEMS trades its excess and required energy on the energy market and a controller schedules the device's operation accordingly. After successful interaction with the energy market, the HEMS can start the flexibility calculation.

2.3. Flexibility Offers

Based on the optimal operating strategy of the devices described in the previous subsection, the HEMS calculates flexibility offers. Such a flexibility offer consists of the flexible power they can offer, the duration they can offer it, at what time, at which position in the grid, and at what price. The following subsections describe the calculation of these parameters in detail.

2.3.1. Location, Negative, and Positive Flexibility

Since in the setting considered here all flexible devices are stationary, the location of a flexible device is considered to be constant and is described by a unique identifier. In Germany, the Bundesnetzagentur introduced a 11-digit identifier (MaLo-ID: market location identifier) to simplify the market communication. Therefore, each HEMS that offers flexibility must attach the MaLo-ID to their bids.

Generally, all flexible devices are able to offer positive and negative flexibility, some even at the same time. For example, an EV charging station can offer positive flexibility by stopping an ongoing charging process or by reducing the charging power. Negative flexibility can be offered by charging a vehicle even though it has not been scheduled or by increasing the charging power while charging.

2.3.2. Power, Duration, and Energy

The DERs have different operating types. For both operating types, flexibility can be determined using Equations (11) and (12).

$$p_{pos}^{\delta} = \begin{cases} P_{max}^{\delta} - p^{\delta} & \forall \delta \in G \\ p^{\delta} & \forall \delta \in C \end{cases} \tag{11}$$

$$p_{neg}^{\delta} = \begin{cases} -p^{\delta} & \forall \delta \in G \\ p^{\delta} - P_{max}^{\delta} & \forall \delta \in C \end{cases} \tag{12}$$

As mentioned in Section 2.2, p^{δ} denotes the power of the electricity consumer (C) and generator (G). P_{max}^{δ} is the maximal power of each flexible device. p_{pos}^{δ} and p_{neg}^{δ} represent the resulting positive and negative flexibility power for each device. Note that the positive and negative flexibility power is always positive and negative, respectively, or zero. As described above, one device can offer positive and negative flexibility at the same time.

Equations (13)–(15) describe the duration that flexibility is available. d_{flex}^{δ} is the maximal duration that flexibility can be offered by a flexible device.

$$\max_{t_{flex}^e \in [t_{flex}^s,\, T]} d_{flex}^{\delta} = \left(t_{flex}^e - t_{flex}^s\right)\Delta t \tag{13}$$

s.t.

$$f_t\left(\hat{p}^{\delta'},\, p^{\delta}_{flex}\right) = 0 \qquad \begin{matrix}\forall \delta' \in A_f - \delta \\ \forall t \in \left[t^s_{flex}, t^e_{flex}\right]\end{matrix} \tag{14}$$

$$g_t\left(\hat{p}^{\delta'},\, p^{\delta}_{flex}\right) \leq 0 \qquad \begin{matrix}\forall \delta' \in A_f - \delta \\ \forall t \in \left[t^s_{flex}, t^e_{flex}\right]\end{matrix} \tag{15}$$

This optimization problem is solved for each time step. The start time t^s_{flex} of each flexibility is exactly the time step chosen by each iteration. t^e_{flex} is variable in this problem and should be maximized without violating constraints f_t and g_t, which are abstracted from the equality and inequality constraints discussed in Section 2.2, respectively. Subscript t for f and g indicates that the constraints shall be satisfied in the whole domain of t. p^{δ}_{flex} is the positive or negative power of one specific flexible appliance, whereas $\hat{p}^{\delta'}$ refers to all other flexible appliances that still follow the cost-optimal schedules.

Once the flexibility duration has been acquired, the flexible energy is calculated by Equation (16).

$$e^{\delta}_{flex,t} = \sum_{s=t}^{t+d^{\delta}_{flex}-1} p^{\delta}_{flex,t} \cdot \Delta t \tag{16}$$

Hence, the duration for which flexibility can be offered depends on the device's current state. In the case of an EV, the flexibility that can be offered depends on the battery's SoC, maximal charging power and availability.

In a final step, the flexibility would need a price tag in order to be offerable on a flexibility platform. However, this paper focuses on the quantification of flexibility of EVs and therefore the pricing is excluded from this analysis. Nevertheless, one possible pricing mechanism for flexibility of EV is described in [9].

Finally, the HEMS transfers the calculated flexibility parameters to a flexibility platform and waits for flexibility calls. Once a provider is called for flexibility, user preferences change, or new forecasts are available, the HEMS reinitiates the entire procedure from optimization to flexibility calculation and updates the offers on the flexibility platform.

The model is open-source and accessible via the link in the Supplementary Material.

3. Case Study

Figure 2 visualizes the general design of the case study. In a first step, we computed vehicle availabilities based on field trial data, collected by the California Department of Transportation and the Karlsruhe Institute of Technology. After gathering and pre-processing the vehicle availabilities and electricity tariffs, the cost-optimal charging schedules and the flexibility for each vehicle availability is calculated using the model described in Section 2. In order to analyze the aggregated flexibility potential of more than 4000 Californian and more than 11,000 German vehicle availabilities, the final results are aggregated. The following paragraphs describe the case study setup in detail. The link in the Supplementary Material contains an open-source script for the case study.

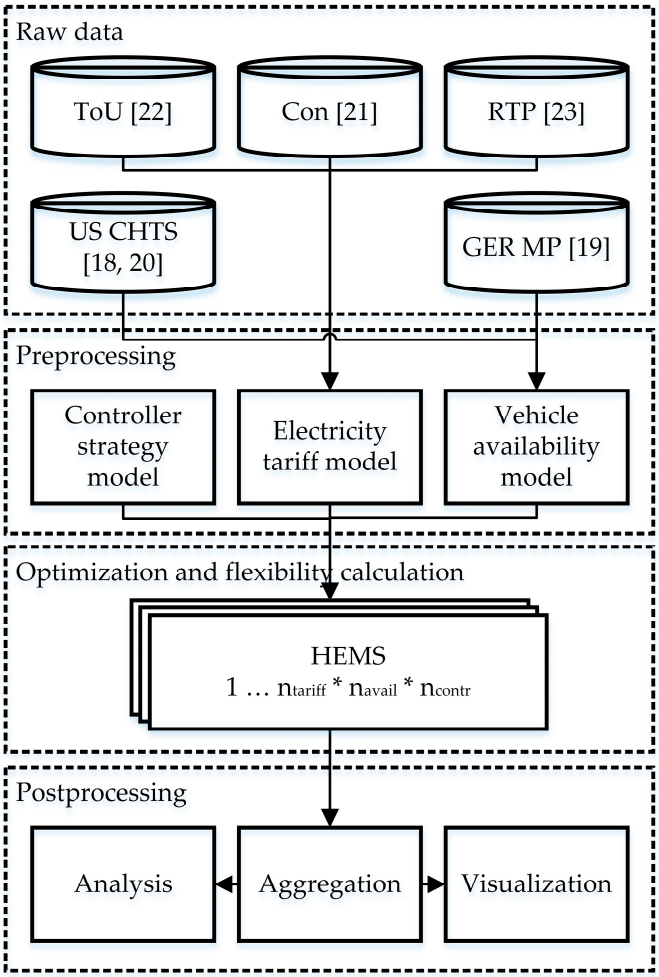

Figure 2. Case study design, US CHTS, and GER MP refers to the Californian and German field trial data used to calculate the vehicle availabilities [18–20]. Con refers to the constant electricity rate in California [21], ToU refers to the 'ToU-D-Prime' electricity tariff of Southern California Edison [22], and RTP refers to the Hourly Real-Time prices of ComEd in Illinois [23], US. n_{tariff} refers to the number of electricity tariffs, n_{avail} refers to the number of vehicle availabilities, and n_{contr} refers to the number of controller strategies investigated in this case study.

3.1. Data Input and Preprocessing

For the case study, vehicle availabilities at home are computed based on the data sets of the Californian Household Travel Survey (US CHTS) and the German Mobility Panel (GER MP) [20,21]. Table 1 summarizes the parameters that characterize a vehicle availability.

Table 1. Vehicle availability characterizing parameters.

Parameter	Unit	Description
ID_{veh}	-	Vehicle identifier
$t_{arrival}$	Timestamp	Arrival time at home
$t_{departure}$	Timestamp	Departure time from home
$d_{travelled}$	km	Distance traveled since last departure from home
$\Delta t_{available}$	s	Available time at home

The following subsections provide a brief summary of the most important characteristics and differences of the data sets used, as well as a short analysis of the computed vehicle availabilities.

3.1.1. Californian Household Travel Survey

Between February 2012 and March 2013, 677 Californian vehicles were equipped with in-vehicle GPS tracking devices. Every trip made by each vehicle was tracked for one week. The publicly available data set contains information about start and end times, start and end location, average speed and miles driven for every trip [22]. In the data set, 19,075 trips by 662 unique vehicles are recorded. The distance traveled varies from less than 0.5 km up to 1289 km. The average distance traveled is 35 km for all conducted trips (see Table 2). Start and end locations are categorized in four categories: HOME, WORK, SCHOOL, and OTHER.

Table 2. Mean, maximum, minimum and 95%-ile of distance traveled since last departure from home.

Parameter	Unit	US CHTS	GER MP
$d_{\text{travelled,avg}}$	km	35	38
$d_{\text{travelled,max}}$	km	1289	1992
$d_{\text{travelled,min}}$	km	0.5	0.2
$d_{\text{travelled,95\%}}$	km	131	130

Based on these parameters, the availability of vehicles at 'HOME' can be extracted, with arrival and departure time. Furthermore, the distance traveled is used to calculate the energy used by an average vehicle from its last departure from home. This procedure results in 4062 vehicle availabilities of 592 unique vehicles that contain a vehicle identifier, the distance traveled since the vehicle's last departure from home, its arrival time at and departure time from home. Inconsistencies in the GPS data set, e.g., a vehicle arrives at home but departs for the next trip from another location, are neglected in this analysis.

3.1.2. German Mobility Panel

Between September and November 2017, 3867 persons from 1881 households logged their daily mobility behavior in a travel diary. After plausibility checks conducted by the Karlsruhe Institute of Technology (KIT), a total of 70,252 trips were gathered from 1850 persons [21]. The final trip data set includes information about the date, the trip's start and end time, purpose, mode of transport used, duration, distance, and household. In 33,250 of the 70,252 trips logged, the person recorded having driven a vehicle as a driver either as a first, second or third "mode of transport used". In 13,550 of the 33,250 trips, the purpose of the trip was to return home.

Based on the 33,250 trips, a total of 11,458 vehicle availabilities at home are computed by considering household and person identifier, trip purpose, and the trips' chronology.

3.1.3. Vehicle Availabilities

In this subsection, the calculated vehicle availabilities are visualized and analyzed. In order to analyze the number of available vehicles at home during an average week, all vehicle availabilities are summed up for each time step of the week. Thereafter, the sums are averaged over all weeks of the field trials. Figure 3 shows the results for the Californian and German data sets. The average number of vehicles available in the Californian data set is 4.5 vehicles and for the German data set 21.3 vehicles. This can be explained by the compressed German field trial period of three months and the higher number of field trial participants (see [20,21]). Despite the differences in quantity, the vehicle availabilities indicate the same trends. At night, the number of vehicles increases until 12 a.m. and then decreases until 12 p.m. This behavior is repeated every day of the week. On weekends, however, the magnitude of the oscillation decreases approximately by a factor of three.

Figure 4 visualizes a histogram of the total number of available vehicles over the distance traveled since their last departure from home. The results of both data sets show an exponential decay with

only a few outliers. Ninety-five percent of the American and German vehicles arrive at home with less than 130 km driven since their last departure from home (see Table 2).

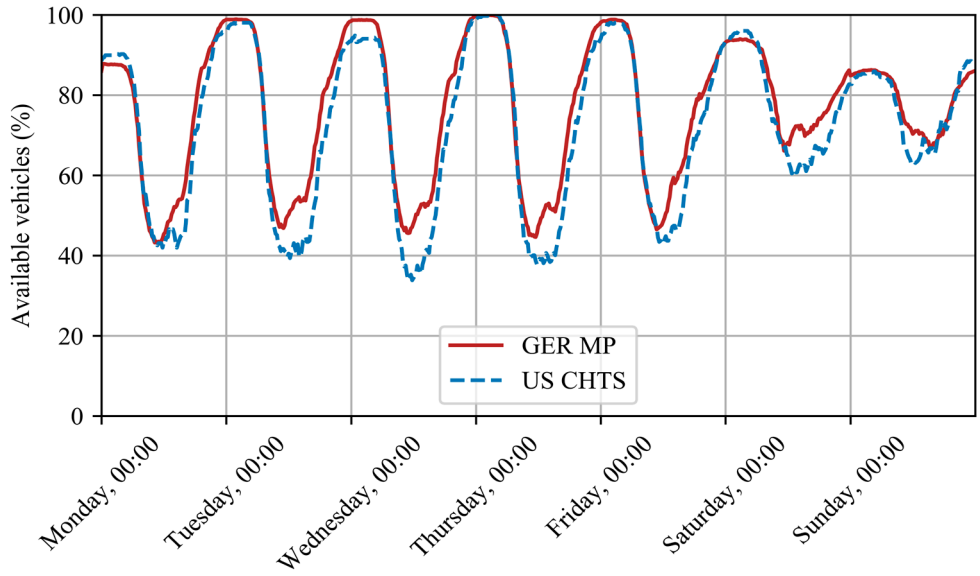

Figure 3. Percentage of vehicles available at home during an average week. The maximum number of vehicles available at home is 6 for the US CHTS data and 120 for the GER MP.

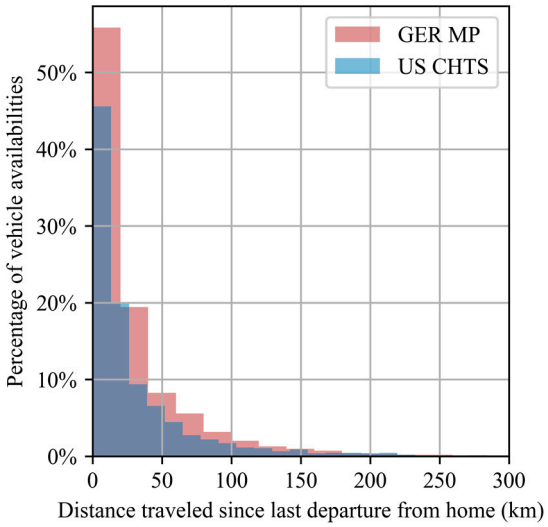

Figure 4. Distribution of the distance traveled since the vehicle's last departure from home—sampled from all modeled vehicle availabilities.

Figure 5 visualizes a relative frequency histogram of the total number of vehicles over the period the vehicles are available at home. Both data sets (US CHTS and GER MP) indicate a periodic behavior with a decreasing amplitude for an increasing time of availability. Most vehicles are available either for less than 1 to 3 h or for 7 to 25 h. Far fewer vehicles are available for 4 to 6 h or for more than 25 h. Table 3 summarizes the mean, maximum, minimum and 95%-ile of the available time for both data sets.

Figure 6 visualizes the distribution of the number of vehicles arriving at home over the hour of the day and the day of the week. Most vehicles arrive at home during the afternoon hours from 3 to 6 p.m. and depart from home between 6 and 9 a.m. Vehicles arrive at and depart from home more frequently during the week than on the weekend. Neither result is surprising considering conventional 9 to 5 working hours.

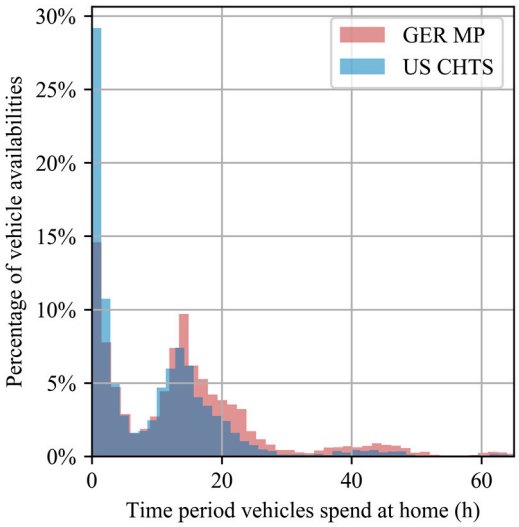

Figure 5. Distribution of the time period vehicles spend at home—sampled from all modeled vehicle availabilities.

Table 3. Mean, maximum, minimum, and 95%-ile of time of availability at home.

Parameter	Unit	US CHTS	GER MP
$\Delta t_{\text{available, avg}}$	h	10.43	16.16
$\Delta t_{\text{available, max}}$	h	142.38	148.67
$\Delta t_{\text{available, min}}$	h	0	0.02
$\Delta t_{\text{available, 95\%}}$	h	34	47.5

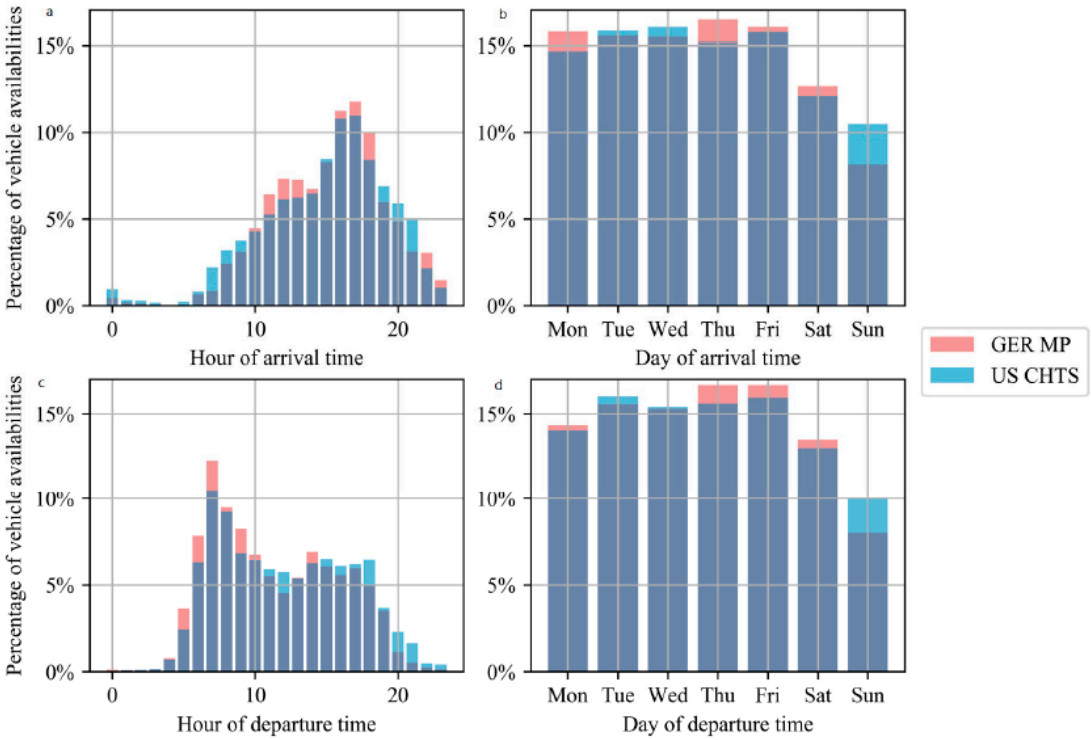

Figure 6. Percentage of vehicle availabilities over (**a**) hour, (**b**) day of arrival time, (**c**) hour, and (**d**) day of departure time.

3.1.4. Electricity Tariffs

In order to quantify the impact of different electricity tariffs on the flexibility potential of electric vehicles, three tariffs are used in this case study.

The first tariff is a constant tariff '*Con*' in which the electricity price does not vary. The price is set to 0.19 $/kWh, which was the average electricity price in California in 2018 [23].

'*ToU*' tariffs are offered throughout the United States and in other countries to motivate the reduction of electricity consumption in peak demand periods. Southern California Edison offers multiple *ToU* tariffs for residential customers on their website. For the simulations, the 'ToU-D-Prime' tariff as published on the website in the beginning of 2020 has been used. The tariff differentiates between winter and summer, weekday and weekend, and hour of day. In the winter, weekdays and weekends are priced equally. Between 4 and 9 p.m. the mid-peak tariff is active during the entire winter (0.36 $/kWh) and on weekends in the summer (0.27 $/kWh). During the summer, on weekdays from 4 to 9 p.m., the on-peak tariff for 0.39 $/kWh is active. From 9 to 4 p.m. the off or super-off-peak tariff at 0.14 and 0.13 $/kWh is active. This tariff motivates customer to reduce their electricity consumption in the late afternoon and early evening.

The third tariff integrated in this analysis is *RTP*. California already implemented two *RTP* programs in 1985 and 1987. However, both *RTP* programs had been canceled by 2003 [16]. Nowadays, California only offers *Con* and *ToU* tariffs. Therefore, a publicly available *RTP* tariff from ComEd, an energy supplier in Illinois, US is chosen [24]. In order to equalize the electricity prices for all tariffs, $p_{\mathrm{RTP,offset}}$ is added to the real-time prices. $p_{\mathrm{RTP,offset}}$ is the equal to the constant electricity price of 0.19 $/kWh minus the mean of all RTP. Since an analysis of the forecasting error of *RTP* is beyond the scope of this publication, the *RTP* tariff is assumed to be a perfect forecast of the electricity prices.

$$p_{\mathrm{RTP,offset}} = p_{\mathrm{Con}} - \frac{1}{N}\sum_{t=1}^{T} p_{\mathrm{RTP,i}} \tag{17}$$

3.1.5. Controller Strategies

In order to quantify the impact of different controller strategies or user preferences on the flexibility potential of electric vehicles, we implemented two controller strategies.

The first controller strategy is to charge the vehicle at minimal costs but as soon as possible. Such behavior can be simulated by adding a minimal price increment onto the electricity prices (see Equation (18)).

$$c_t^{\mathrm{im/ex}} = c_t^{\mathrm{grid,\ im/ex}} + c_t^{\mathrm{contr}} \qquad \forall t \in [1, T] \tag{18}$$

$c_t^{\mathrm{grid,\ im/ex}}$ denotes the actual electricity prices/revenues and c_t^{contr} the term that is added in accordance with the controller strategy. In the case of the first controller strategy, minimal price increments are added in the range of 0.00001 to 0.00002 $/kWh and therefore do not affect the actual price of electricity for the user. In the case of constant electricity prices, the optimizer would choose the first possible time steps in order to charge at minimal costs. For the rest of this publication, this operating strategy is denoted as "+*MI*".

In order to conserve battery life, a second controller strategy is to charge the vehicle as late as possible and therefore to keep the SoC of the EV battery as low as possible as long as possible. This controller strategy can be implemented either by the addition of a minimal price decrement in Equation (18) or in the optimizer by default. In our case, this behavior was implemented by default in the solver. Therefore, this controller strategy is not separately labeled.

Table 4 lists the five simulated operating strategies that represent the combination of the three electricity tariffs and the two controller strategies.

Table 4. Simulated operating strategies that represent the combination of electricity tariffs and controller strategies.

Operating Strategy	Electricity Tariff	Controller Strategy
Con	Con	Minimal decrements
ToU	ToU	Minimal decrements
Con + MI	Con	Minimal increments
ToU + MI	ToU	Minimal increments
RTP	RTP	-

3.2. Flexibility Calculation

In order to use the vehicle availabilities described in Section 3.1 as EV input parameters for the model described in Section 2, the energy demand is calculated based on the distance traveled. The energy required is the product of the specific energy consumption of the EV $e_{\mathrm{kWh/km}}$ and the distance traveled $d_{\mathrm{travelled}}$.

$$E_{\mathrm{EV,i}} = e_{\mathrm{kWh/km}} * d_{\mathrm{travelled}} \tag{19}$$

For this case study, a specific energy consumption of 0.2 kWh/km is used for all vehicle availabilities [25,26]. Furthermore, the user preference for the desired SoC of the vehicle at the time of departure $t_{\mathrm{departure}}$ was set to 100 %. The charging efficiency is set to 98 %.

In order to investigate the impact of the maximal charging power, the maximal charging power is varied in three steps: $P_{\mathrm{charge,max}} \in \{3.7\ \mathrm{kW},\ 11\ \mathrm{kW}, 22\ \mathrm{kW}\}$. This variation allows all current and possible future residential charging station configurations to be analyzed.

While the HEMS is capable of calculating the flexibility of HP, CHP, PV, and batteries, all other possible inputs, such as additional electrical or thermal loads or generation, are set to zero.

For every one of the five operating strategies listed in Table 4 and every $P_{\mathrm{charge,max}}$, the model calculates the optimal charging schedule and flexibility potential as a time series. This procedure resulted in a total of 165,870 for GER MP and 60,930 for US CHTS executions of the model.

3.3. Data Aggregation

Once optimal charging schedules and flexibility have been calculated for more than 15,000 vehicle availabilities for 5 operating strategies and 3 maximal charging powers, the results are aggregated.

First, all available vehicles, charging schedules, flexible power and energies are summed up for every time step of the field trial periods. The result is a data set that shows the total number of available vehicles at home, charging powers, flexible power and energy for every time step of the field trial.

In a final step, the summed data is clustered into weekly time steps (e.g., "Monday, 09:00"), and weekdays and weekends. The clusters are then averaged over the field trial duration.

4. Results

This chapter visualizes and describes the results of the case study in detail. The cost-optimal charging schedules are shown in the top two rows of plots, whereas the flexibility potential is shown in the bottom two rows of plots (Figure 7). The first section describes the cost-optimal charging schedules, and the second section the flexibility potentials of the vehicle availabilities from both data sets for the five operating strategies.

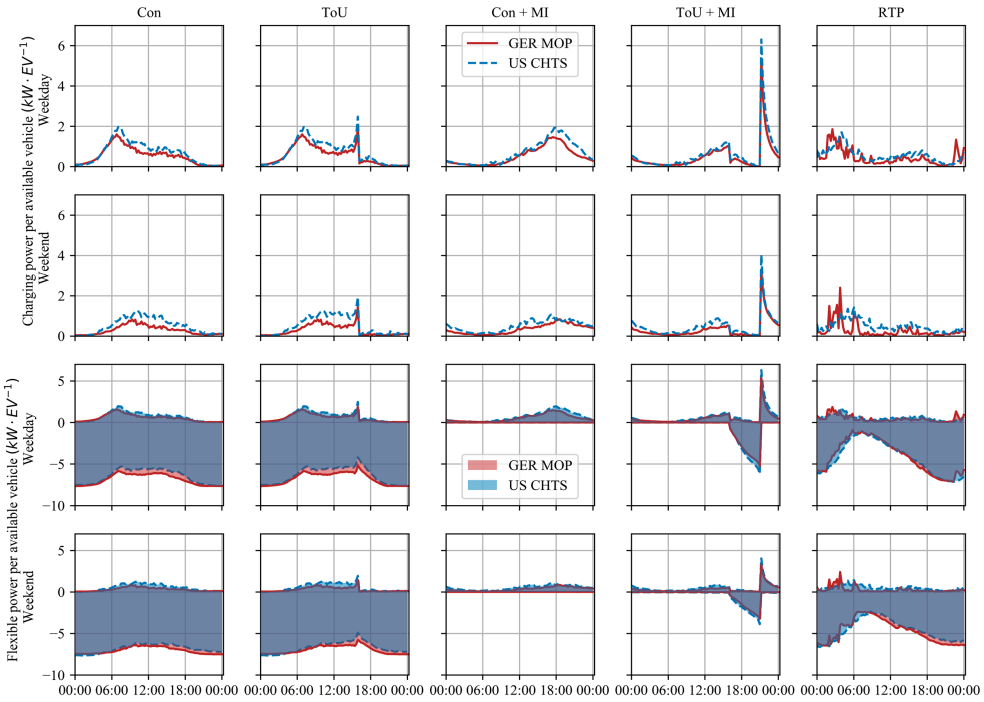

Figure 7. The plot series visualizes the charging and flexible power per available EV. The first two rows of plots show the charging power per available EV for the five operating strategies on weekdays and weekends. The third and fourth rows of plots show the flexible power per available EV for the five operating strategies on weekdays and weekends.

4.1. Cost-Optimal Charging Schedules

In the top two rows of plots, Figure 7 shows the cost-optimal power demand per vehicle for weekdays in the first row and for weekends in the second row. The curves of the *Con* and the *ToU* operating strategy are almost identical and can only be distinguished by their behavior between 3 p.m. and 9 p.m. At 4 p.m., the *ToU* curves show a smaller second peak compared to the early morning hours. This behavior can be explained by the optimizer logic and mid/on-peak tariffs. The optimizer implemented charges the vehicles as late as possible and as cheaply as possible. Considering the mid/on-peak tariffs starting at 4 p.m., the optimizer schedules all vehicles that depart between 4 and 9 PM to charge right before 4 p.m. Therefore, this trend is consistent with the implemented optimizer logic. Besides the difference mentioned in the early afternoon, the power curves for the *ToU* and *Con* operating strategy show the same trend as visualized by the histogram of the departure times in Figure 6. The amplitude ranges from 0 to 2.5 kW/EV for both data sets. On weekends, the power ranges from 0 to 1.9 kW/EV and is more spread out throughout the day. Generally, the results indicate that the Californian vehicles require greater power per vehicle compared to the German vehicles.

The *RTP* operating strategy causes charging peaks that are spread out from 11 p.m. to 8 a.m. The peaks are more irregular than the ones for the *Con* and *ToU* operating strategies. While the power curves for the *Con* and *ToU* operating strategy indicate similar trends for the US CHTS and the GER MP data set, the cost-optimal charging power differ significantly between the German and the Californian data set in the *RTP* operating strategy. The charging power for the Californian data set looks rather smooth, whereas the results of the German vehicles look much spikier. Since the German data set was collected over a period of three months, a single drop in the real-time prices and the corresponding peak of charging power have a greater impact on the average charging power than those that occurred during the 12-month Californian field trial with only a few vehicles. However, the amplitude ranges also from 0 to 2.5 kW/EV for both data sets. Since real-time prices are much more difficult to forecast and exhibit erratic short-term changes, the demand peaks are most probably overestimated in these results.

The cost-optimal charging power for the operating strategy *Con + MI* indicates a shifted charging behavior. Whereas the *Con* operating strategy schedules vehicle charging right before their departure in the morning hours, the minimal price increments force the optimizer to charge the vehicles right after they arrive home. Therefore, the charging power curve for the *Con + MI* follows the almost Gaussian distribution of the arrival times shown in Figure 6. The amplitude ranges from 0 to 2 kW/EV, which is comparable to the curves of the *Con* and *ToU* operating strategies.

Nevertheless, *ToU + MI* cause the greatest charging power peaks (see Figure 7). Every day at 9 p.m., the optimizer schedules the vehicles that arrived between 4 and 9 p.m. to start charging at the same time. This leads to power peaks of more than 6 kW/EV for both data sets.

Overall, the US CHTS and the GER MP results show similar trends for the cost-optimal charging power for the five operating strategies simulated.

4.2. Flexibility

4.2.1. Operating Strategies

In the bottom two plots of Figure 7 the ranges of flexibility for the five operating strategies simulated are visualized.

For EVs, positive flexibility is equivalent to a pause or postponement of the charging process. Therefore, the upper boundary of the flexibility is equal to the optimal charging power.

According to the definition in Section 1, negative flexibility is the ability to consume electricity ahead of its schedule. Considering the operating strategy *Con + MI* and a cost optimization, no negative flexibility can be offered. Therefore, the lower boundary of the simulation results is congruent with the zero line (see Figure 7).

Similar to the aforementioned operating strategy, *ToU + MI* result in no negative flexibility between 9 p.m. and 4 p.m. From 4 p.m. to 9 p.m., the negative flexibility increases linearly as vehicles arrive

home, and their charging process is scheduled from 9 p.m. onwards owing to lower electricity prices. At 9 p.m., negative flexibility drops back to zero.

The operating strategy *Con* and *ToU* result in almost identical negative flexibility results. Furthermore, the negative flexibility that can be offered follows the vehicle availability curves discussed in Section 3.1.3). Periodically, at night time, negative flexibility increases and reaches its maximum around 1 to 3 a.m. During the morning hours before 12 a.m., the flexibility decreases. Negative flexibility ranges from −5 kW/EV to −7.5 kW/EV with the *Con* and *ToU* operating strategies. On weekends, the ranges are smaller since vehicle fluctuations also decrease. At 4 p.m., the *ToU* operating strategy causes a minor drop in negative flexibility due to the charging of vehicles that depart between 4 and 9 p.m.

The *RTP* operating strategy also follows the vehicle availability described in Section 3.1.3). However, in contrast to the results of the *ToU* and *Con* operating strategies, the maximum negative flexibility is available right before midnight. After midnight, when electricity prices are the lowest, the vehicles are charged and the available negative flexibility decreases. On weekends, the range of negative flexibility that can be offered decreases slightly as the fluctuations in vehicle availabilities also decrease. The negative flexibility that can be offered ranges between −2 kW/EV and −7 kW/EV for both data sets. Therefore, *RTP* prices lead to less offerable negative flexibility than a *Con* or *ToU* operating strategy.

Having described the impact of the five operating strategies, the next subsections describe the impact of the maximal charging power on the offerable flexibility of EVs.

4.2.2. Maximal Charging Power

To analyze the impact of the maximum charging power level, the optimization and flexibility calculation for all vehicle availabilities are repeated for three maximum charging power levels: 3.7 kW, 11 kW, and 22 kW. Figure 8 shows the positive and negative flexible power that can be offered for the GER MP data set. Each operating strategy corresponds to a row and each maximum charging power level to a column of heat maps. Tables 5 and 6 summarize the maximal flexible power and average flexible power for all five operating strategies. Generally, the positive flexibility is also representative of the cost-optimal charging power.

Table 5. Maximum and average positive flexible power for five operating strategies and three maximum charging powers.

Operating Strategy	$P_{pos,max}$ [kW/EV]			$P_{pos,avg}$ [kW/EV]		
	3.7 kW	**11 kW**	**22 kW**	**3.7 kW**	**11 kW**	**22 kW**
Con	1.1	1.8	2.1	0.4	0.5	0.5
ToU	1.1	2.1	2.8	0.4	0.5	0.5
Con + MI	1.1	1.6	2.0	0.4	0.5	0.5
ToU + MI	2.4	5.7	9.1	0.4	0.4	0.5
RTP	1.9	4.0	6.2	0.4	0.4	0.4

Table 6. Maximum and average negative flexible power for five operating strategies and three maximum charging powers.

Operating Strategy	$P_{neg,max}$ [kW/EV]			$P_{neg,avg}$ [kW/EV]		
	3.7 kW	**11 kW**	**22 kW**	**3.7 kW**	**11 kW**	**22 kW**
Con	−2.9	−7.8	−12.8	−1.9	−6.9	−11.3
ToU	−2.9	−7.8	−12.8	−1.9	−6.8	−11.1
Con + MI	0.0	0.0	0.0	0.0	0.0	0.0
ToU + MI	−2.3	−5.6	−9.0	0.0	−0.6	−0.9
RTP	−2.9	−7.6	−12.2	−0.2	−4.3	−6.7

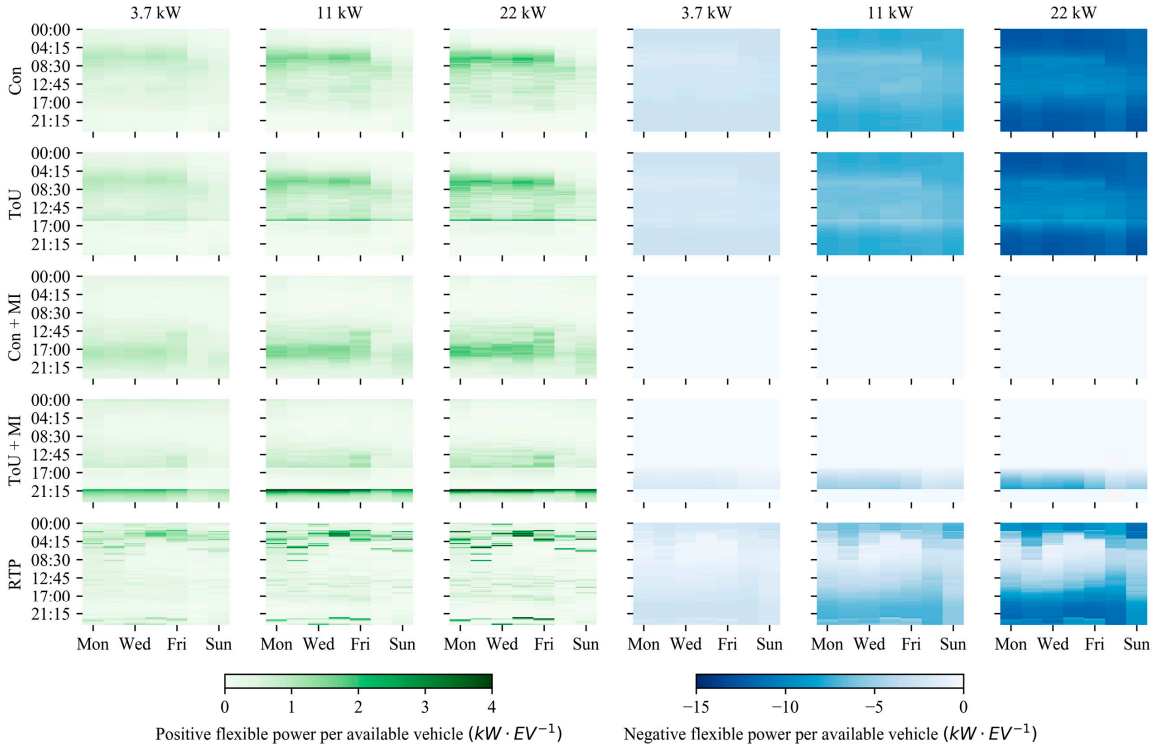

Figure 8. Resulting positive and negative flexible power per available EV. These results are based on the GER MP vehicle availabilities, the five operating strategies {*Con*, *ToU*, *Con + MI*, *ToU + MI*, *RTP*}, and three maximal charging power levels {3.7, 11, 22 kW}.

The results of the *ToU* and *Con* operating strategy show similar behavior. As described in Section 4.1, the optimizer schedules EV chargings at the latest possible time. This leads to higher charging powers and a high level of positive flexibility from 3 a.m. to 8 a.m. on weekdays. A higher maximum charging power increases the maximal and average positive flexible power that can be offered (see Figure 8). However, the duration of positive flexibility seems to decrease with increasing maximum charging power in Figure 8. With a higher charging power level, the energy required is charged over a shorter time period, and therefore leads to a compressed availability of positive flexibility. The increase of maximal and average positive flexible power with an increasing maximum charging power can be explained by assuming that with a low charging power, e.g., 3.7 kW, not all vehicles are completely charged. In this case, the vehicle cannot offer any flexibility. With a higher maximum charging power, the charging station charges the EV over a shorter period and can therefore offer more flexibility. However, this relation is not linear, since the average positive flexible power seems to only change insignificantly from 11 to 22 kW. Therefore, the two observations described complement each other.

Considering the cost optimization described in IV.A, the results for positive flexible power for the *ToU + MI*, *Con + MI*, and *RTP* operating strategies indicate a similar behavior. With an increasing charging power, the positive flexible power that can be offered is compressed in time whereas the maximal power increases. Furthermore, the average quantity of positive flexibility increases (see Table 5). Both effects are explained in the previous paragraph.

Nevertheless, the *ToU + MI* and *RTP* operating strategies cause such high charging peaks at 9 p.m. (*ToU + MI*) and overnight (*RTP*) that the average maximal positive flexible power is three and two times higher than in the remaining operating strategies. Whereas the impact of the *RTP* might be overestimated since in a real-world scenario prices cannot be predicted as easily, the *ToU + MI* operating strategy can pose a major threat to grid stability.

Considering *ToU* and *Con* operating strategies, most negative flexibility can be offered at night and on weekends, when most vehicles are at home. Operating strategies with minimal price increments result in no flexibility (*Con + MI*) or only for short durations from 4 to 9 p.m. (*ToU + MI*). The causes have been discussed in the previous section. An *RTP* operating strategy shows similar trends as the *ToU* and *Con* operating strategies for weekdays. Most negative flexibility is offered at nighttime, from 5 p.m. to 3 p.m. On weekends, negative flexibility is at a high level and homogenously distributed for the *Con* and *ToU* operating strategy, whereas *RTP* results indicate a similar behavior as during the week. Such behavior can be explained by the time-varying electricity prices that are lower at nighttime throughout the entire week.

As discussed in the previous subsection the *ToU*, *Con*, and *RTP* operating strategies show similar trends in offerable negative flexibility. Table 6 displays the absolute differences between the operating strategies and the maximal charging power.

A variation in charging power results in an increase in maximal and average negative flexibility for all five simulated pricing scenarios. In order to identify a mathematical relationship between the maximum charging power and the amount of negative flexibility further simulations are required.

With all results summarize, the next chapter discusses the validity and limitations of the applied method.

5. Discussion

This paper presents a thorough analysis of cost-optimal charging schedules and flexibility potential of more than 15,000 vehicle availabilities at home for five operating strategies, and three maximal charging power levels. While the calculation of cost-optimal charging schedules is state of the art, the quantification and analysis of the available flexibility of EV complements and enhances existing literature.

In this analysis, perfect price forecasts have been used to analyze the flexibility of EVs. For the first four operating strategies, which were based on *Con* and *ToU* tariffs, the consideration of perfect

price forecasts would not have led to any other results. However, in the case of *RTP* the effect of the perfect price forecast is not negligible. Since *RTP* cannot be forecasted precisely and multiple methods lead to a range of results, the absolute impact of *RTP* is expected to be smaller in reality. Therefore, future research will investigate the impact of the uncertainty of price forecasts on the flexibility that can be offered.

Overall, the *ToU + MI* operating strategy leads to the least favorable charging behavior and flexibility offers. The average charging power indicates major peaks at 9 p.m. and a smaller peak at 3:45 p.m. Both peaks are caused by the mid- and on-peak prices between 4 and 9 p.m. These peaks occur every weekday with similar power levels and therefore represent a significant stress for grid operation. The original assumption that the network could be relieved by time-varying discrete tariffs will become obsolete in the near future, when charging processes will be optimized and automated. This conclusion is in line with the existing literature [13,17]. Nevertheless, *ToU* operating strategies lead to the overall minimum charging costs compared to the other operating strategies (see Figure 9). Despite the seemingly cheaper *ToU* tariffs, regulators should omit operating strategies that offer pre-known price differences in the future for the sake of grid stability and security of supply.

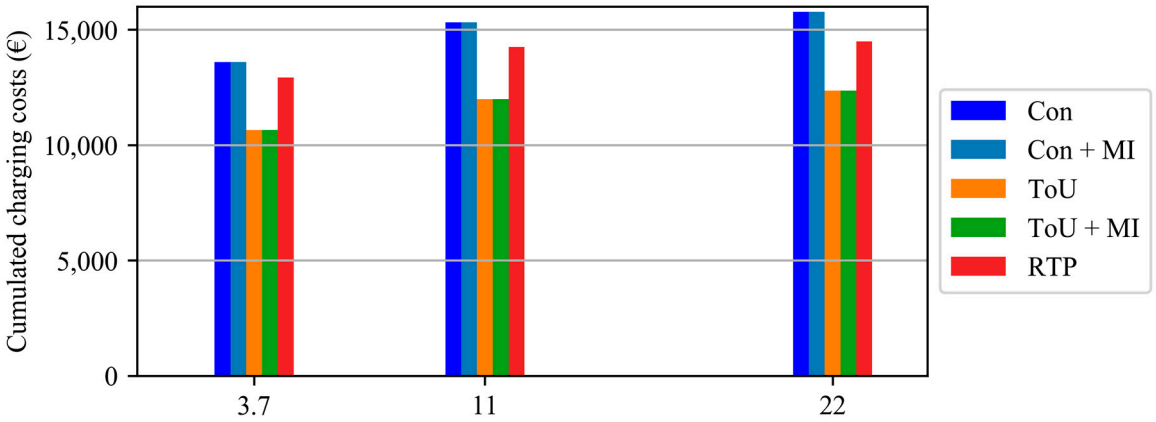

Figure 9. Cumulated charging costs in € for five operating strategies and three maximum charging power levels. For this analysis, the 11,103 vehicle availabilities of the GER MP field trial were used.

In order to achieve grid-friendly user behavior and not to create further grid congestions, we will investigate the integration of local energy markets (LEM). LEM enable participants to trade and exchange their electricity locally. Market agents within HEMS predict the vehicle availability, post bids on the LEM, and adjust their bids automatically based on market results. With this approach, different prices are calculated locally, and users are motivated to consume electricity in times of high generation and to generate electricity in times of high demand.

For this case study, the most recent publicly available data sets with all required parameters were chosen. Since the field trial data was collected from a wide variety of households with different types of vehicles and only contain information about the distances traveled, departure and arrival times, the results can only be representative for realistic user behavior but not for specific types of vehicles. The energy demands of the vehicles were calculated based on the distances traveled. Even though the two data sets are not from the same year (2012/2013 and 2017), the results do not indicate any major differences. Furthermore, the report on the GER MP state that the trends in transportation and individual mobility have remained almost constant over the last 10 years [21]. Therefore, the effect of the different survey periods is considered insignificant. Nevertheless, the continuation of the coronavirus pandemic may mean that employees will be able to work from home to a greater extent, and that vehicle availability may therefore change in the long term. This effect has not yet been taken into account in this study but would be an interesting new aspect.

The gathered flexibility results of this case study are based on availabilities of vehicles at home. However, the method described is neither limited to those two regions nor to quantify flexibility based on EVs at home. This method is applicable to any region/data set that contains information about trip start and end times, purpose or start and end location of the trip, means of transport and distance travelled. Further investigations will investigate differences from other world regions and the quantification of flexibility at other locations, such as workplaces.

6. Conclusions

This paper describes in detail a model that calculates cost-optimal charging schedules and quantifies the flexibility of EV. A case study with more than 15,000 vehicle availabilities from Germany and the USA was conducted and the results visualized for weekdays, weekends, and an average week. Furthermore, the impact of five operating strategies and three charging power levels on the offerable flexibility were analyzed.

Based on these results, the following key findings can be drawn:

1. *ToU* tariffs in combination with the user preference to charge the vehicle as soon as possible (*ToU* + *MI*) leads to significant increased grid congestions.
2. Positive flexibility is mostly available during either the evening hours or early morning hours depending on the user's preferred charging time (*MI*).
3. No negative flexibility is available if the user is charged a constant electricity rate and chooses to charge as soon as possible (*Con* + *MI*).
4. Negative flexibility follows the periodic availability of vehicle availabilities at home if the user chooses to charge the vehicle as late as possible (*Con*).
5. Increased charging power levels lead to higher absolute positive and negative flexibility power levels and also increase the total offerable flexibility of EVs.

In conclusion, the model presented in Section 2 is able to quantify EV flexibility. Regulators, researchers, and system operators can use this model to investigate various influences such as tariff structures, user preferences, charging power levels etc. on the flexibility of EVs. Furthermore, the presented HEMS model can calculate the flexibility of heat pumps, combined heat and power, photovoltaic and battery systems. Once completed, this model will be a new helpful tool for tasks such as flexibility calculation, grid expansion planning, and the design and implementation of future electricity regulations.

Supplementary Materials: The model and the script to perform the ev case study is open-source and accessible via the following link: https://zenodo.org/badge/latestdoi/212816117.

Author Contributions: Conceptualization, M.Z.; data curation, M.Z.; formal analysis, M.Z. and P.T. funding acquisition, P.T. and U.W.; investigation, M.Z. and Z.Y.; methodology, M.Z. and Z.Y.; project administration, P.T. and U.W.; software, M.Z., Z.Y., and B.K.N.; supervision, P.T. and U.W.; validation, M.Z.; visualization, M.Z.; writing—original draft, M.Z. and Z.Y.; writing—review and editing, M.Z., Z.Y., B.K.N., P.T. and U.W. All authors have read and agreed to the published version of the manuscript.

Funding: The German Federal Ministry for Economic Affairs and Energy, Bundesministerium für Wirtschaft und Energie, funded this research under the grant number 03SIN109.

Conflicts of Interest: The authors declare no conflict of interest. The funders had no role in the design of the study; in the collection, analyses, or interpretation of data; in the writing of the manuscript, or in the decision to publish the results.

References

1. Ma, J.; Silva, V.; Belhomme, R.; Kirschen, D.S.; Ochoa, L.F. Evaluating and Planning Flexibility in Sustainable Power Systems. *IEEE Trans. Sustain. Energy* **2012**, *4*, 200–209. [CrossRef]
2. Eurelectric (2014)—Flexibility-and-Aggregation. 2014. Available online: https://www.usef.energy/app/uploads/2016/12/EURELECTRIC-Flexibility-and-Aggregation-jan-2014.pdf (accessed on 26 October 2020).

3. Paulus, M.; Borggrefe, F. The potential of demand-side management in energy-intensive industries for electricity markets in Germany. *Appl. Energy* **2011**, *88*, 432–441. [CrossRef]
4. Strbac, G. Demand side management: Benefits and challenges. *Energy Policy* **2008**, *36*, 4419–4426. [CrossRef]
5. Zhou, K.; Yang, S. Demand side management in China: The context of China's power industry reform. *Renew. Sustain. Energy Rev.* **2015**, *47*, 954–965. [CrossRef]
6. Radecke, J.; Hefele, J.; Hirth, L. Markets for Local Flexibility in Distribution Networks. Kiel, Hamburg. 2019. Available online: https://www.econstor.eu/bitstream/10419/204559/1/Radecke%2C%20Hefele%20%26%20Hirth%202019%20%20Markets%20for%20Local%20Flexibility%20in%20Distribution%20Networks.pdf (accessed on 1 June 2020).
7. Nalini, B.K.; Eldakadosi, M.; You, Z.; Zade, M.; Tzscheutschler, P.; Wagner, U. Towards Prosumer Flexibility Markets: A Photovoltaic and Battery Storage Model. In Proceedings of the 2019 IEEE PES Innovative Smart Grid Technologies Europe (ISGT-Europe), Bucharest, Romania, 29 September 2019–2 October 2019; pp. 1–5.
8. You, Z.; Nalini, B.K.; Zade, M.; Tzscheutschler, P.; Wagner, U. Flexibility quantification and pricing of household heat pump and combined heat and power unit. In Proceedings of the 2019 IEEE PES Innovative Smart Grid Technologies Europe (ISGT-Europe), Bucharest, Romania, 29 September 2019–2 October 2019; pp. 1–5.
9. Zade, M.; Incedag, Y.; El-Baz, W.; Tzscheutschler, P.; Wagner, U. Prosumer Integration in Flexibility Markets: A Bid Development and Pricing Model. In Proceedings of the 2018 2nd IEEE Conference on Energy Internet and Energy System Integration (EI2), Beijing, China, 20–22 October 2018; pp. 1–9.
10. Kumar, A.; Srivastava, S.; Singh, S. Congestion management in competitive power market: A bibliographical survey. *Electr. Power Syst. Res.* **2005**, *76*, 153–164. [CrossRef]
11. Yusoff, N.I.; Zin, A.A.M.; Bin Khairuddin, A. Congestion management in power system: A review. In Proceedings of the 2017 3rd International Conference on Power Generation Systems and Renewable Energy Technologies (PGSRET), Johor Bahru, Malaysia, 4–6 April 2017; pp. 22–27.
12. Beaudin, M.; Zareipour, H. Home energy management systems: A review of modelling and complexity. *Renew. Sustain. Energy Rev.* **2015**, *45*, 318–335. [CrossRef]
13. Yan, X.; Ozturk, Y.; Hu, Z.; Song, Y. A review on price-driven residential demand response. *Renew. Sustain. Energy Rev.* **2018**, *96*, 411–419. [CrossRef]
14. Eurelectric—Union of the Electricity Industry. Dynamic Pricing in Electricity Supply. February 2017. Available online: http://www.eemg-mediators.eu/downloads/dynamic_pricing_in_electricity_supply-2017-2520-0003-01-e.pdf (accessed on 18 June 2020).
15. Limmer, S. Dynamic Pricing for Electric Vehicle Charging—A Literature Review. *Energies* **2019**, *12*, 3574. [CrossRef]
16. Barbose, G.; Goldman, C.; Neenan, B. *A Survey of Utility Experience with Real Time Pricing*; LBNL: Berkeley, CA, USA, 2004.
17. Muratori, M.; Rizzoni, G. Residential Demand Response: Dynamic Energy Management and Time-Varying Electricity Pricing. *IEEE Trans. Power Syst.* **2015**, *31*, 1108–1117. [CrossRef]
18. Veldman, E.; Verzijlbergh, R.A. Distribution Grid Impacts of Smart Electric Vehicle Charging From Different Perspectives. *IEEE Trans. Smart Grid* **2014**, *6*, 333–342. [CrossRef]
19. Atabay, D. An open-source model for optimal design and operation of industrial energy systems. *Energy* **2017**, *121*, 803–821. [CrossRef]
20. NuStats, L.L.C. 2010–2012 California Household Travel Survey: Final Report. June 2013. Available online: https://www.nrel.gov/transportation/secure-transportation-data/assets/pdfs/calif_household_travel_survey.pdf (accessed on 23 July 2020).
21. Ecke, L.; Chlond, B.; Magdolen, M.; Hilgert, T.; Vortisch, P. Deutsches Mobilitätspanel (MOP): Wissenschaftliche Begleitung und Auswertung Bericht 2018/2019: Alltagsmobilität und Fahrleistung. *Ger. Mobil. Panel* **2020**.
22. California Department of Transportation. 2010–2012 California Household Travel Survey. National Renewable Energy Laboratory. Available online: https://www.nrel.gov/transportation/secure-transportation-data/tsdc-california-travel-survey.html (accessed on 23 July 2020).
23. U.S. Energy Information Administration. 2018 Average Monthly Bill—Residential: (Data from Forms EIA-861- Schedules 4A-D, EIA-861S and EIA-861U). 2018. Available online: https://www.eia.gov/electricity/sales_revenue_price/pdf/table5_a.pdf (accessed on 23 July 2020).

24. Commonwealth Edison Company. Comed's Hourly Pricing Program. Available online: https://hourlypricing.comed.com/ (accessed on 23 July 2020).
25. Electric Vehicle Database: Energy Consumption of Full Electric Vehicles. Available online: https://ev-database.org/cheatsheet/energy-consumption-electric-car (accessed on 23 July 2020).
26. Hao, X.; Wang, H.; Lin, Z.; Ouyang, M. Seasonal effects on electric vehicle energy consumption and driving range: A case study on personal, taxi, and ridesharing vehicles. *J. Clean. Prod.* **2020**, *249*, 119403. [CrossRef]

Chapter 4

Conclusion and future research

This dissertation describes how formerly passive consumers and prosumers are integrated and coordinated as active participants in LEMs and are transforming into flexumers preventing grid congestions and enabling a continuous expansion of renewable energies.

4.1 Conclusion

The articles presented in this dissertation introduce new coordination mechanisms, an innovative flexibility model, and the results of three analyses that provide new insights on how to coordinate increasingly decentralized, renewable, and electrified energy systems. Based on these findings, the RQs formulated in section 1.1 are answered.

RQ#1 addressed coordination mechanisms that allow consumers and prosumers to be integrated as active participants into energy systems, to trade energy locally, and to take into account their preferences for energy qualities such as *green* or *local*. Simulation results show that the newly developed library of IMCAs and bidding format fulfill the aforementioned criteria. With the help of these algorithms, consumers and prosumers can verifiably supply their energy demand with electricity of their preferred energy quality and adapt their feed-in and consumption behavior based on the availability of renewable or local electricity. This enables consumers and prosumers to support the decarbonization of the energy system and the reduction of both transmission losses and grid expansion costs.

RQ#2 asked how consumers and prosumers can support grid operations by providing market-based flexibility to grid operators and how much flexibility at what time and price could be expected from them. A case study with real world mobility data demonstrated the functionality of the introduced flexibility quantifying and pricing model and visualized the flexibility potential of EVs that can be used to prevent future grid congestions. This model represents the first approach transforming consumers and prosumers into flexumers who can decentrally offer market-based flexibility as requested in the EU's Clean Energy Package directive 2019/944 [15]. Ideally, these flexumers help to efficiently avoid grid congestions, which reduces grid management costs and enables the continued expansion of renewable energies.

RQ#3 concerned the potential added value the blockchain technology could provide in coordinating consumers and prosumers compared to centralized implementations, particularly in LEMs. The results of a comparative performance analysis show that the blockchain-based LEM implementation does not fulfill essential LEM requirements such as data privacy and scalability and only adds value in the category of tamper resistance. Therefore, I conclude that the blockchain technology at its current stage of development does not help to coordinate or empower consumers and prosumers to host their own energy trading applications.

With the help of the presented models, scientists, energy experts, and regulators are able to model the coordination of consumers, prosumers and flexumers and their preferences, thus facilitating their efficient integration into energy systems.

4.2 Future research

I conclude this dissertation with the following recommendations for future research.

Consumer- and prosumer-centric energy markets

After investigating consumer preferences for heterogeneous energy qualities in detail in community-based LEMs, an interesting field of research is to incorporate consumer preferences also in centralized optimizations and pure P2P approaches and to compare the results with each other.

In the future, LEMs are going to be coupled either directly to whole-sale markets or to neighbouring platforms to increase liquidity. In chapter 2, market coupling is modelled with a retailer that is connected to both markets and bears the entire whole-sale market risk by setting fixed upper and lower price boundaries on the LEM. Future research should investigate how LEMs can be coupled with each other, to whole-sale and flexibility markets, and evaluate the markets' interdependencies.

While the newly developed clearing algorithms were tested and analyzed for local electricity-only markets, an interesting RQ could be whether the presented clearing algorithms for heterogeneous energy qualities can be used for other commodities such as heat or in whole-sale markets with interconnected bidding blocks.

Within this dissertation, I modelled auction-based LEMs without grid constraints. Future research should investigate how grid constraints can be considered in community-based LEMs and what impact they have on consumer preferences. *lemlab* offers the basis for modelling grid constraints and load-dependent grid fees, thereby allowing to investigate how grid congestions can be prevented in dispatching processes.

Hybrid blockchain solutions

With regard to RQ#3, I introduced an experimental test setup comparing a fully blockchain-based implementation with a centralized LEM. Future work should study how the fulfillment of the technology-independent LEM requirements changes with a hybrid implementation to combine the advantages of a central and a blockchain-based LEM structure. The developed add-on for the open-source project *lemlab* can help to quickly implement

different variants and assess their performances similar to section 2.2. Additionally, *lemlab* is extendable to support other blockchain protocols such as Tendermint and Hyperledger to analyze alternative blockchain protocols and their suitability for LEM applications.

Further flexibilization of energy systems

The presented model, which quantifies and prices flexibility potentials of consumers and prosumers, can only be the first step in the field of market-based procurement of flexibility with flexumers. Future research should investigate how uncertainties and probabilistic forecasts can be considered in the model, how regulatory decisions impact flexibility potentials, and how the model can be used for commercial and industrial sites.

In order to further validate the flexibility offers of flexumers and assess whether investments in flexible infrastructures could be stimulated by flexibility markets, research on flexibility demands, market platform designs, and the interdependencies between energy and flexibility markets needs to be intensified.

Appendix A

List of publications

A.1 First-authored publications

1. M. Zade, S. D. Lumpp, P. Tzscheutschler, and U. Wagner. Satisfying user preferences in community-based local energy markets — Auction-based clearing approaches. Applied Energy, 306:118004, 2022. URL: https://doi.org/10.1016/j.apenergy.2021.118004.
2. M. Zade, M. Feroce, A. Guridi, S. D. Lumpp, and P. Tzscheutschler. Evaluating the added value of blockchains to local energy markets — Comparing the performance of blockchain–based and centralised implementations. IET Smart Grid, 2022. URL: https://doi.org/10.1049/stg2.12058.
3. M. Zade, Y. Incedag, W. El-Baz, P. Tzscheutschler, and U. Wagner. Prosumer integration in flexibility markets: A bid development and pricing model. In 2018 2nd IEEE Conference on Energy Internet and Energy System Integration (EI2), pages 1–9. IEEE, 2018. URL: https://doi.org/10.1109/EI2.2018.8582022.
4. M. Zade, Z. You, B. Kumaran Nalini, P. Tzscheutschler, and U. Wagner. Quantifying the flexibility of electric vehicles in Germany and California — A case study. Energies, 13 (21): 5617, 2020. URL: https://doi.org/10.3390/en13215617.
5. M. Zade, J. Myklebost, P. Tzscheutschler, and U. Wagner. Is bitcoin the only problem? A scenario model for the power demand of blockchains. Frontiers in Energy Research, 7, 2019. URL: https://doi.org/10.3389/fenrg.2019.00021.

A.2 Co-authored publications

1. B. K. Nalini, M. Eldakadosi, Z. You, M. Zade, P. Tzscheutschler, and U. Wagner. Towards prosumer flexibility markets: A photovoltaic and battery storage model. In 2019 IEEE PES Innovative Smart Grid Technologies Europe (ISGT-Europe), pages 1–5. IEEE, 29.09.2019 - 02.10.2019. URL: https://doi.org/10.1109/isgteurope.2019.8905622.
2. G. C. Okwuibe, M. Zade, P. Tzscheutschler, T. Hamacher, and U. Wagner. A blockchain-based double-sided auction peer-to-peer electricity market framework. In 2020 IEEE Electric Power and Energy Conference (EPEC), pages 1–8. IEEE, 09.11.2020

- 10.11.2020. URL: https://doi.org/10.1109/EPEC48502.2020.9320030.

3. C. Weinhardt, E. Mengelkamp, W. Cramer, S. Hambridge, A. Hobert, E. Kremers, W. Otter, P. Pinson, V. Tiefenbeck, and M. Zade. How far along are local energy markets in the DACH+ region? In Proceedings of the Tenth ACM International Conference on Future Energy Systems, pages 544–549, New York, NY, USA, 2019. ACM. URL: https://doi.org/10.1145/3307772.3335318.
4. Z. You, B. K. Nalini, M. Zade, P. Tzscheutschler, and U. Wagner. Flexibility quantification and pricing of household heat pump and combined heat and power unit. In 2019 IEEE PES Innovative Smart Grid Technologies Europe (ISGT-Europe), pages 1–5. IEEE, 29.09.2019 - 02.10.2019. URL: https://doi.org/10.1109/isgteurope.2019.8905594.
5. Z. You, M. Zade, B. Kumaran Nalini, and P. Tzscheutschler. Flexibility estimation of residential heat pumps under heat demand uncertainty. Energies, 14 (18): 5709, 2021. URL: https://doi.org/10.3390/en14185709.

A.3 Open-source repositories

1. S. D. Lumpp, M. Zade, and M. Doepfert. *lemlab*. [Computer software]. URL: https://github.com/tum-ewk/lemlab, 2021.
2. Z. You, M. Zade, and B. Kumaran Nalini. *OpenTUMFlex*. [Computer software]. URL: https://github.com/tum-ewk/opentumflex, 2020.
3. M. Zade, J. Myklebost. Bitcoin and Ethereum mining hardware. [Data collection]. URL: https://doi.org/10.17632/4dw6j3pxz5.1, 2018.

Appendix B

Preparatory study on the power demand of Bitcoin and Ethereum

Publication #5: Is Bitcoin the Only Problem? A Scenario Model for the Power Demand of Blockchains

Authors Michel Zade, Jonas Myklebost, Peter Tzscheutschler, Ulrich Wagner

Publication medium Frontiers in Energy Research, Volume 7, Article 21

Digital object identifier https://doi.org/10.3389/fenrg.2019.00021

Open-source repository all data sets collected for this study can be found in [115], Etherscan (2018), and Blockchain Luxembourg S.A. (2018).

Author contributions

Michel Zade:	75 %	Conceptualization, Methodology, Software, Investigation, Visualization, Writing – original draft, Writing – review & editing.
Jonas Myklebost:	10 %	Software, Investigation, Writing – review & editing.
Peter Tzscheutschler:	10 %	Conceptualization, Methodology, Investigation, Writing – review & editing, Project administration, Funding acquisition.
Ulrich Wagner:	5 %	Investigation, Writing – review & editing, Supervision, Funding acquisition.

frontiers in Energy Research

ORIGINAL RESEARCH
published: 13 March 2019
doi: 10.3389/fenrg.2019.00021

Is Bitcoin the Only Problem? A Scenario Model for the Power Demand of Blockchains

Michel Zade, Jonas Myklebost, Peter Tzscheutschler and Ulrich Wagner*

Chair of Energy Economy and Application Technology, Department of Electrical and Computer Engineering, Technical University of Munich, Munich, Germany

When an author under the pseudonym Satoshi Nakamoto published the paper "Bitcoin: A Peer-to-Peer Electronic Cash System" in 2008, the first cryptocurrency using the new blockchain technology was introduced. Over the last decade, more than 1,000 different cryptocurrencies, such as Ethereum, Ripple, and Litecoin were developed and Bitcoin's currency had almost reached an equivalent value of 20,000 $/BTC. After recognizing the disrupting momentum that the blockchain technology generated, scientists started to develop blockchain use cases for the energy sector. However, the scientific literature so far offers only rough and incomplete estimations when questions about the current and future energy consumption of the Bitcoin network are raised. This paper introduces a new scenario model to estimate the mining power demand of the Bitcoin and Ethereum network. Six scenarios are developed on the basis of mining hardware efficiency and network parameter data. The results show that an increase of the mining hardware efficiency will only have a limited impact on the overall power demand of blockchain networks. Furthermore, the current power demand of the Ethereum network is in the range from 0.6 to 3 GW and therefore, is similar to the one of Bitcoin. In case of linear growth of the block difficulty and sigmoidal increase of the hardware efficiency until the year of 2025, the mining power demand for the Bitcoin blockchain will be approximately 8 GW. Furthermore, the model and the scenarios are adaptable to other cryptocurrencies that use the proof-of-work consensus algorithm to create scenarios for their future power demand.

Keywords: blockchain, bitcoin, ethereum, mining power demand, scenario, block difficulty, hardware efficiency

OPEN ACCESS

Edited by:
Sonia Yeh,
Chalmers University of Technology, Sweden

Reviewed by:
Eric Hittinger,
Rochester Institute of Technology, United States
David Malone,
Maynooth University, Ireland

****Correspondence:***
Michel Zade
michel.zade@tum.de

Specialty section:
This article was submitted to Energy Systems and Policy, a section of the journal Frontiers in Energy Research

Received: *03 January 2019*
Accepted: *13 February 2019*
Published: *13 March 2019*

Citation:
Zade M, Myklebost J, Tzscheutschler P and Wagner U (2019) Is Bitcoin the Only Problem? A Scenario Model for the Power Demand of Blockchains. Front. Energy Res. 7:21. doi: 10.3389/fenrg.2019.00021

1. INTRODUCTION

In 2008, an author under the pseudonym Satoshi Nakamoto published the idea of a decentralized cryptocurrency based on the blockchain technology (Nakamoto, 2008). The idea became reality in 2009 when the Bitcoin network was launched. Since then, and especially in 2017, when the Bitcoin price nearly reached 20,000 $/BTC, the blockchain technology witnessed an immense growth of attention. Many research papers have so far focused on the usability of the blockchain technology on the peer-to-peer (P2P) level, and in micro-grid energy markets (Sabounchi and Wei, 2017; Wang et al., 2017; Mengelkamp et al., 2018). However, since 2017, the public raises questions about the current, and future energy consumption, and environmental impact of the Bitcoin blockchain and other cryptocurrencies (altcoins) (DiChristopher, 2017; Popper, 2018). The scientific literature currently offers few, and incomplete models to answer these questions.

Economical models to estimate the energy consumption of blockchains were introduced in 2015. Hayes presented the first model that estimated the energy consumption of the Bitcoin network based on the marginal product and costs. The break-even points are based on the market prices, the difficulty of the network (an indicator for the computing power in the blockchain), and an average price for electricity (see Hayes, 2015). Vries argues that Hayes' model does not cover the investment costs of the mining hardware and concludes that only 60 % of the marginal product is used to cover the electricity demand (de Vries, 2018b). The latter approach is used on the website of the Digiconomist (de Vries, 2018a). At the end of 2017, the Bitcoin market price fluctuated heavily, whereas the Bitcoin block difficulty grew steadily (see **Figure 1**). As a result of this development, the aforementioned economical approaches can only offer an upper bound of the overall energy consumption of the network.

Hashrate-based, bottom-up models were first introduced by Malone and O'Dwyer (2014). The calculation of the Bitcoin power demand considered the Bitcoin block difficulty and the efficiency of the mining hardware (Malone and O'Dwyer, 2014). Malone et al. calculated only lower and upper bounds of the mining power demand with the most and least efficient hardware available in 2014 because of an unknown combination of the actual operating hardware. Mora et al. used the equations developed in the aforementioned model (Mora et al., 2018). However, the researchers picked for each mined block in 2017 an arbitrary hardware efficiency to calculate the power demand. The procedure was repeated 1,000 times, in order to reduce the impact of the randomness (Mora et al., 2018). Unfortunately, the latter approach does not consider the release date and the profitability of the randomly picked mining hardware. Therefore, the estimate for the power demand and the resulting CO_2 emissions is most likely unrealistically high for 2017. Krause et al. presented a model that estimates the annual average power demand of Bitcoin, Ethereum, Litecoin, and Monero for the years of 2016, 2017, and partially 2018 by multiplying an average hardware efficiency to the network's hashrate (Krause et al., 2018). The network's hashrate is calculated by dividing the block difficulty by the mining rate.

Models, that estimate the future power demand of blockchains, have for the first time been introduced in 2018. Vries proposed the idea to forecast the future power demand by analyzing the supply chain of hardware manufacturers such as Bitmain (de Vries, 2018b). This approach relies on business secrets that are publicly not accessible and therefore, can hardly be objectively verified. Mora et al. fit a logistic curve to the adoption rates of 40 different technologies and use random samples of the 2017 mined blocks to estimate the future CO_2 emissions (Mora et al., 2018). This approach neglects any future improvements of mining hardware. Furthermore, Mora et al. consider mining hardware that is uneconomic already in 2017, and fit the adoption rate of Bitcoin to household appliances that offer insufficient parallels.

In 2017 Vranken, and Giungato et al. published reviews summarizing the previously mentioned approaches but did not introduce new methods (Giungato et al., 2017; Vranken, 2017). Other estimates presented on the Internet claiming to estimate the energy consumption of blockchains often are not reproducible, and therefore are excluded from this scientific discussion.

In conclusion, a reliable hashrate-based scenario model for the future power demand of blockchains is a research gap in the scientific literature (de Vries, 2018b).

This paper presents a new hashrate-based, bottom-up model that allows the creation of scenarios for the future mining power demand of the Bitcoin, and Ethereum blockchain. The model is based on the past development of the mining hardware efficiency, and mining difficulty of the network and is applicable to other blockchains, that use the proof-of-work (POW) consensus algorithm. Section 2 describes the analysis of the network difficulty, mining hardware efficiency, and the setup of the scenarios. In section 3, the results of the model are presented and finally discussed in section 4.

2. METHODS

This section describes the scenario model for the future mining power demand of the Bitcoin and Ethereum blockchain. The first subsection covers the block difficulty, and the second one the mining hardware efficiency. Each subsection is split in two parts: (a) a brief summary of the past evolution and (b) the created scenarios. The final subsection describes the combination of the two isolated scenarios into the final model for the future mining power demand.

2.1. Block Difficulty

The block difficulty is a network parameter in the Bitcoin and Ethereum blockchain that automatically adapts its value to the recent block mining rates of the blockchain. Therefore, the block difficulty can be used as an indicator for the computational power of the blockchain network. In order to create reasonable scenarios, it is crucial to understand the way the block difficulty changes.

2.1.1. Bitcoin Protocol

According to the Bitcoin protocol, the block mining rate shall stay constant at $T_{\mathrm{BTC}} = 10\,\mathrm{min/block}$. Every 2016 blocks $T_{\mathrm{BTC,Adjust,Period}} = 2016\,\mathrm{block}$, the block difficulty is automatically adjusted to make up for the deviations from the intended block mining rate of T_{BTC}. Equation (1) shows the adjustment formula.

$$d_{\mathrm{BTC}} = d_{\mathrm{BTC,prev}} \times (T_{\mathrm{BTC}} \times T_{\mathrm{BTC,Adjust,Period}}) / t_{\mathrm{BTC,2016,blocks}} \quad (1)$$

The block difficulty (d_{BTC}) is calculated by multiplying the previous difficulty ($d_{\mathrm{BTC,prev}}$) with a correction factor. The correction factor is the quotient of the scheduled time $T_{\mathrm{BTC}} \times T_{\mathrm{BTC,Adjust,Period}}$ and the actual time to mine the last 2016 blocks $t_{\mathrm{BTC,2016,blocks}}$. Therefore, the block difficulty increases when the actual time $t_{\mathrm{BTC,2016,blocks}}$ is smaller than the intended time $T_{\mathrm{BTC}} \times T_{\mathrm{BTC,Adapt,Period}}$ to mine the last 2016 blocks. Furthermore, the correction factor is limited to not fall below 25 %, and to not exceed 400% (Nakamoto and The Bitcoin Developers, 2012).

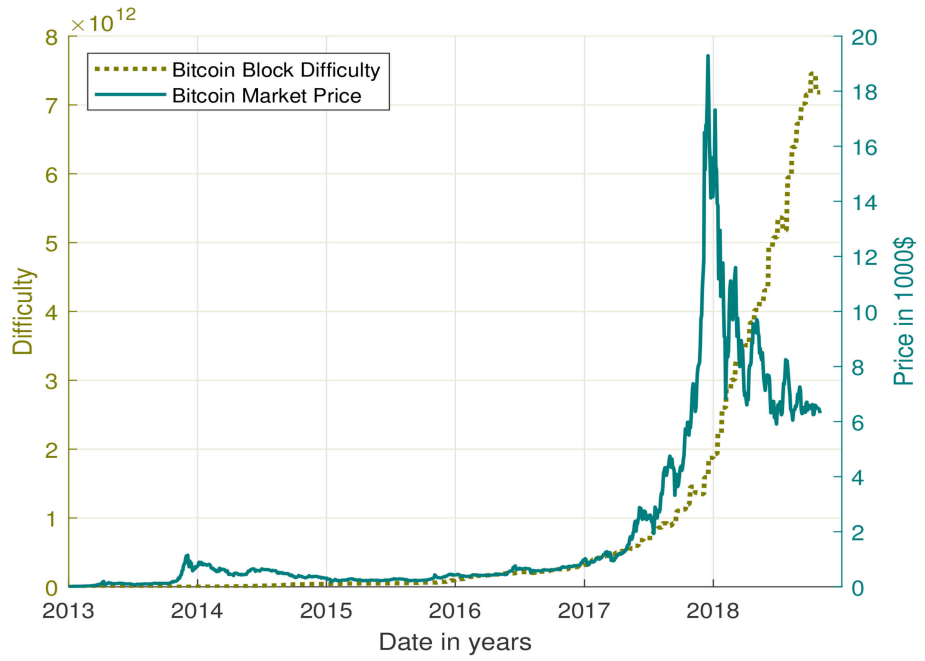

FIGURE 1 | Development of the Bitcoin block difficulty and the market price from January 2013 until October 2018 (Blockchain Luxembourg S.A., 2018).

Figure 1 visualizes the development of the Bitcoin block difficulty and the market price from January 2013 to October 2018. Since the beginning of 2014 until October 2018, the difficulty shows an exponential growth. This growth correlated with the development of the Bitcoin price until December 2017. However, since January 2018 the Bitcoin price shows great fluctuations, whereas the network difficulty constantly rises (see **Figure 1**). Considering the adjustment formula of the mining difficulty in Equation (1) it can be concluded that the computing power added to the Bitcoin network has been exponentially growing since 2014.

While preparing this article from November 2018 until the end of December 2018, the Bitcoin block difficulty decreased for four consecutive 2-week-periods for the first time in Bitcoin history. This decrease coincides to a significant price drop from 6,400 to 3,200$ as of December 16, 2018. However in January 2019, the block difficulty has again increased for two consecutive 2-week-periods. These fluctuations make it difficult to foresee, and extrapolate future developments of the Bitcoin block difficulty. Therefore, a range of possible scenarios are presented in the next section.

2.1.2. Bitcoin Scenarios

Considering the exponential growth of the block difficulty in **Figure 1**, three basic scenarios for the difficulty are employed that seem most convenient. The first one is assuming a continuous exponential increase of the difficulty with a least-squares fit. One data point per day has been used for the fitting. The second scenario is a linear interpolation of the difficulty from January 1st, 2013 and October 31st, 2018. The third scenario is considering a stagnating difficulty. **Figure 2** shows the three chosen scenarios.

The next sections focus on the Ethereum protocol and the scenarios for the Ethereum block difficulty.

2.1.3. Ethereum Protocol

The Ethereum network is designed to offer a "more secure, trustworthy and globally accessible internet," and will undergo multiple development phases and versions to reach this goal (Buterin, 2015b). Those updates had in the past and likely will in the future continue to have direct impact on the calculation of the block difficulty. In the original implementation of 2015, the Ethereum block difficulty (d_{ETH}) was calculated from the previous block difficulty ($d_{\mathrm{ETH,prev}}$) and two additional arithmetic expressions (see Equation 2).

$$\begin{aligned} d_{\mathrm{ETH}} = d_{\mathrm{ETH,prev}} + d_{\mathrm{ETH,prev}}//2048 \\ \times(1 \text{ if } t_{\mathrm{block}} - t_{\mathrm{block,prev}} < 13 \text{ else } -1) \\ +2^{((n_{\mathrm{block}}//100000)-2)} \end{aligned} \tag{2}$$

The first expression is a correction factor, including the spend time to mine the previous block. If the calculated time is shorter or longer than 13 s a correction factor is added or subtracted from the difficulty of the previously mined block. The second expression is called the difficulty bomb. Every 100,000 blocks this expression grows exponentially, starting at block 300,000. The difficulty bomb was implemented to move toward an "ice age" with the POW algorithm, in order to pressure the transition to proof-of-stake (POS), an alternative consensus algorithm. Double dashes symbolize an integer division, curtailing the remainder (Buterin, 2015a).

Equation (3) shows the updated adjustment formula for the block difficulty after the Homestead release, which was the

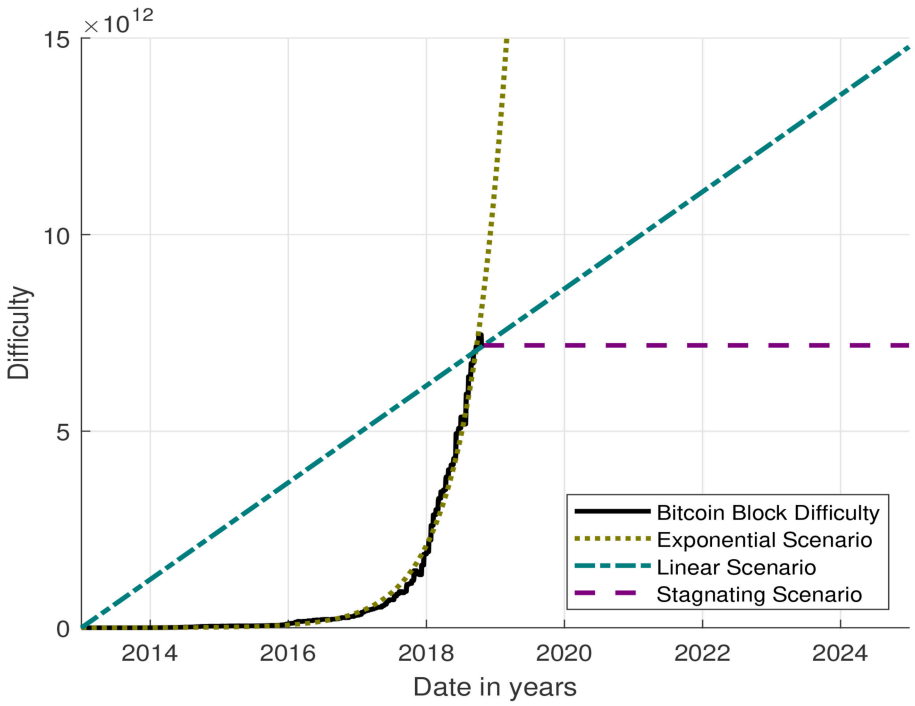

FIGURE 2 | Exponential, linear, and stagnating scenario for the future development of the Bitcoin block difficulty fitted to the past difficulty. Data for the Bitcoin block difficulty from Blockchain Luxembourg S.A. (2018).

second version of the Ethereum platform and included multiple protocol and network changes (Jeffrey Wilcke, 2016).

$$d_{\text{ETH}} = d_{\text{ETH,prev}} + d_{\text{ETH,prev}}//2048 \times \max(1 - (t_{\text{block}} - t_{\text{block,prev}})//10, -99) + 2^{((n_{\text{block}}//100000)-2)} \quad (3)$$

In the Homestead update released in March 2016, the difficulty formula was adjusted in such a way that the difficulty does not change when the time necessary to mine a block stays in the range from 10 to 19 s. The block difficulty increases whenever the time drops below the range, and when it exceeds the range it decreases. The difficulty bomb was not altered in the Homestead update (Buterin, 2015a).

Equations (4–6) show the updated adjustment formula and current state of the Ethereum protocol for the block difficulty after the Byzantium and Constantinople hard forks, which are updates of the Ethereum protocol (Schoedon and Buterin, 2017; Schoedon, 2018). The Byzantium and Constantinople hard forks are part of the Metropolis release, which is the third version of the Ethereum platform. The Byzantium hard fork happened in October 2017 and Constantinople is planned for early 2019 (Foundation, Ethereum, 2018).

$$d_{\text{ETH}} = \max[d_{\text{ETH,prev}} + (d_{\text{ETH,prev}}// D_{\text{ETH,constant}}) \times adj,\ \min(d_{\text{ETH,prev}}, D_{\text{MIN}})] + 2^{((n_{\text{block,fake}}//100000)-2)} \quad (4)$$

$$adj = \max((2 \text{ if } len(uncles_{\text{prev}}) \text{ else } 1) - ((t_{\text{block}} - t_{\text{block,prev}})//9), -99) \quad (5)$$

$$n_{\text{block,fake}} = \max(0, n_{\text{block}} - 5,000,000 \text{ block}) \quad (6)$$

With the introduction of the adjustment factor (*adj*) the existence of uncles is factored in the calculation of the block difficulty. Uncles are blocks that are correctly mined but are not included into the blockchain, and were not considered until the Byzantium hard fork. Furthermore, the range in which the block difficulty stays constant was altered from 9 to 18 s (Buterin, 2016). **Figure 3** visualizes the evolution of the Ethereum block difficulty from March 2015 to October 2018 with a solid black line.

Until the beginning of 2017, the graph shows a steady and continuous growth of the block difficulty. Especially in mid-2017, an increasing impact of the difficulty bomb becomes visible from the exponential steps towards the Byzantium update. In October 2017, the difficulty drops from 3×10^{15} to 1.5×10^{15}, due to the reset of the difficulty bomb in the Byzantium update, by 3,000,000 blocks (Schoedon and Buterin, 2017). Since the Byzantium update, the block difficulty exponentially rose again after reaching a level of saturation at approximately 3×10^{15}. For the Constantinople release, the Ethereum developers already agreed on delaying the difficulty bomb for another 2,000,000 blocks (Schoedon, 2018), resulting in a total delay of 5,000,000 blocks Equation (6). Therefore, the impact of the difficulty bomb will not be visible before 2020 assuming an average mining rate of 15.9 s (see **Figure 3**).

2.1.4. Ethereum Scenarios

Three scenarios for the future development of the Ethereum block difficulty are presented in **Figure 3**. The first scenario is the development of the difficulty bomb only, according to Equations (4–6). The second scenario is a linear interpolation of the block difficulty on October 31, 2018 and the initial block difficulty in 2015. The last scenario is a stagnating block difficulty. Stagnation of the block difficulty is only realistic if the Ethereum community agrees to further delay the difficulty bomb.

2.2. Mining Hardware

This section summarizes the development of the efficiency of the currently available mining hardware and describes the creation of the efficiency scenarios for Bitcoin and Ethereum. A pessimistic, and an optimistic scenario for each the Bitcoin and the Ethereum mining hardware efficiency is shown until 2025.

2.2.1. Evolution of Bitcoin Hardware

Bitcoin mining hardware witnessed many advancements in the past decade. In the first years of the Bitcoin network, mining was still possible with conventional computers and laptops (Bitcoin Forum, 2012; Bitcoin Wiki, 2018). As Bitcoin became more popular and the price increased, field programmable gate arrays (FPGA) and then application specific integrated circuits (ASIC) were developed (Bitcoin Wiki, 2018). In 2018, the most powerful ASIC calculates up to 16 Th/s (Shivam Chawla, 2017).

The investigation of the development of the hardware efficiency requires a data set, that contains information about the energy consumption, the hashrate, and the release date of the mining hardware. The data, used in this paper, is available in Zade and Myklebost (2018). **Figure 4** visualizes the efficiency of the mining hardware as crosses at the date corresponding to their release date or the date the information of the hardware was originally retrieved. The data starts in 2013 because beforehand Bitcoin mining was mostly done on personal computers (PC) and graphical processing units (GPU). Around 2013, FPGAs were introduced to mine Bitcoins, however were quickly outrun by ASICs. Since 2013, the efficiency of the mining hardware grows steadily.

2.2.2. Efficiency Scenarios for Bitcoin Hardware

In order to create reasonable scenarios of the hardware efficiency of the Bitcoin network, it is necessary to consider a certain time lag until the network adopts the newly released hardware. In **Figure 4**, a 6 months time lag, which is equivalent to 1/4 of the duration of use, has been added to the release dates to make up for the adoption time (see de Vries, 2018b). The scenarios are then created with one pessimistic and one optimistic least-squares fits. The data that has been fitted are the release dates in Zade and Myklebost (2018) delayed by the time lag and the corresponding efficiency (see **Figure 4**). In the fitting, one data point per release date was used.

The first one, is a standardized second order polynomial fit, and returns the parameters in Equation (7).

$$\eta_{2\mathrm{nd}}(t) = 3.0 \times 10^{-13} \times t^2 - 8.0 \times 10^{-4} \times t + 5.4 \times 10^{5} \quad (7)$$

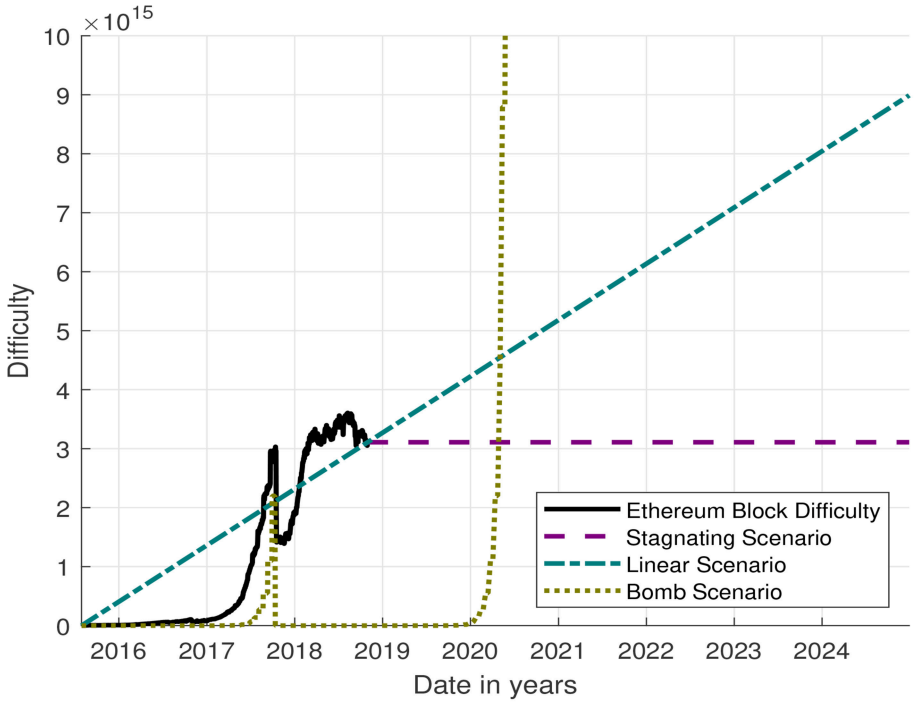

FIGURE 3 | Past Ethereum block difficulty development according to Etherscan (2018) and exponential, linear, and stagnating scenarios for the future.

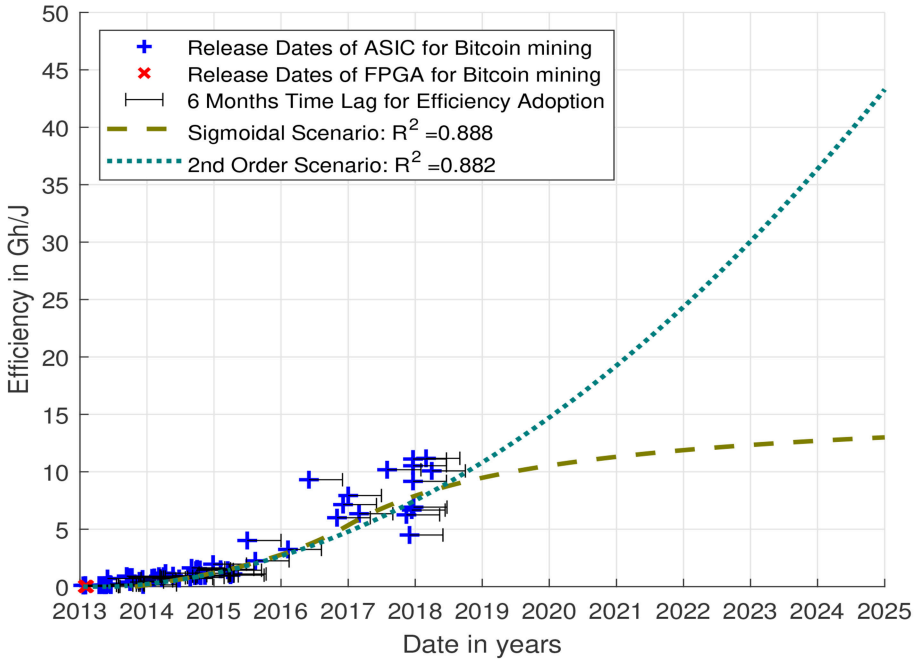

FIGURE 4 | Quadratic and sigmoid scenario for the development of the Bitcoin mining hardware efficiency fitted to the past development. Data for the hardware release dates from Zade and Myklebost (2018).

The second fitting curve is a sigmoid curve, which was derived from Equation (8).

$$y = \frac{x}{|x| + 1} \tag{8}$$

Equation (9) is a modification of Equation (8), so that it is applicable to the data with UNIX timestamps. Therefore, additional parameters are introduced.

$$\eta_{\text{sigm}}(t) = A \times \left(\frac{t - B}{C + |t - B|} + D \right) \tag{9}$$

A variation of the parameter `A` results in an amplification of the function values. Altering `B` causes a shift on the x-axis and `C` affects the gradient of the curve. Finally, the parameter `D` creates a shift on the y-axis. A least-square curve fitting function fitted the parameters. The initial parameters, the lower and the upper bounds and the optimized values are summarized in **Table 1**.

Figure 4 displays the results of the two fitting functions. The curves are congruent until the last data point. The quadratic curve indicates a scenario in which the hardware efficiency will increase to approximately 45 Gh/J in 2025. The sigmoid curve shows a rather pessimistic scenario in which the hardware efficiency reaches a saturation at approximately 13 Gh/J in 2025. The actual development of the hardware efficiency will most probably be in between the proposed scenarios, as long as no breakthrough technology is developed for Bitcoin mining (see **Figure 4**).

TABLE 1 | The parameters used to fit the hardware mining data to a sigmoid curve [see Equation (9)].

	A	B	C	D
Initial values	1.12×10^4	1.52×10^9	5×10^8	0.5
Lower bound	5.59×10^3	1.48×10^9	1×10^8	0
Upper bound	4.47×10^4	1.53×10^9	1×10^9	1
Optimized values	1.22×10^4	1.48×10^9	1.12×10^8	0.51

2.2.3. Evolution of Ethereum Hardware

The mining process in the Ethereum network was built to be ASIC-resistant, in order to keep mining profitable for ordinary computers (Ethereum Wiki, 2018). This ASIC-resistance was originally implemented by the Dagger-Hashimoto algorithm and currently is used in the Ethash implementation. Ethash forces full clients to create a 1 GB dataset which is updated every 30,000 blocks, grows linearly over time, and has to be stored. Mining is only possible, if random parts of the dataset can be accessed, combined with the block data, and altogether hashed. Therefore, a GPU is the best mining hardware, due to its built-in memory and high access rate (Ethereum Wiki, 2017).

Analogous to the hardware evolution analysis for Bitcoin, a data set for the Ethereum mining hardware was needed that includes information about the energy consumption, hashrate, and release date. However, manufacturers of GPUs do not normally state the reachable hashes per second nor the hashes per joule in the technical data, because mining

Ethers is a new field of application. Therefore, the energy consumption of GPUs are from technical data sheets, whereas the hashrates are from different websites that offer test results (Zade and Myklebost, 2018).

Figure 5 shows the evolution of the mining hardware efficiency over time in Mh/J. The displayed data starts in 2012, since already earlier produced GPUs are likely to be used for mining Ethers. Unlike the hardware to mine Bitcoins, the development of the Ethereum mining hardware is widely spread. This is most probably due to the fact, that GPUs are not primarily developed to mine Ethers, but instead to enable advanced computer gaming, image processing, and artificial intelligence applications (Karpištšenko, 2017).

2.2.4. Efficiency Scenarios for Ethereum Hardware

Analogous to Bitcoin, it is reasonable to consider a certain time lag until the network adopts the newly released hardware. Therefore, the release dates in **Figure 4** indicate a 6 months time lag, which is equivalent to 1/4 of the duration of use (see de Vries, 2018b). The scenarios are then created with one pessimistic and one optimistic least-squares fit. The data that has been fitted are the release dates from Zade and Myklebost (2018) delayed by the time lag and the corresponding efficiency (see **Figure 4**). In the fitting, one data point per release date was used.

Figure 5 shows the results of the two least-squares fits. First, the historical data shows, that GPUs are primarily not optimized or developed to increase the mining efficiency. Secondly, manufacturers of GPUs will have limited interest in optimizing their processing units for mining Ethers, when Ethereum developers want to shift toward a less computational expensive protocol with POS. Therefore, the first scenario for the development of the Ethereum mining hardware efficiency is rather pessimistic and follows a linear trend. The second scenario assumes an optimistic exponential evolution of the hardware efficiency. The second scenario would propose a mining efficiency of 0.8 Mh/J in 2025.

2.3. Future Mining Power

This section describes the calculation of the future power demand for Bitcoin and Ether mining. The formula for the Bitcoin mining power demand is shown in Equation (10) (Malone and O'Dwyer, 2014).

$$P_{\mathrm{BTC\_mining}} = n_{\mathrm{miner}} \times P_{\mathrm{HW}} = \frac{D_{\mathrm{BTC}} \times 2^{32}}{\Delta t \times R_{\mathrm{HW}}} \times P_{\mathrm{HW}} = \frac{D_{\mathrm{BTC}} \times 2^{32}}{\Delta t \times \eta_{\mathrm{HW}}} \tag{10}$$

TABLE 2 | Block difficulty and hardware efficiency combination for each scenario for the Bitcoin network.

Scenario	Difficulty	Hardware efficiency
1	Stagnating	Sigmoid
2	Linear	Sigmoid
3	Exponential	Sigmoid
4	Stagnating	2nd order
5	Linear	2nd order
6	Exponential	2nd order

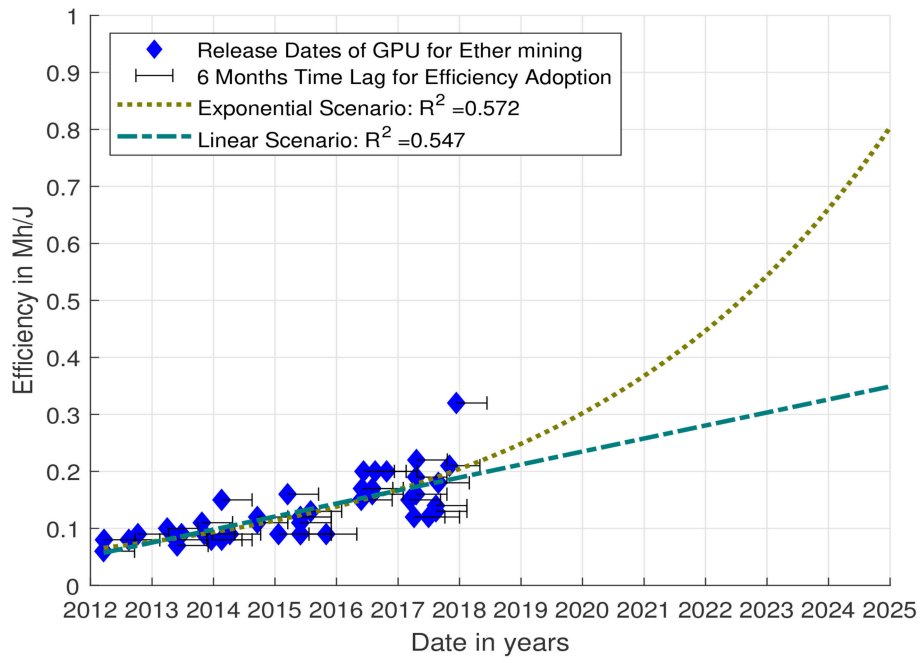

FIGURE 5 | Exponential and linear scenario for the development of the Ethereum hardware efficiency fitted to the past development. Data for the hardware release dates from Zade and Myklebost (2018).

$P_{\text{BTC\_mining}}$ represents the power demand for Bitcoin mining, n_{miner} the number of miners within the network, P_{HW} the power demand of a certain mining hardware, D_{BTC} the difficulty of the Bitcoin network, Δt the preset time to mine a block (for Bitcoin 10 min), and R_{HW} the hashrate. The hashrate and the power demand can be summarized in the mining efficiency η_{HW}.

Equation (11) calculates the network-wide power demand to mine Ethers. The main difference is the absence of the lower bound factor 2^{32}.

$$P_{\text{ETH\_mining}} = n_{\text{miner}} \times P_{\text{HW}} = \frac{D_{\text{ETH}}}{\Delta t \times R_{\text{HW}}} \times P_{\text{HW}} = \frac{D_{\text{ETH}}}{\Delta t \times \eta_{\text{HW}}} \tag{11}$$

Section 3 displays the results of the different scenarios.

3. RESULTS

This section presents the results of the scenario model for the power demand of the Bitcoin and Ethereum blockchain.

3.1. Bitcoin Mining Power Demand Scenarios

Six scenarios are investigated for the Bitcoin blockchain, in order to analyze the future mining power demand. The development of the scenarios is described in section 2. **Table 2** lists the combinations of the hardware efficiency and block difficulty for each scenario.

TABLE 3 | Block difficulty and hardware efficiency variations for each scenario for the Ethereum network.

Scenario	Difficulty	Hardware efficiency
1	Stagnating	Linear
2	Linear	Linear
3	Bomb	Linear
4	Stagnating	Exponential
5	Linear	Exponential
6	Bomb	Exponential

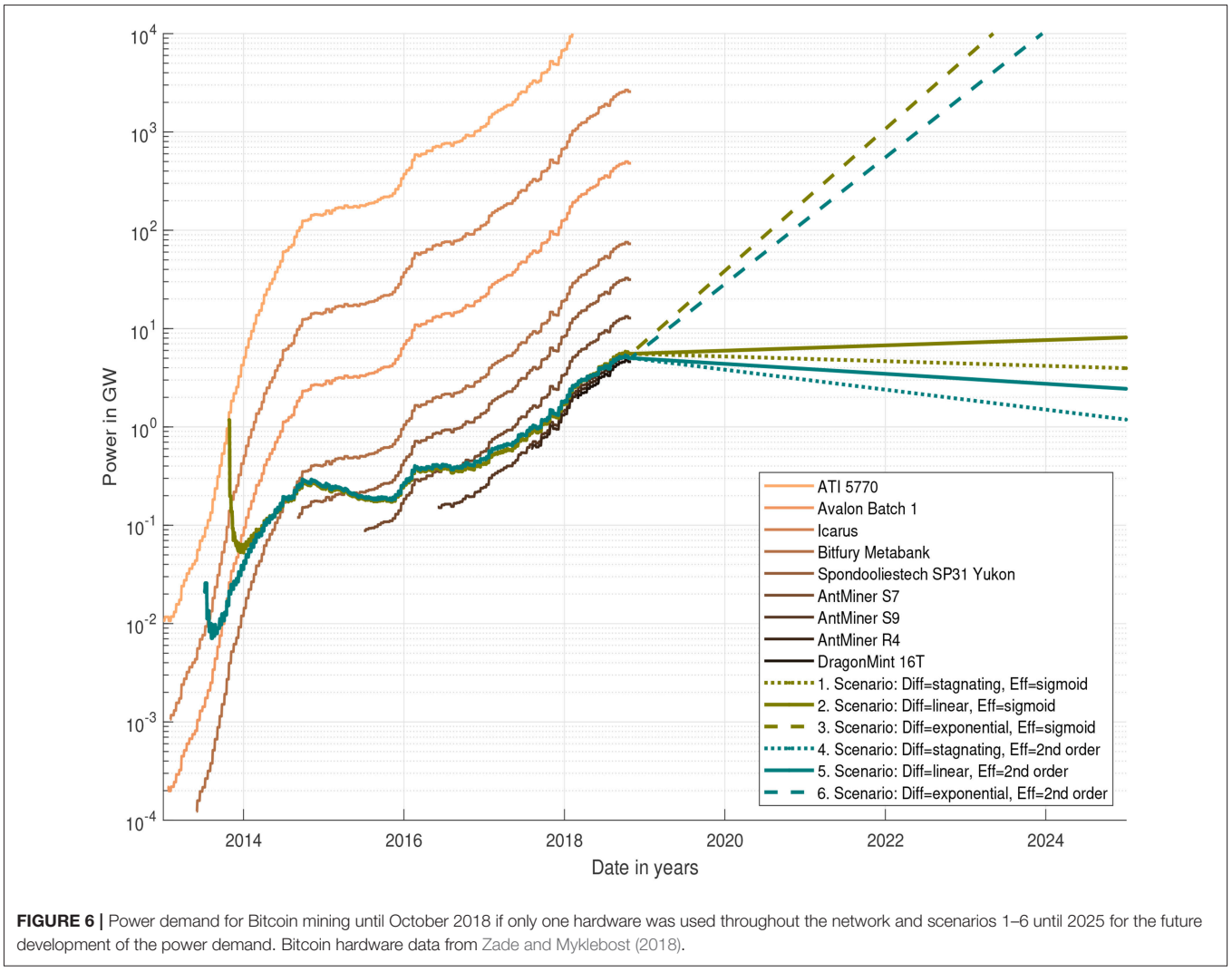

FIGURE 6 | Power demand for Bitcoin mining until October 2018 if only one hardware was used throughout the network and scenarios 1–6 until 2025 for the future development of the power demand. Bitcoin hardware data from Zade and Myklebost (2018).

Figure 6 visualizes three results:

1. How much power the Bitcoin blockchain demanded in the past, if the entire mining process would have followed the fitted curves in section 2.
2. How much power the Bitcoin blockchain demanded in the past, if the entire mining process would have been done on one of the selected hardware.
3. How much power the Bitcoin blockchain will demand, if one of the scenarios from **Table 2** materializes.

Even though the Bitcoin network went live in 2009, the data starts in 2013, because mining was done on conventional CPUs beforehand, and the release of Bitcoin specific hardware started in 2013 (Malone and O'Dwyer, 2014).

The y-axis is a logarithmic scale, in order to show the vast range of mining power demand. The curves of the hardware start at their release date or at the time, when the information about the hardware was first made available. For a better visualization, only a selection of 9 hardware mining machines are shown in **Figure 6**. In 2013, the first data points are FPGAs (e.g., Icarus) and were quickly followed by ASICs (e.g., Antminer). The mining power demand approximately was in the range from 0.1 MW to 10 MW in 2013. With the releases of the first ASICs in 2014, the mining power demand rose drastically to the range from 0.01 GW to 5 GW. In the beginning of 2018, the range of the mining power demand was already from 1.5 GW to more than 5,000 GW. The power demand approximately is at 5 GW, if Bitcoin mining was done in October 2018 with a mix of the three most efficient, displayed ASICs. In 2018, the mining power demand could be higher than 10,000 GW, if mining was entirely done with the FPGAs that were released in 2013.

The curves for the six scenarios indicate the potential development of the power demand of the Bitcoin and Ethereum blockchain. Green curves show sigmoidal, and turquoise curves exponential scenarios for the hardware efficiency of the Bitcoin mining hardware. Dashed lines indicate the exponential increase, solid lines a linear rise, and dotted lines the effect of a stagnating block difficulty.

The curves for scenario 1–3 and 4–6 are congruent to each other from 2014 until the beginning of 2018. The congruence of the curves is a result of the usage of the historical block difficulty data that was for all scenarios the same. Furthermore, the hardware efficiency only show slight deviations between the sigmoidal and exponential fit between 2014 and the beginning of 2018. In 2013, the differences of the curves are caused by the deviating scenarios for the hardware efficiency in **Figure 4**. Differences from mid-2018 onwards are a result of the deviating scenarios for the hardware efficiency and block difficulty.

In 2025, the power demand of the Bitcoin network will be greater than 10,000 GW, if the block difficulty continues to rise exponentially and the hardware efficiency either follows a sigmoidal or an exponential growth. Considering the worldwide installed generation capacity for electricity of 6,300 GW in 2015, these two scenarios are highly unlikely (Central Intelligence Agency, 2018). In the case of a linear growth of the block difficulty, the expected power demand of the Bitcoin network is in the range from 2.5 to 8 GW. A stagnating difficulty results in an overall power demand in the range from 1.2 to 4 GW in 2025.

Conclusively, **Figure 6** shows that the greatest impact results from the development of the block difficulty and that the Bitcoin power demand can potentially decrease, if the block difficulty stagnates or even decreases. Improvements in the hardware efficiency will have limited influence on the power demand of the Bitcoin network.

3.2. Ethereum Mining Power Demand Scenarios

Six scenarios are investigated for the future mining power demand of the Ethereum blockchain. **Table 3** shows the combinations of the hardware efficiency and block difficulty within each scenario.

Figure 7 shows three results:

1. How much power the Ethereum blockchain demanded in the past, if the entire mining process would have followed the fitted curves in section 2.
2. How much power the Ethereum blockchain demanded, if the entire mining process would have been performed using the same hardware.
3. How much power the Ethereum blockchain will demand, if one of the scenarios from **Table 3** materializes.

calculated mining power demand of the Ethereum blockchain for the researched data in Zade and Myklebost (2018) and the above mentioned six scenarios.

For a better visualization, only 10 of the 45 listed mining machines are visualized, in order to display the full range of the power demand in **Figure 6** (Zade and Myklebost, 2018). The x-axis starts at the beginning of the Ethereum network in July 2015, and ends with the forecast in 2025. The curves of the hardware start at their release date. In January 2016, the mining power demand ranged from 3 to 9 MW. In January 2017, the mining power demand was in the range from 25 to 90 MW. After the Byzantium update in October 2017, the demand dropped shortly to a range from 0.45 to 1.5 GW but increased again until January 2018 up to 0.5 to 2 GW.

The mining power demand of the Ethereum blockchain would have been at approximately 0.9 GW on October 31st, 2018, if the network used a mixture of the five most efficient GPUs to mine Ethers. This estimate and the one in section 3.1 about a similar mixture for the Bitcoin network conclude that the mining power demand of the Bitcoin and the Ethereum blockchain are in similar ranges.

The two dashed lines show the development of the power demand when the block difficulty grows according to the difficulty bomb and the hardware efficiency either increases linearly (dashed brown line) or exponentially (dashed green line). The average power demand of the scenarios 1 and 4 would exceed 10,000 GW before the beginning of 2020. These scenarios seem, from the energy system's perspective highly unlikely, considering the worldwide installed generation capacity for electricity of 6,300 GW in 2015 (Central Intelligence Agency, 2018). The green, and turquoise solid lines show the mining power demand if the block difficulty rises linearly. The average power demand in 2025

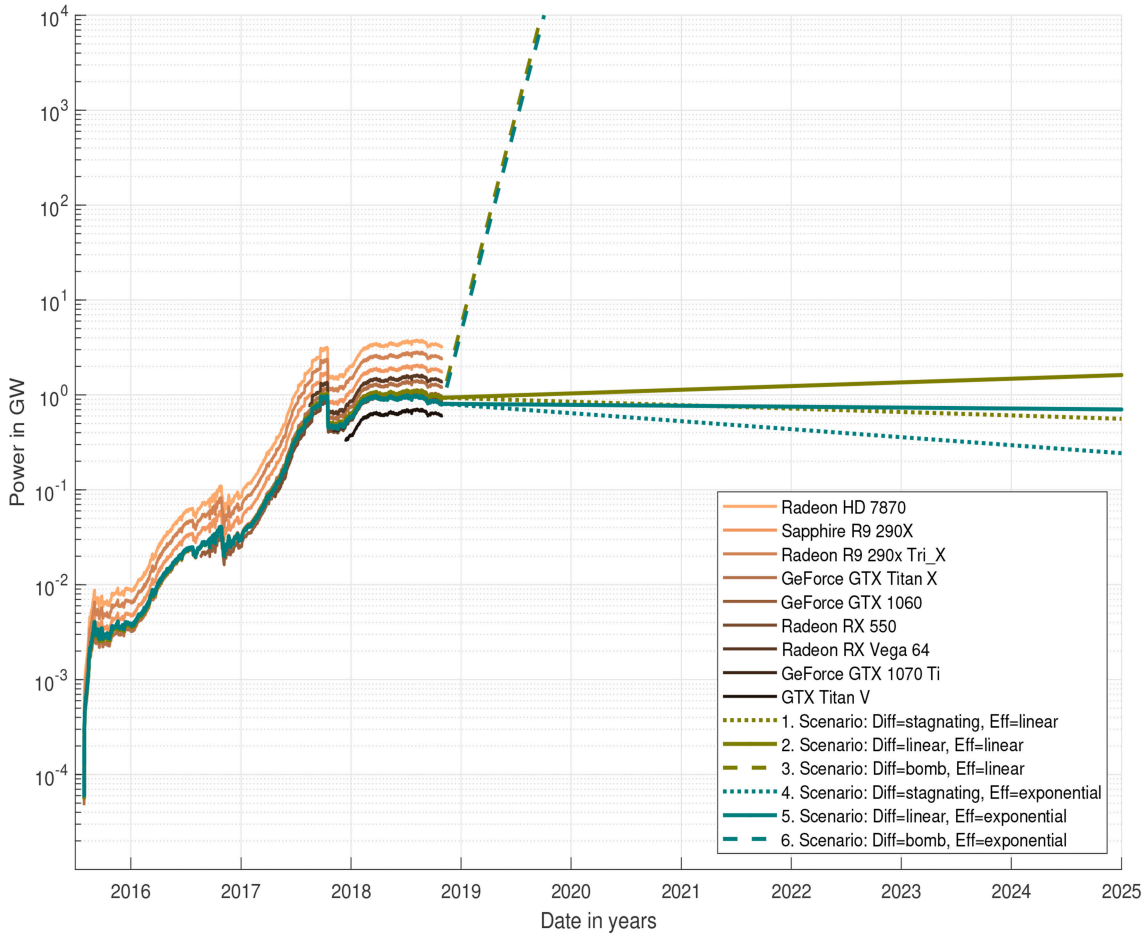

FIGURE 7 | Mining power demand of the Ethereum blockchain until October 2018 if only one hardware was used throughout the network and scenarios 1–6 until 2025 for the future development of the power demand. Ethereum hardware data from Zade and Myklebost (2018).

of the scenarios 2 and 5 would be at 1.4 GW. The dotted lines represent the scenarios 3 and 6 in which the difficulty stagnates at the level of the October 31, 2018 and the hardware efficiency increases exponentially or linearly. The average power demand would be in 0.4 GW in 2025. Therefore, a stagnating block difficulty will result in a mining power demand by 2025 of less than half compared to the scenarios with an linearly increasing block difficulty.

Similarly to section 3.1, the scenarios for the Ethereum blockchain indicate that the future power demand most significantly depends on the block difficulty. The hardware efficiency has a limited impact.

4. DISCUSSION

This paper presents a scenario model that estimates the future mining power demand of the Bitcoin and Ethereum blockchain. This section discusses the selected model's input scenarios, limitations, results, and compares them with the scientific literature.

The model creates scenarios for the efficiency of mining machines, based on release dates and efficiencies of hardware from the last decade. The chosen scenarios follow the trend of processor efficiencies described in (Hasler and Marr, 2013; Marr et al., 2013; Rupp, 2013). However, they do not assume any breakthrough technology that would improve the efficiency of mining hardware by more than 400% in 2025 compared to October 2018. This method allows the creation of efficiency scenarios for mining hardware, which can also be applied to other technologies.

In the Bitcoin blockchain, the block difficulty only depends on the block mining rate. In the Ethereum network, the block difficulty also is affected by the difficulty bomb. The different influences on the block difficulty were analyzed, extrapolated, and fitted with multiple functions, in order to create reasonable scenarios for the future. The developed scenarios offer a wide range of possible developments, because the computing power in a blockchain is amongst others dependent on the market price which is hard to predict. Furthermore, this method cannot cover the impact of protocol changes, such as in the Byzantium and Constantinople release. However, the creation of scenarios for the block difficulty based on the past development appears to be the most appropriate approach.

TABLE 4 | Annual average powerdemand of bitcoin and ethereum.

Blockchain	Bitcoin				Ethereum	
Model	O'Dwyer	Mora et al	Krause et al.	This study	Krause et al.	This study
	in MW	in MW	in MW	in MW	in MW	in MW
2014	10–10,000	-	-	168	-	-
2015	100–100,000	-	-	202	-	3
2016	1,000–1,000,000	-	283	364	24	19
2017	-	11,959–12,538[a]	948	843	299	367
2018	-	-	3,441[b]	3,852[c]	1,165[b]	991[c]

[a]*Since the model of Mora et al. provides only the energy per block in GWh. The annual average power demand has been calculated by dividing the energy per block by the expected block mining time of* 0.167 h.
[b]*Average from January 1 to June 30, 2018.*
[c]*Average from January 1 to October 31, 2018.*

Large mining farms that were built to pool the computing power of multiple thousands of mining machines require extra cooling elements (de Vries, 2018b). However, the analyzed hardware does only consider on-board cooling elements. Moreover, the power demand of the GPU's auxiliary equipment is not considered. Therefore, the results presented in this paper are a lower bound of the power demand of the Bitcoin and Ethereum blockchain. The investigation of the cooling demand requires further research.

In consideration of the aforementioned limitations, this model calculates the power demand of the Bitcoin and Ethereum blockchain, and provides the following answers:

1. Mining efficiency has increased significantly over the past years. Today's mining would result in a power demand of more than 1,000 GW in 2018 if mining was done on a mix of hardware that was released in 2013.
2. Future hardware efficiency improvements will have only a limited impact on the total power demand of the Bitcoin and Ethereum blockchain if the block difficulty follows similar growth patterns as in the past decade.
3. The power demands of the Bitcoin and Ethereum blockchain are expected to decrease if the block difficulty stagnates. However, the demand will stay constant if the block difficulty only grows linearly.
4. The power demands of the Bitcoin and Ethereum blockchain are estimated to be in similar ranges, at least 5 and 0.9 GW, respectively as of October 2018.

For comparison and verification of the presented model, **Table 4** shows the average annual power demand of the Bitcoin and Ethereum blockchain from the scientific literature and the presented scenario model for the years from 2014 to 2018.

For the years 2014 and 2015, the model calculates power demands for Bitcoin that correspond to the results presented in O'Dwyer (2017). For 2016, 2017, and 2018, the model's results for Bitcoin are in similar ranges as the results presented by Krause et al. (2018). The scenario model does not match the results of O'Dwyer in 2016 because the hardware selection in O'Dwyer (2017) was not updated from the author's original selection from 2014 and therefore calculated with less efficient hardware a higher power demand range for 2016 (see Malone and O'Dwyer, 2014). For 2017, the scenario model calculates an annual average power demand for Bitcoin of 843 MW and for Ethereum of 367 MW. Mora et al. (2018) published a model that calculates a power demand for Bitcoin in the range from 11,959 to 12,538 MW. The reason behind this high power demand can be explained with the random selection of hardware that was already uneconomic and out-dated in 2017 (see section 1). In summary, the comparison of the results in **Table 4** verifies the output of the scenario model and provides explanations for deviations to other scientific models for the years from 2014 to 2018.

5. CONCLUSION

This paper presented a new hashrate-based model for the creation of scenarios for the future mining power demand of the Bitcoin and Ethereum blockchain. Hence, providing an alternative to economical models that require business secrets, or technical models that use unrelated adoption rates. The developments of the block difficulty and the hardware efficiency of the last decade provided the basis for the developed scenarios. The investigation of six scenarios until 2025 revealed that the hardware improvements will have only a limited impact on the total power demand of the Bitcoin and Ethereum blockchain, and that the mining power demand of the Ethereum network is in a similar range as the one of Bitcoin. Furthermore, the presented methodology can be applied to create scenarios for the power demand of any other blockchain that uses the POW consensus algorithm by adjusting the formulas to the network's characteristics.

Future research shall investigate the impact of the market price on the block difficulty and the consideration of cooling equipment in the overall power demand of the Bitcoin and Ethereum blockchain.

DATA AVAILABILITY

The datasets analyzed for this study can be found in Zade and Myklebost (2018), Etherscan (2018), and Blockchain Luxembourg S.A. (2018).

AUTHOR CONTRIBUTIONS

JM, PT, and MZ contributed conception and design of the study. JM and MZ organized the database. JM performed the statistical analysis. MZ wrote the first draft of the manuscript. All authors contributed to manuscript revision, read and approved the submitted version.

REFERENCES

Bitcoin Forum (2012). *The First Miners*. Available online at: https://bitcointalk.org/index.php?topic=99265.0 (Accessed February 14, 2018).

Bitcoin Wiki (2018). *Mining.* Available online at: https://en.bitcoin.it/wiki/Mining (Accessed February 14, 2018).

Blockchain Luxembourg S.A. (2018). *Bitcoin Charts & Graphs - Blockchain.* Available online at: https://www.blockchain.com/charts (Accessed November 18, 2018).

Buterin, V. (2015a). *Eip 2: Homestead Hard-Fork Changes.* Repository. Available online at: https://github.com/ethereum/EIPs/blob/master/EIPS/eip-2.md (Accessed May 16, 2018).

Buterin, V. (2015b). *The Evolution of Ethereum.* Available online at: https://blog.ethereum.org/2015/09/28/the-evolution-of-ethereum/ (Accessed November 29, 2018).

Buterin, V. (2016). *Eip 100: Change Difficulty Adjustment to Target Mean Block Time Including Uncles.* Available online at: https://github.com/ethereum/EIPs/blob/984cf5de90bbf5fbe7e49be227b0c2f9567e661e/EIPS/eip-100.md (Accessed May 16, 2018).

Central Intelligence Agency (2018). *The world factbook: Electricity - Installed Generating Capacity (kw).* Available Online at: https://www.cia.gov/library/publications/the-world-factbook/fields/2236.html#xx (Accessed May 16, 2018).

de Vries, A. (2018a). *Bitcoin Energy Consumption Index.* Available online at: https://digiconomist.net/bitcoin-energy-consumption (Accessed November 20, 2018).

de Vries, A. (2018b). Bitcoin's growing energy problem.c *Joule* 2, 801–805. doi: 10.1016/j.joule.2018.04.016

DiChristopher, T. (2017). *No, Bitcoin Isn't Likely to Consume All the World's Electricity in 2020.* Available online at: https://www.cnbc.com/2017/12/21/no-bitcoin-is-likely-not-going-to-consume-all-the-worlds-energy-in-2020.html (Accessed April 4, 2018).

Ethereum Wiki (2017). *Ethash.* Repository. Available online at: https://github.com/ethereum/wiki/wiki/Ethash (Accessed February 14, 2018).

Ethereum Wiki (2018). *Dagger Hashimoto.* Repository. Available online at: https://github.com/ethereum/wiki/blob/master/Dagger-Hashimoto.md (Accessed February 14, 2018).

Etherscan (2018). *Ethereum Block Difficulty Growth Chart.* Available Online at: https://etherscan.io/chart/difficulty (Accessed November 18, 2018).

Foundation, Ethereum (2018). *Byzantium hf Announcement.* Available online at: https://blog.ethereum.org/2017/10/12/byzantium-hf-announcement/ (Accessed November 27, 2018).

Giungato, P., Rana, R., Tarabella, A., and Tricase, C. (2017). Current trends in sustainability of bitcoins and related blockchain technology. *Sustainability* 9:2214. doi: 10.3390/su9122214

Hasler, J., and Marr, B. (2013). Finding a roadmap to achieve large neuromorphic hardware systems. *Front. Neurosci.* 7:118. doi: 10.3389/fnins.2013.00118

Hayes, A. (2015). A cost of production model for bitcoin. *SSRN Electr. J.* doi: 10.2139/ssrn.2580904

Jeffrey Wilcke (2016). *Homestead Release.* Available online at: https://blog.ethereum.org/2016/02/29/homestead-release/ (Accessed November 18, 2018).

Karpištšenko, A. (2017). Use of graphics processing units on the rise – future tech – medium. Available online at: https://medium.com/futuretech/use-of-graphics-processing-units-on-the-rise-390696fd8d8 (Accessed February 22, 2019).

Krause, M. J., Tolaymat, T., and (2018). Quantification of energy and carbon costs for mining cryptocurrencies. *Nat. Sustain.* 1, 711–718. doi: 10.1038/s41893-018-0152-7

Malone, D., and O'Dwyer, K. J. (2014). "Bitcoin mining and its energy footprint," in *25th IET Irish Signals & Systems Conference 2014 and 2014 China-Ireland International Conference on Information and Communities Technologies (ISSC 2014/CIICT 2014)* (Limerick: Institution of Engineering and Technology), 280–285.

Marr, B., Degnan, B., Hasler, P., and Anderson, D. (2013). Scaling energy per operation via an asynchronous pipeline. *IEEE Trans. Very Large Scale Integr. Syst.* 21, 147–151. doi: 10.1109/TVLSI.2011.2178126

Mengelkamp, E., Gärttner, J., Rock, K., Kessler, S., Orsini, L., and Weinhardt, C. (2018). Designing microgrid energy markets. *Appl. Ener.* 210, 870–880. doi: 10.1016/j.apenergy.2017.06.054

Mora, C., Rollins, R. L., Taladay, K., Kantar, M. B., Chock, M. K., Shimada, M., et al. (2018). Bitcoin emissions alone could push global warming above 2° c. *Nat. Clim. Change* 8, 931–933. doi: 10.1038/s41558-018-0321-8

Nakamoto, S. (2008). *Bitcoin: A Peer-to-Peer Electronic Cash System.* Available Online at: https://bitcoin.org/bitcoin.pdf (Accessed May 5, 2018).

Nakamoto, S., and The Bitcoin Developers (2012). main.cpp: Getnextworkrequired(). Available Online at: https://github.com/bitcoin/bitcoin/blob/d62a1947be5350ed60066ccacc7aba43bbdf48fb/src/main.cpp#L865 (Accessed January 30, 2019).

O'Dwyer, K. (2017). *Topics in Power Usage in Network Services*. Dissertation, National University of Ireland Maynooth.

Popper, N. (2018). *There Is Nothing Virtual About Bitcoin's Energy Appetite.* New York Times. Available online at: https://www.nytimes.com/2018/01/21/technology/bitcoin-mining-energy-consumption.html (Accessed April 4, 2018).

Rupp, K. (2013). *CPU GPU and MIC Hardware Characteristics Over Time.* Available at: https://www.karlrupp.net/2013/06/cpu-gpu-and-mic-hardware-characteristics-over-time/ (Accessed April 4, 2018).

Sabounchi, M., and Wei, J. (2017). *Towards Resilient Networked Microgrids: Blockchain-Enabled Peer-to-Peer Electricity Trading Mechanism.* IEEE. Available online at: https://ieeexplore-ieee-org.eaccess.ub.tum.de/document/8245449/

Schoedon, A. (2018). *Eip 1234: Constantinople Difficulty Bomb Delay and Block Reward Adjustment.* Repository. Available online at: https://github.com/ethereum/EIPs/blob/master/EIPS/eip-1234.md (Accessed November 27, 2018).

Schoedon, A., and Buterin, V. (2017). *Eip 649: Metropolis Difficulty Bomb Delay and Block Reward Reduction.* Repository. Available online at: https://github.com/ethereum/EIPs/blob/abcf1153ae3939fab9dd30fae8a94c26c9d18db6/EIPS/eip-649.md (Accessed May 5, 2018).

Shivam Chawla (2017). *Dragonmint 16t: Halongmining Releases Competitor to Bitmain.* Online. Available online at: https://blockchaind.net/dragonmint-halongmining-releases-competitor-bitmain/ (Accessed December 17, 2018).

Vranken, H. (2017). Sustainability of bitcoin and blockchains. *Curr. Opin. Environ. Sustain.* 28, 1–9. doi: 10.1016/j.cosust.2017.04.011

Wang, J., Wang, Q., Zhou, N., and Chi, Y. (2017). A novel electricity transaction mode of microgrids based on blockchain and continuous double auction. *Energies* 10:1971. doi: 10.3390/en10121971

Zade, M., and Myklebost, J. (2018). *Bitcoin and Ethereum Mining Hardware*. Munich: Mendeley. doi: 10.17632/4dw6j3pxz5.1

Conflict of Interest Statement: The authors declare that the research was conducted in the absence of any commercial or financial relationships that could be construed as a potential conflict of interest.

Appendix C

Acronyms

CC	Check and Curtail	12
Con	Constant	54
DER	Distributed Energy Resource	6
EU	European Union	10
EV	Electric Vehicle	1
HEMS	Home Energy Management System	3
HP	Heat Pump	1
IMCA	Iterative Market Clearing Algorithm	5
LEM	Local Energy Market	2
P2P	Peer-to-Peer	6
PDA	Periodic Double Auction	8
PP	Preference Prioritization	12
REC	Renewable Energy Certificate	11
RQ	Research Question	2
RT	Real-Time	3
SM	Smart Meter	3
ToU	Time-of-Use	54
VRE	Variable Renewable Electricity	1
WTPP	Willingness To Pay a Premium	5

List of Figures

List of Tables

Bibliography

[1] H.-O. Pörtner, D. Roberts, M. Tignor, K. M. E.S. Poloczanska, A. Alegría, M. Craig, S. Langsdorf, V. M. S. Löschke, A. Okem, and B. R. (eds.) *Climate Change 2022: Impacts, Adaptation, and Vulnerability. Contribution of Working Group II to the Sixth Assessment Report of the Intergovernmental Panel on Climate Change*. Ed. by Cambridge University Press. Cambridge, United Kingdom and New York, USA, 2022. URL: https://report.ipcc.ch/ar6wg2/pdf/IPCC_AR6_WGII_FinalDraft_FullReport.pdf (visited on 03/03/2022).

[2] International Renewable Energy Agency. *World Energy Transitions Outlook: 1.5°C Pathway*. Abu Dhabi, 2021. URL: https://irena.org/publications/2021/Jun/World-Energy-Transitions-Outlook (visited on 03/11/2022).

[3] International Renewable Energy Agency. *Renewable Capacity Statistics 2021*. 2021. URL: https://www.irena.org/publications/2021/March/Renewable-Capacity-Statistics-2021 (visited on 04/19/2021).

[4] *Glasgow Climate Pact: Decision -/CP.26*. Glasgow, 2022. URL: https://unfccc.int/sites/default/files/resource/cop26_auv_2f_cover_decision.pdf (visited on 03/11/2022).

[5] G. Luderer, S. Madeddu, L. Merfort, F. Ueckerdt, M. Pehl, R. Pietzcker, M. Rottoli, F. Schreyer, N. Bauer, L. Baumstark, C. Bertram, A. Dirnaichner, F. Humpenöder, A. Levesque, A. Popp, R. Rodrigues, J. Strefler, and E. Kriegler. Impact of declining renewable energy costs on electrification in low-emission scenarios. In: *Nature Energy* (2021). DOI: 10.1038/s41560-021-00937-z.

[6] Bundesnetzagentur and Bundeskartellamt, eds. *Monitoringbericht 2016: Monitoringbericht gemäß § 63 Abs. 3 i. V. m. § 35 EnWG und § 48 Abs. 3 i. V. m. § 53 Abs. 3 GWB*. Bonn, Germany, 2016. URL: https://www.bundesnetzagentur.de/SharedDocs/Mediathek/Monitoringberichte/Monitoringbericht2016.pdf?__blob=publicationFile&v=2 (visited on 04/20/2021).

[7] Bundesnetzagentur and Bundeskartellamt, eds. *Monitoringbericht 2020: Monitoringbericht gemäß § 63 Abs. 3 i. V. m. § 35 EnWG und § 48 Abs. 3 i. V. m. § 53 Abs. 3 GWB*. Bonn, Germany, 2021. URL: https://www.bundesnetzagentur.de/SharedDocs/Mediathek/Berichte/2020/Monitoringbericht_Energie2020.pdf?__blob=publicationFile&v=6 (visited on 04/20/2021).

[8] Bundesnetzagentur, ed. *Monitoringbericht 2011: Monitoringbericht gemäß § 63 Abs. 4 EnWG i.V.m. § 35 EnWG*. Bonn, Germany, 2012. URL: https://www.bundesnetzagentur.de/SharedDocs/Downloads/DE/Allgemeines/Bundesnetzagentur/Publikationen/Berichte/2011/MonitoringBericht2011.pdf?__blob=publicationFile (visited on 02/20/2022).

[9] Bundeskartellamt and Bundesnetzagentur, eds. *Monitoringbericht 2012: Monitoringbericht gemäß § 63 Abs. 3 i.V.m. § 35 EnWG und § 48 Abs. 3 i.V.m. § 53 Abs. 3 GWB*. 2013. URL: https://www.bundesnetzagentur.de/SharedDocs/Downloads/DE/Allgemeines/Bundesnetzagentur/Publikationen/Berichte/2012/MonitoringBericht2012.pdf?__blob=publicationFile (visited on 02/20/2022).

[10] A. Feicht. *Schriftliche Frage an die Bundesregierung im Monat Oktober 2019 - Fragen Nr. 497 und Nr. 498*. Ed. by Bundesministerium für Wirtschaft und Energie. Berlin, 2019. URL: https://www.bmwi.de/Redaktion/DE/Parlamentarische-Anfragen/2019/10-497-498.pdf?__blob=publicationFile&v=2 (visited on 02/20/2022).

[11] Bundesnetzagentur, ed. *Quartalsbericht Netz- und Systemsicherheit - Gesamtes Jahr 2020*. 2021. URL: https://www.bundesnetzagentur.de/SharedDocs/Mediathek/Berichte/2020/Quartalszahlen_Gesamtjahr_2020.pdf?__blob=publicationFile&v=3 (visited on 02/20/2022).

[12] Umweltbundesamt. *Anteil erneuerbarer Energien am Bruttostromverbrauch und am Bruttoendenergieverbrauch*. Dessau-Roßlau, 2021. URL: https://www.umweltbundesamt.de/sites/default/files/medien/384/bilder/dateien/de_indikator_ener-04_erneuerbare-energien_2021-12-02.pdf (visited on 01/31/2022).

[13] Deutsche Bundesregierung, ed. *Mehr Fortschritt wagen - Bündnis für Freiheit, Gerechtigkeit und Nachhaltigkeit: Koalitionsvertrag 2021 - 2025 zwischen der Sozialdemokratischen Partei Deutschlands (SPD), Bündnis 90 / Die Grünen und den Freien Demokraten (FDP)*. Berlin, 2021. URL: https://www.spd.de/fileadmin/Dokumente/Koalitionsvertrag/Koalitionsvertrag_2021-2025.pdf (visited on 02/20/2022).

[14] Committee on Climate Change, ed. *Net Zero: The UK's contribution to stopping global warming*. 2019. URL: https://www.theccc.org.uk/wp-content/uploads/2019/05/Net-Zero-The-UKs-contribution-to-stopping-global-warming.pdf (visited on 01/31/2022).

[15] European Parliament. *Directive (EU) 2019/944 of the European Parliament and of the Council of 5 June 2019 on common rules for the internal market for electricity and amending Directive 2012/27/EU: DIRECTIVE (EU) 2019/944*. 2019. URL: https://eur-lex.europa.eu/legal-content/EN/TXT/PDF/?uri=CELEX:32019L0944 (visited on 02/19/2022).

[16] R.E.H. Sims, R.N. Schock, A. Adegbululgbe, J. Fenhann, I. Konstantinaviciute, W. Moomaw, H.B. Nimir, B. Schlamadinger, J. Torres-Martínez, Y. U. C. Turner, S.J.V. Vuori, N. Wamukonya, and X. Zhang. *Energy supply: Contribution of Working Group III to the Fourth Assessment Report of the Intergovernmental Panel on Climate Change*. Ed. by Cambridge University Press. Cambridge, United Kingdom and New York,

USA, 2007. URL: https://www.ipcc.ch/site/assets/uploads/2018/02/ar4-wg3-chapter4-1.pdf (visited on 04/22/2021).

[17] M. Gough, S. F. Santos, M. Javadi, R. Castro, and J. P. S. Catalão. Prosumer Flexibility: A Comprehensive State-of-the-Art Review and Scientometric Analysis. In: *Energies* 13.11 (2020), p. 2710. ISSN: 1996-1073. DOI: 10.3390/en13112710.

[18] M. Zeinali, J. Thompson, C. Khirallah, and N. Gupta. Evolution of home energy management and smart metering communications towards 5G. In: *2017 8th International Conference on the Network of the Future (NOF)*. 2017, pp. 85–90. DOI: 10.1109/NOF.2017.8251225.

[19] M. Beaudin and H. Zareipour. Home energy management systems: A review of modelling and complexity. In: *Renewable and Sustainable Energy Reviews* 45 (2015), pp. 318–335. ISSN: 13640321. DOI: 10.1016/j.rser.2015.01.046.

[20] V. Heinisch, M. Odenberger, L. Göransson, and F. Johnsson. Prosumers in the Electricity System—Household vs. System Optimization of the Operation of Residential Photovoltaic Battery Systems. In: *Frontiers in Energy Research* 6 (2019). ISSN: 2296-598X. DOI: 10.3389/fenrg.2018.00145.

[21] D. Fox. Smart Meter. In: *Datenschutz und Datensicherheit* 6 (2010), p. 408. URL: https://www.secorvo.de/publikationen/smartmeter-fox-2010.pdf (visited on 03/11/2022).

[22] B. Haller, O. Langniß, A. Reuter, and N. Spengler, eds. 1.5°*Csellsius: Energiewende zellulär - partizipativ - vielfältig umgesetzt*. 1. Auflage. Stuttgart: C/sells Verlag, 2020. ISBN: 978-3-00-067236-1. URL: https://www.csells.net/media/com_form2content/documents/c12/a357/f122/CSells_Buch_15GradCSellsius_WEB_20201209_compressed.pdf (visited on 03/11/2022).

[23] E. Al Kawasmi, E. Arnautovic, and D. Svetinovic. Bitcoin-Based Decentralized Carbon Emissions Trading Infrastructure Model. In: *Systems Engineering* 18.2 (2015), pp. 115–130. ISSN: 10981241. DOI: 10.1002/sys.21291.

[24] T. Dimitriou and G. Karame. Privacy-friendly tasking and trading of energy in smart grids. In: *Proceedings of the 28th Annual ACM Symposium on Applied Computing - SAC '13*. Ed. by S. Y. Shin and J. C. Maldonado. New York, New York, USA: ACM Press, 2013, p. 652. ISBN: 9781450316569. DOI: 10.1145/2480362.2480488.

[25] J. Frizzo-Barker, P. A. Chow-White, P. R. Adams, J. Mentanko, D. Ha, and S. Green. Blockchain as a disruptive technology for business: A systematic review. In: *International Journal of Information Management* 51 (2020), p. 102029. ISSN: 02684012. DOI: 10.1016/j.ijinfomgt.2019.10.014.

[26] M. Mihaylov, S. Jurado, N. Avellana, K. van Moffaert, I. M. de Abril, and A. Nowe. NRGcoin: Virtual currency for trading of renewable energy in smart grids. In: *2014 11th International Conference on the European Energy Market (EEM)*. Piscataway, NJ: IEEE, 2014, pp. 1–6. ISBN: 978-1-4799-6095-8. DOI: 10.1109/EEM.2014.6861213.

[27] A. von Perfall, T. Hillebrand, E. Smole, L. Lay, and M. Charlet. *Blockchain - Chance für Energieverbraucher? Kurzstudie für die Verbraucherzentrale NRW, Düsseldorf*. Ed. by PricewaterhouseCoopers AG. 2016. URL: https://www.verbraucherzentrale.nrw/sites/default/files/migration_files/media242403A.pdf (visited on 08/10/2018).

[28] A. Bogensperger, A. Zeiselmair, and M. Hinterstocker. *Die Blockchain-Technologie: Chance zur Transformation der Energieversorgung? Berichtsteil Technologiebeschreibung*. Ed. by Forschungsstelle für Energiewirtschaft e.V. 2018. URL: https://www.ffe.de/veroeffentlichungen/neue-studie-grundlagen-der-blockchain-technologie-in-der-energiewirtschaft-berichtsteil-technologiebeschreibung/ (visited on 03/06/2022).

[29] Alexander Bogensperger, Andreas Zeiselmair, Michael Hinterstocker, and Christa Dufter. Die Blockchain-Technologie: Chance zur Transformation der Energiewirtschaft? Berichtsteil Anwendungsfälle. In: (2018). Ed. by Forschungsstelle für Energiewirtschaft e.V. URL: https://www.ffe.de/veroeffentlichungen/neue-studie-anwendungsfaelle-der-blockchain-technologie-in-der-energiewirtschaft-berichtsteil-anwendungsfaelle/ (visited on 03/06/2022).

[30] C. Burger, A. Kuhlmann, P. Richard, and J. Weinmann. *Blockchain in der Energiewende*. Ed. by Deutsche Energie-Agentur GmbH and European School of Management and Technology GmbH. Berlin, GER, 2016. URL: https://www.esmt.org/system/files_force/dena_esmt_studie_blockchain_deutsch_0.pdf?download=1&download=1 (visited on 08/10/2018).

[31] V. Peter, K. Tidten, P. Hahn, Y. Bendjebbour, and G. Stolzenburg. *Blockchain in der Energiewirtschaft: Potenziale für Energieversorger*. Ed. by Bundesverband der Energie- und Wasserwirtschaft e.V. 2017. URL: https://www.bdew.de/service/publikationen/blockchain-energiewirtschaft/ (visited on 08/10/2018).

[32] S. D. Lumpp, M. Zade, and M. Doepfert. *LEMLab*. https://github.com/tum-ewk/lemlab. [Computer Software]. 2021.

[33] Z. You, M. Zade, and B. Kumaran Nalini. *OpenTUMFlex*. https://github.com/tum-ewk/opentumflex. [Computer Software]. 2020.

[34] A. Burkhalter, J. Kaenzig, and R. Wüstenhagen. Kundenpräferenzen für leistungsrelevante Attribute von Stromprodukten. In: *Zeitschrift für Energiewirtschaft* 33 (2009), pp. 161–172. DOI: 10.1007/s12398-009-0019-8.

[35] J. Kaenzig, S. L. Heinzle, and R. Wüstenhagen. Whatever the customer wants, the customer gets? Exploring the gap between consumer preferences and default electricity products in Germany. In: *Energy Policy* 53 (2013), pp. 311–322. ISSN: 03014215. DOI: 10.1016/j.enpol.2012.10.061.

[36] E. M. Mengelkamp. *Engineering Local Electricity Markets for Residential Communities*. 2019. DOI: 10.5445/IR/1000095229.

[37] Alvin E. Roth. The art of designing markets. In: *Harvard Business School Publishing Corporation* (2007). URL: https://scholar.harvard.edu/files/roth/files/hbr.artofdesigningmarkets.pdf (visited on 05/01/2021).

[38] W. Tushar, C. Yuen, T. K. Saha, T. Morstyn, A. C. Chapman, M. J. E. Alam, S. Hanif, and H. V. Poor. Peer-to-peer energy systems for connected communities: A review of recent advances and emerging challenges. In: *Applied Energy* 282 (2021), p. 116131. ISSN: 03062619. DOI: 10.1016/j.apenergy.2020.116131.

[39] T. Sousa, T. Soares, P. Pinson, F. Moret, T. Baroche, and E. Sorin. Peer-to-peer and community-based markets: A comprehensive review. In: *Renewable and Sustainable Energy Reviews* 104 (2019), pp. 367–378. ISSN: 13640321. DOI: 10.1016/j.rser.2019.01.036.

[40] M. Khorasany, Y. Mishra, and G. Ledwich. Market framework for local energy trading: a review of potential designs and market clearing approaches. In: *IET Generation, Transmission & Distribution* 12.22 (2018), pp. 5899–5908. ISSN: 1751-8687. DOI: 10.1049/iet-gtd.2018.5309.

[41] B. J. Kalkbrenner, K. Yonezawa, and J. Roosen. Consumer preferences for electricity tariffs: Does proximity matter? In: *Energy Policy* 107 (2017), pp. 413–424. ISSN: 03014215. DOI: 10.1016/j.enpol.2017.04.009.

[42] C. Plum, R. Olschewski, M. Jobin, and O. van Vliet. Public preferences for the Swiss electricity system after the nuclear phase-out: A choice experiment. In: *Energy Policy* 130 (2019), pp. 181–196. ISSN: 03014215. DOI: 10.1016/j.enpol.2019.03.054.

[43] N. Günther, L. Fait, E. Groh, and H. Wetzel. Gibt es eine Zahlungsbereitschaft für regionalen Grünstrom? In: *Energiewirtschaftliche Tagesfragen* 11 (2019), pp. 35–38.

[44] D. Friedman and J. Rust, eds. *The double auction market: Institutions, theories, and evidence ; proceedings of the Workshop on Double Auction Markets held June, 1991 in Santa Fe, New Mexico*. Vol. 14. Santa Fe Institute studies in the sciences of complexity. Cambridge, Mass.: Perseus Publ, 1993. ISBN: 978-0-201-62459-5.

[45] Y. Shoham and K. Leyton-Brown. *Multiagent systems: Algorithmic, game-theoretic, and logical foundations*. Cambridge: Cambridge University Press, 2009. DOI: 10.1017/CBO9780511811654.

[46] G. Wood. *Ethereum: A secure decentralised generalised transaction ledger*. 2022. URL: https://ethereum.github.io/yellowpaper/paper.pdf (visited on 02/11/2022).

[47] T. W. Edgar and D. O. Manz. Science and Cyber Security. In: *Research Methods for Cyber Security*. Elsevier, 2017, pp. 33–62. ISBN: 9780128053492. DOI: 10.1016/B978-0-12-805349-2.00002-9.

[48] Union of the Electricity Industry, ed. *Flexibility and Aggregation: Requirements for their interaction in the market*. Brussels, 2014. URL: https://www.usef.energy/app/uploads/2016/12/EURELECTRIC-Flexibility-and-Aggregation-jan-2014.pdf (visited on 03/11/2022).

[49] O. Risse, C. Stephanos, and B. Erlach, eds. *Netzengpässe als Herausforderung für das Stromversorgungssystem: Optionen zur Weiterentwicklung des Marktdesigns*. Version 1.01. Stellungnahme / Deutsche Akademie der Naturforscher Leopoldina. Halle (Saale), Mainz, and München: Deutsche Akademie der Naturforscher Leopoldina e.V. - Nationale Akademie der Wissenschaften, Union der deutschen Akademien der Wissenschaften e. V, and acatech - Deutsche Akademie der Technikwissenschaften e.V., 2020. ISBN: 978-3-8047-4116-4. URL: http://nbn-resolving.org/urn:nbn:de:gbv:3:2-126924 (visited on 03/11/2022).

[50] M. Zade, Z. You, B. Kumaran Nalini, P. Tzscheutschler, and U. Wagner. Quantifying the Flexibility of Electric Vehicles in Germany and California—A Case Study. In: *Energies* 13.21 (2020), p. 5617. ISSN: 1996-1073. DOI: 10.3390/en13215617.

[51] H. Weigt. *A Review of Liberalization and Modeling of Electricity Markets*. MPRA Paper 65651. University Library of Munich, Germany, Oct. 2009. URL: https://ideas.repec.org/p/pra/mprapa/65651.html (visited on 03/11/2022).

[52] K. Lenz, T. Lenck, and F. Peter. *The Liberalisation of Electricity Markets in Germany History, Development and Current Status*. Ed. by Agora Energiewende. Berlin, 2019. URL: https://static.agora-energiewende.de/fileadmin/Projekte/2019/Liberalisation_Power_Market/Liberalisation_Electricity_Markets_Germany_V1-0.pdf (visited on 02/28/2022).

[53] European Parliament. *Directive 96/92/EC of the European Parliament and of the Council of 19 December 1996 concerning common rules for the internal market in electricity*. 1996. URL: https://eur-lex.europa.eu/legal-content/EN/TXT/?uri=CELEX%5C%3A31996L0092 (visited on 02/28/2022).

[54] European Parliament. *Directive 2003/54/EC of the European Parliament and of the Council of 26 June 2003 concerning common rules for the internal market in electricity and repealing Directive 96/92/EC - Statements made with regard to decommissioning and waste management activities*. 2003. URL: https://eur-lex.europa.eu/legal-content/EN/TXT/?uri=celex%5C%3A32003L0054 (visited on 02/28/2022).

[55] European Parliament. *Directive 2009/28/EC of the European Parliament and of the Council of 23 April 2009 on the promotion of the use of energy from renewable sources and amending and subsequently repealing Directives 2001/77/EC and 2003/30/EC*. 2009. URL: https://eur-lex.europa.eu/legal-content/EN/TXT/?uri=CELEX%5C%3A32009L0028&qid=1646075609140 (visited on 02/28/2022).

[56] J. Hu, R. Harmsen, W. Crijns-Graus, E. Worrell, and M. van den Broek. Identifying barriers to large-scale integration of variable renewable electricity into the electricity market: A literature review of market design. In: *Renewable and Sustainable Energy Reviews* 81 (2018), pp. 2181–2195. ISSN: 1364-0321. DOI: 10.1016/j.rser.2017.06.028.

[57] P. Fekete. *Redispatch in Deutschland: Auswertung der Transparenzdaten - April 2013 bis einschließlich Dezember 2020*. Ed. by Bundesverband der Energie- und Wasserwirtschaft e.V. Berlin, 2021. URL: https://www.bdew.de/media/documents/2021_Q2_Bericht_Redispatch.pdf (visited on 03/11/2022).

[58] E. Hauser, S. Heib, J. Hildebrand, I. Rau, A. Weber, J. Welling, J. Güldenberg, C. Maaß, J. Mundt, R. Werner, A. Schudak, and T. Wallbott. *Marktanalyse Ökostrom II: Marktanalyse Ökostrom und HKN, Weiterentwicklung des Herkunftsnachweissystems und der Stromkennzeichnung*. Ed. by Umweltbundesamt. Dessau-Roßlau, 2019. URL: https://www.umweltbundesamt.de/sites/default/files/medien/1410/publikationen/2019-08-15_cc_30-2019_marktanalyse_oekostrom_ii.pdf (visited on 02/14/2022).

[59] A. A. Goett, K. Hudson, and K. E. Train. Customers' Choice Among Retail Energy Suppliers: The Willingness-to-Pay for Service Attributes. In: *The Energy Journal* 21.4 (2000). ISSN: 01956574. DOI: 10.5547/ISSN0195-6574-EJ-Vol21-No4-1.

[60] D. A. Hensher, N. Shore, and K. Train. Willingness to pay for residential electricity supply quality and reliability. In: *Applied Energy* 115 (2014), pp. 280–292. ISSN: 03062619. DOI: 10.1016/j.apenergy.2013.11.007.

[61] N. Lienhoop. Acceptance of wind energy and the role of financial and procedural participation: An investigation with focus groups and choice experiments. In: *Energy Policy* 118 (2018), pp. 97–105. ISSN: 03014215. DOI: 10.1016/j.enpol.2018.03.063.

[62] A. Mattes. Grüner Strom: Verbraucher sind bereit, für Investitionen in erneuerbare Energien zu zahlen. In: *DIW Wochenbericht* 79.7 (2012), pp. 2–9. URL: https://EconPapers.repec.org/RePEc:diw:diwwob:79-7-1 (visited on 03/11/2022).

[63] R. Menges and G. Beyer. Consumer Preferences for Renewable Energy. In: *Marketing Renewable Energy*. Ed. by C. Herbes and C. Friege. Management for Professionals. Cham: Springer International Publishing, 2017, pp. 49–73. ISBN: 978-3-319-46426-8. DOI: 10.1007/978-3-319-46427-5_3.

[64] P. Mozumder, W. F. Vásquez, and A. Marathe. Consumers' preference for renewable energy in the southwest USA. In: *Energy Economics* 33.6 (2011), pp. 1119–1126. ISSN: 01409883. DOI: 10.1016/j.eneco.2011.08.003.

[65] J. Rommel, J. Sagebiel, and J. R. Müller. Quality uncertainty and the market for renewable energy: Evidence from German consumers. In: *Renewable Energy* 94 (2016), pp. 106–113. ISSN: 09601481. DOI: 10.1016/j.renene.2016.03.049.

[66] J. Sagebiel, J. R. Müller, and J. Rommel. Are consumers willing to pay more for electricity from cooperatives? Results from an online Choice Experiment in Germany. In: *Energy Research & Social Science* 2 (2014), pp. 90–101. ISSN: 22146296. DOI: 10.1016/j.erss.2014.04.003.

[67] J.-J. Soon and S.-A. Ahmad. Willingly or grudgingly? A meta-analysis on the willingness-to-pay for renewable energy use. In: *Renewable and Sustainable Energy Reviews* 44 (2015), pp. 877–887. ISSN: 13640321. DOI: 10.1016/j.rser.2015.01.041.

[68] A. Tabi, S. L. Hille, and R. Wüstenhagen. What makes people seal the green power deal? — Customer segmentation based on choice experiment in Germany. In: *Ecological Economics* 107 (2014), pp. 206–215. ISSN: 09218009. DOI: 10.1016/j.ecolecon.2014.09.004.

[69] D. Vecchiato and T. Tempesta. Public preferences for electricity contracts including renewable energy: A marketing analysis with choice experiments. In: *Energy* 88 (2015), pp. 168–179. ISSN: 03605442. DOI: 10.1016/j.energy.2015.04.036.

[70] A. C. Atkinson. Optimal Experimental Design. In: *International Encyclopedia of the Social & Behavioral Sciences*. Elsevier, 2015, pp. 256–262. ISBN: 9780080970875. DOI: 10.1016/B978-0-08-097086-8.42041-6.

[71] B. Richter, E. Mengelkamp, and C. Weinhardt. Vote for your energy: a market mechanism for local energy markets based on the consumers' preferences. In: *16th International Conference on the European Energy Market (EEM)*. [Piscataway, New Jersey]: IEEE, 2019, pp. 1–6. ISBN: 978-1-7281-1257-2. DOI: 10.1109/EEM.2019.8916544.

[72] C. Senkpiel, A. Dobbins, C. Kockel, J. Steinbach, U. Fahl, F. Wille, J. Globisch, S. Wassermann, B. Droste-Franke, W. Hauser, C. Hofer, L. Nolting, and C. Bernath. Integrating Methods and Empirical Findings from Social and Behavioural Sciences into Energy System Models—Motivation and Possible Approaches. In: *Energies* 13.18 (2020), p. 4951. ISSN: 1996-1073. DOI: 10.3390/en13184951.

[73] E. Mengelkamp, J. Gärttner, K. Rock, S. Kessler, L. Orsini, and C. Weinhardt. Designing microgrid energy markets - A case study. In: *Applied Energy* 210 (2018), pp. 870–880. ISSN: 03062619. DOI: 10.1016/j.apenergy.2017.06.054.

[74] T. Morstyn, N. Farrell, S. J. Darby, and M. D. McCulloch. Using peer-to-peer energy-trading platforms to incentivize prosumers to form federated power plants. In: *Nature Energy* 3.2 (2018), pp. 94–101. DOI: 10.1038/s41560-017-0075-y.

[75] S. Aggarwal and N. Kumar. Blockchain 2.0: Smart contracts. In: *The Blockchain Technology for Secure and Smart Applications across Industry Verticals*. Vol. 121. Advances in Computers. Elsevier, 2021, pp. 301–322. ISBN: 9780128219911. DOI: 10.1016/bs.adcom.2020.08.015.

[76] L. Ante, F. Steinmetz, and I. Fiedler. Blockchain and energy: A bibliometric analysis and review. In: *Renewable and Sustainable Energy Reviews* 137 (2021), p. 110597. ISSN: 13640321. DOI: 10.1016/j.rser.2020.110597.

[77] A. Hasankhani, S. Mehdi Hakimi, M. Bisheh-Niasar, M. Shafie-khah, and H. Asadolahi. Blockchain technology in the future smart grids: A comprehensive review and frameworks. In: *International Journal of Electrical Power & Energy Systems* 129 (2021), p. 106811. ISSN: 01420615. DOI: 10.1016/j.ijepes.2021.106811.

[78] Q. Wang, R. Li, and L. Zhan. Blockchain technology in the energy sector: From basic research to real world applications. In: *Computer Science Review* 39 (2021), p. 100362. ISSN: 15740137. DOI: 10.1016/j.cosrev.2021.100362.

[79] K.-L. Brousmichc, A. Anoaica, O. Dib, T. Abdellatif, and G. Deleuze. Blockchain Energy Market Place Evaluation: An Agent-Based Approach. In: *2018 IEEE 9th Annual Information Technology, Electronics and Mobile Communication Conference (IEMCON)* (Nov. 1–3, 2018). IEEE, pp. 321–327. ISBN: 978-1-5386-7266-2. DOI: 10.1109/IEMCON.2018.8614924.

[80] G. C. Okwuibe, M. Zade, P. Tzscheutschler, T. Hamacher, and U. Wagner. A Blockchain-based Double-sided Auction Peer-to-peer Electricity Market Framework. In: *2020 IEEE Electric Power and Energy Conference (EPEC)* (Nov. 9–10, 2020). IEEE, pp. 1–8. ISBN: 978-1-7281-6489-2. DOI: 10.1109/EPEC48502.2020.9320030.

[81] C. Zhang, T. Yang, and Y. Wang. Peer-to-Peer energy trading in a microgrid based on iterative double auction and blockchain. In: *Sustainable Energy, Grids and Networks* 27 (2021), p. 100524. ISSN: 23524677. DOI: 10.1016/j.segan.2021.100524.

[82] H. T. Doan, J. Cho, and D. Kim. Peer-to-Peer Energy Trading in Smart Grid Through Blockchain: A Double Auction-Based Game Theoretic Approach. In: *IEEE ACCESS* 9 (2021), pp. 49206–49218. ISSN: 2169-3536. DOI: 10.1109/ACCESS.2021.3068730.

[83] S. Chen, Z. Shen, L. Zhang, Z. Yan, C. Li, N. Zhang, and J. Wu. A trusted energy trading framework by marrying blockchain and optimization. In: *Advances in Applied Energy* 2 (2021), p. 100029. ISSN: 26667924. DOI: 10.1016/j.adapen.2021.100029.

[84] K. Heck, E. Mengelkamp, and C. Weinhardt. Blockchain-based local energy markets: Decentralized trading on single-board computers. In: *Energy Systems* 12.3 (2021), pp. 603–618. ISSN: 1868-3967. DOI: 10.1007/s12667-020-00399-4.

[85] T. Machacek, M. Biswal, and S. Misra. Proof of X: Experimental Insights on Blockchain Consensus Algorithms in Energy Markets. In: *2021 IEEE Power & Energy Society Innovative Smart Grid Technologies Conference (ISGT)* (Feb. 16–18, 2021). IEEE, pp. 1–5. ISBN: 978-1-7281-8897-3. DOI: 10.1109/ISGT49243.2021.9372194.

[86] F. Blom and H. Farahmand. On the Scalability of Blockchain-Supported Local Energy Markets. In: *2018 International Conference on Smart Energy Systems and Technologies (SEST)* (Sept. 10–12, 2018). IEEE, pp. 1–6. ISBN: 978-1-5386-5326-5. DOI: 10.1109/SEST.2018.8495882.

[87] A. Esmat, M. de Vos, Y. Ghiassi-Farrokhfal, P. Palensky, and D. Epema. A novel decentralized platform for peer-to-peer energy trading market with blockchain technology. In: *Applied Energy* 282 (2021), p. 116123. ISSN: 03062619. DOI: 10.1016/j.apenergy.2020.116123.

[88] M. Foti and M. Vavalis. Blockchain based uniform price double auctions for energy markets. In: *Applied Energy* 254 (2019), p. 113604. ISSN: 03062619. DOI: 10.1016/j.apenergy.2019.113604.

[89] S. Liu, F. Chen, L. Shen, Y. Hu, and Y. Ding. A high-performance local energy trading cyber-physical system based on blockchain technology. In: *IOP Conference Series: Earth and Environmental Science* 227 (2019), p. 032009. DOI: 10.1088/1755-1315/227/3/032009.

[90] D. Han, C. Zhang, J. Ping, and Z. Yan. Smart contract architecture for decentralized energy trading and management based on blockchains. In: *Energy* 199 (2020), p. 117417. ISSN: 03605442. DOI: 10.1016/j.energy.2020.117417.

[91] D. Son, S. Al Zahr, and G. Memmi. Performance Analysis of an Energy Trading Platform Using the Ethereum Blockchain. In: *2021 IEEE International Conference on Blockchain and Cryptocurrency (ICBC)* (May 3–6, 2021). IEEE, pp. 1–3. ISBN: 978-1-6654-3578-9. DOI: 10.1109/ICBC51069.2021.9461115.

[92] G. Vieira and J. Zhang. Peer-to-peer energy trading in a microgrid leveraged by smart contracts. In: *Renewable and Sustainable Energy Reviews* 143 (2021), p. 110900. ISSN: 13640321. DOI: 10.1016/j.rser.2021.110900.

[93] G. Tsaousoglou, K. Steriotis, N. Efthymiopoulos, P. Makris, and E. Varvarigos. Truthful, Practical and Privacy-Aware Demand Response in the Smart Grid via a Distributed and Optimal Mechanism. In: *IEEE Transactions on Smart Grid* 11.4 (2020), pp. 3119–3130. ISSN: 1949-3053. DOI: 10.1109/TSG.2020.2965221.

[94] S. V. Oprea, A. Bara, and A. I. Andreescu. Two Novel Blockchain-Based Market Settlement Mechanisms Embedded Into Smart Contracts for Securely Trading Renewable Energy. In: *IEEE ACCESS* 8 (2020), pp. 212548–212556. ISSN: 2169-3536. DOI: 10.1109/ACCESS.2020.3040764.

[95] M. Zade, M. Feroce, A. Guridi, S. D. Lumpp, and P. Tzscheutschler. Evaluating the added value of blockchains to local energy markets—Comparing the performance of blockchain–based and centralised implementations. In: *IET Smart Grid* (2022). ISSN: 2515-2947. DOI: 10.1049/stg2.12058.

[96] A. Hayes. A Cost of Production Model for Bitcoin. In: *SSRN Electronic Journal* (2015). ISSN: 1556-5068. DOI: 10.2139/ssrn.2580904.

[97] D. Malone and K. J. O'Dwyer. Bitcoin Mining and its Energy Footprint. In: *25th IET Irish Signals & Systems Conference 2014 and 2014 China-Ireland International Conference on Information and Communities Technologies (ISSC 2014/CIICT 2014)*. Institution of Engineering and Technology, 2014, pp. 280–285. ISBN: 978-1-84919-924-7. DOI: 10.1049/cp.2014.0699.

[98] C. Mora, R. L. Rollins, K. Taladay, M. B. Kantar, M. K. Chock, M. Shimada, and E. C. Franklin. Bitcoin emissions alone could push global warming above 2°C. In: *Nature Climate Change* 8.11 (2018), pp. 931–933. ISSN: 1758-678X. DOI: 10.1038/s41558-018-0321-8.

[99] H. Vranken. Sustainability of bitcoin and blockchains. In: *Current Opinion in Environmental Sustainability* 28 (2017), pp. 1–9. ISSN: 18773435. DOI: 10.1016/j.cosust.2017.04.011.

[100] N. Alzahrani and N. Bulusu. Towards True Decentralization: A Blockchain Consensus Protocol Based on Game Theory and Randomness. In: *Decision and Game Theory for Security*. Ed. by L. Bushnell, R. Poovendran, and T. Başar. Vol. 11199. Lecture Notes in Computer Science. Cham: Springer International Publishing, 2018, pp. 465–485. ISBN: 978-3-030-01553-4. DOI: 10.1007/978-3-030-01554-1_27.

[101] M. Zade, Y. Incedag, W. El-Baz, P. Tzscheutschler, and U. Wagner. Prosumer Integration in Flexibility Markets: A Bid Development and Pricing Model. In: *2018 2nd IEEE Conference on Energy Internet and Energy System Integration (EI2)*. IEEE, 2018, pp. 1–9. ISBN: 978-1-5386-8549-5. DOI: 10.1109/EI2.2018.8582022.

[102] D. P. Oyinloye, J. S. Teh, N. Jamil, and M. Alawida. Blockchain Consensus: An Overview of Alternative Protocols. In: *Symmetry* 13.8 (2021), p. 1363. DOI: 10.3390/sym13081363.

[103] Deutscher Bundestag. *EnWG § 13 Systemverantwortung der Betreiber von Übertragungsnetzen, Verordnungsermächtigungen*. 2015. URL: https://beck-online.beck.de/Print/CurrentDoc?vpath=bibdata/komm/britzhehekoenwg_3/enwg/cont/britzhehekoenwg.enwg.p13.htm&printdialogmode=CurrentDoc&hlword= (visited on 02/19/2022).

[104] Deutscher Bundestag. *Gesetz über die Elektrizitäts- und Gasversorgung (Energiewirtschaftsgesetz - EnWG)*. 2021. URL: https://www.gesetze-im-internet.de/enwg_2005/__13.html (visited on 02/19/2022).

[105] Council of European Energy Regulators, ed. *CEER Paper on DSO Procedures of Procurement of Flexibility*. Brussels, 2020. URL: https://www.ceer.eu/documents/104400/-/-/e436ca7f-a0df-addb-c1de-5a3a5e4fc22b (visited on 02/19/2022).

[106] International Renewable Energy Agency. *Innovation landscape for a renewable-powered future: Solutions to integrate variable renewables*. Abu Dhabi, 2019. URL: https://www.irena.org/publications/2019/Feb/Innovation-landscape-for-a-renewable-powered-future (visited on 02/19/2022).

[107] E. Heilmann, N. Klempp, and H. Wetzel. *Market design of regional flexibility markets: A classification metric for flexibility products and its application to German prototypical flexibility markets*. Ed. by Philipps-University Marburg, School of Business and Economics, Marburg. 2020. URL: https://www.econstor.eu/handle/10419/213475 (visited on 02/19/2022).

[108] J. Höckner, S. Voswinkel, and C. Weber. Market distortions in flexibility markets caused by renewable subsidies – The case for side payments. In: *Energy Policy* 137 (2020), p. 111135. ISSN: 03014215. DOI: 10.1016/j.enpol.2019.111135.

[109] J. Radecke, J. Hefele, and L. Hirth. *Markets for Local Flexibility in Distribution Networks*. Ed. by ZBW – Leibniz Information Centre for Economics. Kiel, Hamburg, 2019. URL: https://www.econstor.eu/handle/10419/204559 (visited on 02/19/2022).

[110] O. Valarezo, T. Gómez, J. P. Chaves-Avila, L. Lind, M. Correa, D. Ulrich Ziegler, and R. Escobar. Analysis of New Flexibility Market Models in Europe. In: *Energies* 14.12 (2021), p. 3521. ISSN: 1996-1073. DOI: 10.3390/en14123521.

[111] B. K. Nalini, M. Eldakadosi, Z. You, M. Zade, P. Tzscheutschler, and U. Wagner. Towards Prosumer Flexibility Markets: A Photovoltaic and Battery Storage Model. In: *2019 IEEE PES Innovative Smart Grid Technologies Europe (ISGT-Europe)* (Sept. 29–Oct. 2, 2019). IEEE, pp. 1–5. ISBN: 978-1-5386-8218-0. DOI: 10.1109/isgteurope.2019.8905622.

[112] Z. You, B. K. Nalini, M. Zade, P. Tzscheutschler, and U. Wagner. Flexibility quantification and pricing of household heat pump and combined heat and power unit. In: *2019 IEEE PES Innovative Smart Grid Technologies Europe (ISGT-Europe)* (Sept. 29–Oct. 2, 2019). IEEE, pp. 1–5. ISBN: 978-1-5386-8218-0. DOI: 10.1109/isgteurope.2019.8905594.

[113] Z. You, M. Zade, B. Kumaran Nalini, and P. Tzscheutschler. Flexibility Estimation of Residential Heat Pumps under Heat Demand Uncertainty. In: *Energies* 14.18 (2021), p. 5709. ISSN: 1996-1073. DOI: 10.3390/en14185709.

[114] H. Hahne. *Enhancement of a Flexibility Quantifying and Pricing Model for Electric Vehicles*. Research internship report. 2021.

[115] M. Zade and J. Myklebost. *Bitcoin and Ethereum Mining Hardware*. 2018. DOI: 10.17632/4dw6j3pxz5.1.